Summer 2023

Remote Sensing of Georgia Tidal Marsh Habitats Using Aerial Photography and Planetscope Satellite Imagery

Harrison M. Currin

REMOTE SENSING OF GEORGIA TIDAL MARSH HABITATS USING AERIAL PHOTOGRAPHY AND PLANETSCOPE SATELLITE IMAGERY

by

HARRISON CURRIN

(Advised by Dr. Christine M. Hladik)

ABSTRACT

Globally, tidal marshes cover about 90,800 km. Within the state of Georgia tidal marshes are primarily located behind the barrier islands and total 1,619 km^2. The combination of high salinity environments and daily inundation, and being dependent on river output, make these dynamic systems. Tidal marshes provide numerous ecosystem services such as carbon and nitrogen sequestration, flood control, coastal protection, and numerous biogeochemical processes. Due to their unique position, tidal marshes are under threat from sea level rise, drought, coastal development, and large-scale disturbance events. Tidal freshwater marshes are especially susceptible to these threats due to their geographic location and small extent which have been historically understudied. By mapping tidal marshes, species composition is better understood and can be used to scale up ecosystem services, biogeochemical processes, and above ground biomass using remote sensing imagery. This study uses aerial orthoimagery along with a digital elevation model, National Wetland Inventory, and vegetation indices to map salt, brackish, and tidal freshwater marshes along the entire coast of Georgia. Higher spectral and spatial resolution PlanetScope 4- and 8-band satellite imagery was also used to map salt, brackish, and tidal freshwater marshes of the three main watersheds in coastal Georgia which include the Ogeechee, Altamaha, and Satilla Rivers. The aerial orthoimagery classification had an accuracy of 86.3%

with salt marshes making up 67.8%, brackish 28.7%, and tidal freshwater 3.5% of the classified image and showed the importance of using a DEM and NWI for tidal marsh mapping. The PlanetScope classifications were comparable to the aerial classification with an accuracy of 86.5% (Ogeechee), 88.1% (Altamaha), and 75.9% (Satilla). Differences between the 4-band and 8-band PlanetScope imagery proved to be minimal. Due to the vulnerability of salt marshes to climate change, this study aims to contribute and expand upon current remote sensing studies on tidal marsh mapping.

INDEX WORDS: Georgia coast, remote sensing, aerial imagery, satellite imagery, tidal marshes, habitat mapping, random forest, PlanetScope

REMOTE SENSING OF GEORGIA TIDAL MARSH HABITATS USING AERIAL PHOTOGRAPHY AND PLANETSCOPE SATELLITE IMAGERY

By

HARRISON CURRIN

B.S., Elon University 2020

A Dissertation Submitted to the Graduate Faculty of Georgia Southern University in Partial Fulfillment of the Requirements for the Degree

MASTER OF SCIENCE IN APPLIED GEOGRAPHY

REMOTE SENSING OF GEORGIA TIDAL MARSH HABITATS USING AERIAL PHOTOGRAPHY AND PLANETSCOPE SATELLITE IMAGERY

by

HARRISON CURRIN

Major Professor:	Christine Hladik
Committee:	Chester Jackson
	Munshi Rahman
	John Schalles

Electronic Version Submitted:
July 2023

ACKNOWLEDGEMENTS

This project would not have been possible without the help and support of various individuals. I would like to first thank Jennifer Byrd and Mike Land for inspiring me throughout my time at Greenfield School to pursue a career in science. I would also like to thank the various professors, especially Dr. Jen Hamel and Dr. David Vandermast, for introducing me to the wonderful world of ecology. This would have also not been possible without Dr. John Schalles for whom I was an intern where he introduced me to the world of tidal marshes and remote sensing.

Fieldwork could not have been completed without the combined efforts of Georgia Southern University, the University of Georgia Marine Institute, and the Skidaway Institute of Oceanography which supplied the equipment and people to successfully complete this project. I am indebted to multiple people, including Tommy Pudil who without, this project could not have been completed. Tommy acted as our navigator, and organizer, and provided plenty of laughs during tough field days. Likewise, Elise Diehl, Jonah Rigdon, John Williams, Mike Robinson, Bennett Bacon, and Captain Fran Lapolla masterfully operated the boats allowing access to each of our sites. I would also like to thank people who came out to aid in sampling including Emma Goldsmith, Mara Slatterly, and Emily Klawiter.

Words cannot express the gratitude I have for Dr. Christine Hladik, who over the last two years has served as my advisor. Little did I know that working on one project as an intern would lead me to someone who has consistently pushed me and developed my skills in remote sensing, fieldwork, and experimental design. I could not have asked for a better advisor. I would like to thank my committee Dr. Chester Jackson, Dr. Munshi Rahman, and Dr. John Schalles for providing invaluable feedback and advice throughout this project.

Finally, a huge thank you to my parents, Martin and Monica Currin, my brother Davis Currin, and my fiancé Emma Ebright for constantly providing support throughout this project and being there every step of the way through the ups and downs. To these people and others who have contributed both directly and indirectly, I give you my thanks and deepest gratitude.

TABLE OF CONTENTS

Page

LIST OF FIGURES

Page

LIST OF TABLES

Page

CHAPTER 1

INTRODUCTION

1.1 Tidal Marshes

Tidal marshes can be found in protected, low-energy coastlines, where they form the transitional zone between marine, freshwater, and terrestrial systems (Boström et al., 2011). These systems are defined by daily inundation, herbaceous vegetation, and their salinity tolerance (Baldwin, 2004; Odum, 1988). Tidal marshes are commonly separated into three habitats based on salinity: salt, brackish, and tidal freshwater marshes. Salt marshes are found in polyhaline environments with average annual salinities of 18.0 to 30.0 practical salinity units (PSU), while tidal freshwater marshes are restricted to fresh environments which have an average annual salinity of less than 0.5 PSU (Cowardin et al., 1979; Odum, 1988). The areas that fall between 0.5 and 18.0 PSU are considered to be brackish marshes. It is important to note that these values are an average and can be variable over short and long time periods due to environmental conditions such as drought (Odum, 1988).

Sea level rise is currently predicted to reach 36.56 cm globally by 2050 (Sweet et al., 2022), which can cause tidal marsh submergence and loss due to altered salinity regimes and inundation periods (Craft et al., 2009; Kirwan et al., 2010; Moorhead & Brinson, 1995; Reed, 1995). In response to sea level rise, tidal marshes can maintain their position in the tidal frame by gaining elevation either by accreting sediment or increasing organic matter in an ecogeomorphic feedback (Fagherazzi et al., 2022); or by transgressing inland, replacing other species that are no longer suitable for that area due to inundation or salinity (Craft et al., 2009).

Tidal marshes cover an estimated 90,800 km^2 worldwide, of which 54,951 km^2 consists of salt marshes (Mcowen et al., 2017; Murray et al., 2022). However, this is only a small portion of their historical extent. It is estimated that salt marshes have lost between 25% to 50% of their global area (Crooks et al. 2011, Duarte et al. 2008). While this historical extent has decreased, conservation and restoration efforts over the last 20 years have helped marshes to regain about 100 km^2 worldwide (Murray et al. 2022). Although this is a minor gain globally, it shows that restoration projects can mitigate the local loss of tidal marshes.

Tidal marshes provide a wide range of ecosystem services, which differ based on habitat type (Craft et al. 2009). Historically, the different tidal marsh habitats have not been equally studied, and tidal freshwater marshes have received the least attention, as coastal ecologists focused on saline areas due to the large extent of salt marsh, while river ecologists rarely studied marshes subject to tidal fluctuations. However, in recent years, recognition of the ecological importance of tidal freshwater marshes has spurred increased interest (Barendregt, 2016).

The Georgia coast, where this project is located, contains about 33% (1,619 km^2) of all tidal marshes on the East Coast of the United States, 92% (1,489 km^2) of which are saltwater marshes (Wiegert, & Freeman, 1990; Georgia Department of Natural Resources, 2012). The remaining amount is mostly brackish marshes with a small amount of tidal freshwater marsh, which often occupy areas formerly used for rice cultivation (Seabrook, 2006). While brackish and tidal fresh marshes cover a smaller area than salt marshes, they contribute a greater amount of nutrient accumulation and biogeochemical processes (Loomis & Craft, 2010).

1.2 Importance of Tidal Marshes

Tidal marsh ecosystems have been credited by many for playing an important role in maintaining the health of coastal systems by providing numerous ecosystem services. There has been an attempt to agree upon a singular definition for ecosystem services, such as including only the products of ecosystem processes that benefit or are consumed by people (Boyd & Banzhaf, 2007). In the context of this research, ecosystem services are defined as all components of ecosystems that are actively or passively used to promote a human's health and well-being (Fisher et al., 2009). Under this definition, ecosystem services include the food that tidal marshes provide to humans by providing a safe haven for fish and other animals (Etheridge, 2013; Woolf & Kundell, 1990) and the ability of tidal marshes to fix and store carbon which varies by marsh habitat type (Kirwan & Mudd, 2012; Loomis & Craft, 2010; Shiau et al., 2019).

1.2.1 Salt Marshes

All marshes provide ecosystem services such as carbon sequestration and nitrogen storage, but salt marshes sequester carbon and store nitrogen less effectively than tidal freshwater and brackish marshes (Loomis & Craft, 2010). In total, brackish marshes accumulate 18,096 Mg of carbon per year while salt marshes only accumulate 12,673 Mg per year (Loomins and Craft, 2010). Looking on a per-meter basis, tidal freshwater marshes outperformed both the brackish and salt marshes in total carbon and nitrogen accumulated (Loomis and Craft, 2010). In addition to these biogeochemical services, salt marshes also buffer coastal ecosystems and communities from high-impact events such as storms, tidal events (e.g., high tide flooding), wind events, and tropical weather (Shepard et al., 2011), all which are predicted to increase in magnitude and frequency due to global warming (Hardy & Hauer, 2018; Lin et al., 2013).

Salt marshes can help protect these coastal communities and other tidal marsh habitats from storm surges, increases in sea level from wind events, and by other events that may cause increased water levels in the form of wave attenuation (Gedan et al., 2011; Möller et al., 2014; Shepard et al., 2011). Storm surges occur due to wind and waves, low-pressure systems, rainfall, and tidal conditions (Gönnert et al., 2001). Storm surges can range in height up to 5 m in temperate regions causing devastating impacts on people and the economy due to flood-related damage. Salt marshes provide an estimated $10,900 per hectare (Mazzocco et al., 2022) in ecosystem services every year while tidal freshwater marshes, when adjusted for the time period, are estimated to provide $25,800 per hectare. As discussed in a review by Gedan et al. (2011), the presence of salt marshes reduces storm surges, property damage, and human death. Other studies have found that salt marshes attenuate waves during storm surge events by decreasing wave energy and velocities (Möller et al., 2014). Based on a meta-analysis performed by Shepard *et al.* (2011), 10 studies showed increases in wave and surge attenuation with an increase in marsh extent. Salt marshes can also stabilize shorelines and decrease erosion due to the extensive belowground root and rhizome structures of the dominant macrophyte in Eastern US salt marshes, *Spartina alterniflora,* (Cahoon et al., 1999). Additionally, salt marshes have the ability to trap and add organic material and increase belowground biomass which increases their elevation relative to sea level (Morris et al., 2002; van Eerdt, 1985). The detritus and finer material in the soil creates a more cohesive substrate and decreases the amount of lateral erosion in marshes (Feagin et al., 2009). Along with these ecosystem services, salt marshes provide water filtration, tourism, recreation, and education.

1.2.2 Brackish Marshes and Tidal Freshwater Marshes

Brackish marshes provide more carbon sequestration than salt and tidal freshwater marshes per unit area (Shiau et al., 2019). In brackish marshes, 41 to 46 percent of the fixed carbon remained within the plants while only 18.4% was released into the atmosphere as carbon dioxide or methane while the rest, 8.6 to 13.2 percent, was stored in the soil (Shiau et al., 2019). Brackish marshes also act as nutrient filters for agricultural pollutants by retaining nitrogen as nitrate (Etheridge, 2013), reducing estuarine eutrophication, overgrowth of aquatic plants, and low water oxygen levels (Baden et al., 1990; Vitousek et al., 1997). Like salt marshes, brackish marshes also provide habitat for fish, waterfowl, and other species of plants and animals (Etheridge, 2013).

Tidal freshwater marshes have largely been understudied due to their small geographic extent and hydrologic position between fresh and saltwater environments (Barendregt & Swarth, 2013). In addition to carbon sequestration, these marshes are also important for water quality maintenance, flood and erosion control (Woolf & Kundell, 1990), and nutrient cycling (Tortajada et al., 1990). Tidal fresh marshes also play an important part in nitrogen sequestration, removing 13 to 32% of all nitrogen discharged from the Altamaha, Ogeechee, and Satilla watersheds in coastal Georgia (Loomis & Craft, 2010). These systems also act as places to hunt, trap, and other recreational activities (Woolf & Kundell, 1990).

1.3 Threats to Tidal Marshes

1.3.1 Environmental Threats

Tidal marshes are threatened by sea level rise (Burns et al., 2021; Solohin et al., 2020), coastal development (Baldwin, 2004; Greenberg et al., 2006), drought (Neubauer & Craft, n.d.; Palomo et al., 2013), and large-scale disturbance events (Mo et al., 2020). These forces can reduce marsh biomass (Mo et al., 2020; O'Donnell & Schalles, 2016) and alter natural

biogeochemical processes (Palomo et al., 2013), in turn causing a reduction in ecosystem services. Tidal freshwater marshes are especially vulnerable to these threats because of their low salinity tolerance. Salinization due to low river discharge, sea level rise, or storm surges and wind events, causes an overall loss in tidal freshwater marsh habitat, and the conversion of these systems to less productive brackish and salt marsh ecosystems (Neubauer & Craft, 2009).

Across tidal marshes along the Atlantic coast of North America, it is projected that marsh drowning could occur in 90% of all marshes with sea level rise of 11.2 mm per year or about 65% with a sea level rise of 4.4 mm per year in 2100 based on current accretion rates (Crosby et al., 2016). The Georgia coast is projected to see up to 35.56 cm of SLR by 2050 (Sweet et al., 2022). Using the sea level affecting marsh model (SLAMM) and an average sea level rise of 2.5 mm per year, Craft et al. (2009) found that a 52 cm increase in sea level along the Georgia coast, will cause a 1 percent increase in tidal freshwater marshes, a 10 percent increase in brackish marshes, and a 20 percent reduction in salt marshes. This increase in tidal freshwater marshes and brackish marshes was attributed to the reduction of tidal forest extent (Craft et al., 2009). These changes were predicted to lead to a net reduction in nitrogen sequestration (227 tons per year) and potential denitrification (193 tons per year) (Craft et al., 2009). Tidal freshwater marshes experiencing chronic salt stress (porewater of 2 - 5 PSU) lost 1,333 g/m^2 of belowground biomass and 2.8 cm of elevation in 3.75 years (Solohin et al., 2020). This saltwater inundation also alters the porewater chemistry of tidal freshwater marshes by increasing chlorine, sulfate, dissolved organic nitrogen, and dissolved inorganic phosphorus (Herbert et al., 2018). This converts these once-beneficial sources of carbon sinks to a net source of methane, a relatively short-lived but potent greenhouse gas (Tong et al., 2015).As sea level rise is predicted to increase by 60.96 cm by 2100 (Sweet et al., 2022), sea level rise is predicted to rise by more than

predicted in the studies above, these numbers could be increased if tidal marshes are not able to offset this with vertical accretion rates through biogeomorphic feedbacks. Vertical accretion rates are quite variable based on vegetation type, marsh type, and access to suspended sediment and river outflow (Cahoon et al., 1999). However, a recent study examining Atlantic coast tidal marshes found that the majority of salt marshes are not able to keep up with sea level rise estimates in the short and long term (Moorman et al., 2023). Along the coast of Georgia, Moorman et al. (2023) found that there was only one site (Savannah) that showed some potential for resiliency to sea level rise based on vertical accretion and subsidence which is a subsurface process resulting in the sinking or loss of marshes. The other salt marshes along the Georgia coast, including a brackish marsh moving into tidal freshwater marsh did not show signs of resiliency to sea level rise based on vertical accretion and subsidence rates. The values that determined the resiliency of these marshes was based on the difference of accretion and subsidence rates while also incorporating the most recent sea level rise rates (Moorman et al., 2023). Vertical accretion is just one way to mitigate sea level rise on these marsh systems; transgression or migration to higher elevation is another response of vegetation (Morris et al., 2002; van Eerdt, 1985). However, this is only possible if there is land on which to migrate. Urban landscapes and anthropogenic structures present physical barriers to marsh migration which impacts all marsh systems to some extent (Baldwin, 2004), but tidal freshwater marshes are especially vulnerable to coastal development pressures and human impacts. Filling, dredging, habitat isolation, runoff, and the impoundment of upstream freshwater sources have the potential to cause a drastic shift in species composition or can alternatively convert these marshes to salt or brackish marshes (Baldwin, 2004; Ehrenfeld, 2000; Panno et al., 1999; Reinelt et al., 1998). Reduced freshwater flow can cause severe impacts on water quality (Anisfeld & Benoit, 1997),

and a reduction in above ground biomass (Solohin et al., 2020; O'Donnell & Schalles, 2016), to coastal communities as well as the rich biodiversity that tidal freshwater marshes contain (Neubauer, 2013).

Freshwater input is vital to tidal freshwater marshes, and important to other tidal marsh systems, as even salt-tolerant marsh vegetation is more productive under less saline conditions (Neubauer, 2013). Over a 28-year period, *Spartina alterniflora* marshes in Georgia experienced a loss of aboveground biomass of 33%, 35%, and 39% of the short, medium, and tall forms, respectively, due to drought and other abiotic drivers (O'Donnell & Schalles, 2016). Severe drought events (Palmer Drought Severity Index (PSDI) of -3.0 or below) can also cause biogeochemical and microbial changes in the marshes including oxidation of dissolved metabolites, lowered pH, increased iron reduction over sulfate reduction, induced nitrifying and denitrifying microbial activity, and increased metal availability (Palomo et al., 2013). It is predicted that with longer periods of drought, these conditions may worsen which could lead to a trickle-down effect throughout the ecosystem (Palomo et al., 2013).

Other severe weather events such as tropical storms also play a crucial role in the health of marshes. These events push salty water onto tidal freshwater marshes, with devastating impacts such as "salt burn", increased tidal action, and high wind velocities (Neyland, 2007). However, depending on the extent of the damage within the tidal freshwater marshes, recovery can be fairly rapid (Alper, 1992). The increase in sea level rise and tropical storm events could result in the increase of the 100-year flood events for coastal counties along the Southeastern United States to occur every 1 - 30 years based on location according to modeling techniques (Lin et al., 2019). This increase in flooding and tropical storm events could result in tidal freshwater marshes having difficulty recovering from these large-scale events. Much of the

damage to tidal marsh systems comes from erosion, flooding, and water ponding (Mo et al., 2020). These weather systems can also bring in other chemicals and pollutants which can decrease the belowground biomass and increase the rate of root decomposition (Mo et al., 2020).

1.3.2 Human Threats

Humans contribute to these threats both directly and indirectly. These impacts, at a small and large spatial scale (Gedan & Silliman, 2009), can have profound effects on marsh plant composition (Saintilan et al., 2014) and density (Charles & Dukes, 2009) which can lead to different habitat values in the form of ecosystem services, marsh complexity, and productivity (Gedan et al., 2009). Many different factors threaten marshes due to anthropogenic activities in combination with natural disturbances, creating a multipronged attack on different geographic scales. Studying these interactions on a variety of geographic scales is still in its infancy which slows our efforts to mitigate and prevent tidal marsh degradation and loss (Gilby et al., 2021). While humans contribute to sea level rise and climate change, coastal development is a direct anthropogenic effect. One of these industries, which has had a long history in Georgia since the 1800's is the paper and pulp industry (Dick & Johnson, 2000). The first paper plant along the Savannah River broke ground in 1936 and by 1946, just 10 years later, was known to be larger than 3 or 4 normal paper mills (Dick and Johnson). This helped spark industrialization in Savannah by supplying over 10,000 jobs. Over the years, while it has declined, paper and pulp still make up a good portion of the state's annual income bringing $5,403,251,193 US dollars to the state of Georgia and employ 15,619 people (Jolley et al., 2020). While beneficial for the economy, these mills have been linked to various types of pollutants that can negatively impact tidal marshes (Colodey & Wells, 1992). According to the United States Environmental Protection Agency (USEPA), arsenic, cadmium, chromium, copper, lead, nickel, and zinc are

some of the most common metal contaminants found in soil due to anthropogenic activities (Chintapenta et al., 2022; Olaniran et al., 2013). Many of these, plus other chemicals such as trichlorophenol and tetrachloroguicol, among others, have been shown to be related to the production of paper and pulp mills These heavy metals can lead to many issues within the environment and vegetation in the tidal marshes such as inhibited plant growth which eventually leads to plant death. Other industries also produce heavy metals such as transportation, farming, and sewage treatment (Järup, 2003). Tidal marsh species such as *Spartina alterniflora* and other native plant species can aid in the absorption of these heavy metals however there are complex interactions that determine the bioavailability (Chintapenta et al., 2022). Other differences were observed in vegetated and non-vegetated patches showing the importance of vegetated marshes in the uptake and storage of heavy metals (Chintapenta et al., 2022). If these heavy metals were not stored by marsh plants, they could impact human health (Järup, 2003). The reduction and loss of this ecosystem service due to the loss of tidal marsh extent could pose an increased threat of heavy metal contamination.

This complex relationship and interaction between sea level rise, drought, large-scale disturbance events, and the combination of coastal development and other anthropogenic activities, poses a unique and complex threat to tidal marshes and the people who rely on them for their numerous ecosystem services. In the United States, coastal counties, which contain only 10% of the country's land area, are home to over 40% of its population (128 million people) (NOAA, 2018). In Georgia, 585,700 people, or about 5.6% of all Georgians, live in these coastal counties and employ 280,444 people (NOAA, 2018) While it is a fairly small area of Georgia, these counties contribute $29.19 billion to the state's gross domestic product (GDP) and provide many products to the surrounding area including seafood (NOAA Coastal Economy, 2018). Each

coastal county within Georgia ranked at least a 10 on a social vulnerability score out of 14 based on a variety of factors such as exposure (e.g., temperature change, drought, flood), sensitivity (e.g., age group, poverty, occupation) and adaptive capacity (e.g., education, per capita income, irrigated land) but does not include things such as sea level rise and extreme weather events (Kc et al., 2015). If sea level rise and extreme events were examined similarly to previous studies above, the vulnerability index for these coastal counties may have increased (Hardy and Hauer, 2018).

1.4 Remote Sensing Approaches

Typical approaches to mapping vegetation composition include large field surveying methods that can quickly become expensive in time, money, and labor. This methodology also does not allow for as much area to be covered in a relatively short period of time. Remote sensing provides many advantages for tidal marsh mapping such as repeat coverage, cost effectiveness, it is less time-consuming, and it can cover large geographic areas (Ozesmi & Bauer, 2002). One of the main challenges of remote sensing for tidal marsh mapping is the spectral similarities between and within species, a problem exacerbated by lower spatial- and spectral-resolution satellite imagery (Ozesmi & Bauer, 2002). Remote sensing efforts in *S. alterniflora*-dominated marshes are complicated by the "*Spartina* Problem," which is the confusion between the different height forms of *S. alterniflora*, and additional spectral confusion between plants and mud (Hladik et al., 2013). The height continuum between *S. alterniflora* short, medium, and tall forms make it difficult to separate them depending on spatial resolution. *S. alterniflora* stems stand upright and result in mixed pixels with mud. Studies have also found issues with varying tidal water levels, as this interferes with the vegetation's spectral signals (Narron et al., 2022; Silvestri et al., 2005). Despite these drawbacks, previous research has

demonstrated the feasibility of accurately classifying and mapping both salt and brackish marshes using high-resolution aerial imagery, machine learning (random forest), LIDAR-derived digital elevation models (DEMs), and vegetation indices (Alexander & Hladik, 2015). Elevation information derived from DEMs have been used by multiple studies to separate vegetation by elevation range (Hladik et al., 2013; Zhang et al., 2018). Using aerial imagery, vegetation indices, and DEMs, Alexander and Hladik (2015) mapped salt and brackish marshes in Georgia with county-level overall accuracies ranging from 0.850 to 0.950. The study used the random forest classifier and found that DEM was one of the most important predictors of marsh class based on variable importance. Similar studies have been conducted in tidal freshwater marshes using high-resolution aerial imagery, a DEM, vegetation indices, and texture features which produced an overall accuracy of 0.846 when classifying all marsh types (Zhang et al., 2018). Zhang et al. (2018), also examined differences in a variety of machine learning classifiers where they found no significant difference between random forest, artificial neural networks, and support vector machines when the same dataset is used. When examining studies comparing different machine learning classifiers, random forest differs by less than 1 percent when compared to more complex classifiers such as artificial neural networks and support vector machines (Nitze et al., 2012).

These newer machine learning techniques have proven to be a significant improvement over more common supervised methods such as maximum likelihood which had a six percent difference from that of random forest (Nitze et al., 2012). In both satellite and aerial imagery, the number and quality of inputs make a difference in the overall accuracy of a study. Nitze et al, (2012) found that random forest was one of the worst classifiers among support vector machines and artificial neural networks when using a singular image (55.8 percent accuracy) but found

random forest to also be the best classifier when using a more robust input (87.4% accuracy). Zhang et al. (2018) where fewer inputs resulted in significantly lower accuracies, especially for random forest.

Studies have also frequently used freely available government satellite imagery to classify tidal marshes as they are typically free for the user and have a higher revisit rate than that of aerial imagery. Satellite imagery typically also has more spectral bands such as Sentinel-2's 13 spectral bands and Landsat 9's 11 spectral bands. These bands also cover a larger portion of the electromagnetic spectrum with Landsat having two thermal bands and Sentinel-2 having two shortwave infrared bands. The tradeoff is the obtainable spatial resolution for aerial imagery, depending on flight parameters and equipment, is much higher (0.15 – 2 m) than that of satellite imagery (10 – 30 m). Compared to freely available satellites, commercial satellites have a lower spectral resolution similar to that of aerial imagery but have a higher spatial resolution (< 1 – 5 m). The commercial satellite sensor used in this study, PlanetScope, has a 3 m spatial resolution and has a 4-band product similar to that of aerial imagery, and an 8-band product more similar to that of freely available satellites (Planet, 2021.).

PlanetScope has successfully been used to classify *Striga asiatica* (a small, parasitic weed) with an overall accuracy of 92%, in comparison to Sentinel-2's overall accuracy of 88% (Mudereri et al., 2019). PlanetScope has also been used previously to identify diseases in rice plants using vegetation indices with an accuracy of 75.6% (Shi et al., 2018). Moving towards tidal marshes, PlanetScope has been used along the coast of South Carolina to predict the above ground biomass of Spartina alterniflora with a Wilmott's index of agreement of 0.74 (Miller et al., 20190 While PlanetScope has been used to examine many ecosystems including cropland (Mudereri et al,, 2019; Shi et al., 2018), grasslands (Andreatta et al., 2022; Cheng et al., 2020),

and to some extent, tidal marshes (Miller et al., 2019; Purnamasari et al., 2021). While it has been used to examine these different habitats, we found no evidence that PlanetScope has been previously used to map tidal freshwater marsh species. However, studies using QuickBird imagery, which has similar spatial (2.8m) and spectral resolution (4-band) to PlanetScope, have been able to achieve results comparable to that of hyperspectral imagery (Belluco et al., 2006). This indicates that higher spatial resolution is important when mapping marsh species as it will reduce the number of mixed pixels. Newer PlanetScope imagery includes 8-band imagery which should allow for better spectral separability between vegetation classes and allow for more vegetation indices to be used for a random forest classification. In comparisons of commercial satellites (WorldView 2) to government-operated satellites such as Sentinel 2 and Landsat, the commercial satellites typically performed better with a difference in overall accuracy of 4 to 5 % (Shoko & Mutanga, 2017).

1.5 Study Area

This study will include the entire coastal region of Georgia, focusing on the three tidal marsh habitats (fresh, brackish, and salt). The Georgia coast has semidiurnal tides with a range of -0.24 m to 2.5 m (Fort Pulaski NOAA Tide Gauge: 8670870). Each of these environments offers a unique composition of both flora and fauna. In salt marshes, the dominant macrophyte is *Spartina alterniflora* which has three different height forms. The “short” form is typically found in the higher marsh which does not receive regular flooding and must be under 0.5 m in height. The “medium” form is found in the mid-marsh and ranges in height from 0.5 m and under 1.0 m. The “tall” form is recognized as anything over 1m and is typically found in the low marsh which sees regular flooding (Reimold, Gallagher, & Thompson, 1973; Hladik et al., 2013). Brackish marshes are dominated by *Juncus roemerianus*. These systems also contain *S. alterniflora* and

Spartina cynosuroides. However, there are many more species within these brackish systems depending on the area being sampled (Wieski et al., 2010.). Freshwater marshes tend to be the most complex and biodiverse as they have a wide variety of both flora and fauna, and species composition varies widely along the length of the coast (Więski et al., 2010).

This study, while encompassing the entire Georgia coast (Figure 1.1), will focus on the three largest rivers on the coast of Georgia: the Ogeechee, Altamaha, and Satilla Rivers (Figure 1.1). The Ogeechee River basin has an area of 8,415 km^2 and a median discharge of 61 m^3S^{-1} (Alber & Sheldon, 1999; Schaefer & Alber, 2007). The Altamaha River is the largest undammed river on the east coast and the largest coastal watershed in Georgia with an area of 35,112 km^2 and a median discharge of 250 m^3S^{-1} (Alber & Sheldon, 1999; Schaefer & Alber, 2007). The Satilla is the southernmost coastal watershed and the smallest with an area of 7,348 km^2 and a median discharge of 34 m^3S^{-1} (Alber & Sheldon, 1999; Schaefer & Alber, 2007). Salinity gradients vary across these three systems, but the community structures of their marshes are similar. *Spartina alterniflora* dominates the salt marshes, *Spartina cynosuroides and Juncus roemerianus* dominate brackish marshes, and *Zizaniopsis miliacea* dominates the tidal freshwater marshes. While these were the main species, there were others that were included in the classification when present in the watersheds which included: C*ladium jamaicense,* marsh meadow (*Batis maritima*, *Borrichia frutescens*, *Distichlis spicata*, and *Salicornia virginica*) *Schoenoplectus americanus*, *Schoenoplectus tabernaemontani*, and other non-marsh classes such as high reflectance, mud, and trees (Table 1.1).

1.6 Overview of Thesis

The overall goal of this project is to map the species distribution of all tidal marshes along the Georgia coast using remote sensing. In Chapter 2, I examine the use of high-resolution orthoimagery, in combination with DEMs and vegetation indices, to map salt, brackish, and tidal fresh marshes using the random forest classifier. In Chapter 3, I map species distributions in the three major tidal freshwater watersheds in Georgia using a single image of high-resolution PlanetScope imagery.

With the increasing threat of climate change and a predicted sea level rise of 10 to 12 inches along the East Coast of the United States in the next 30 years, it is of extreme importance to understand and monitor these areas. Remote sensing is an attractive technique, as it allows researchers to monitor large areas at a relatively low cost. This project will expand our understanding of tidal marsh remote sensing, especially tidal freshwater marshes. Creating a high-resolution aerial coast-wide classification will aid in the monitoring of tidal marshes. By creating an accurate classification of tidal marshes using PlanetScope imagery, a coast-wide classification could then be applied with the ability to monitor these areas at a higher frequency than before due to the high revisit time. These classifications can also be used to scale up ecosystem services and track the loss and gain of these vulnerable ecosystems.

1.7 References

Alber, M., & Sheldon, J. E. (1999). Use of a data-specific method to examine variability in the flushing time of Georgia estuaries. *Estuarine, Coastal and Shelf Science*, *49*(4), 469–482. https://doi.org/10.1006/ecss.1999.0515

Alexander, C. R., & Hladik, C. (2015). *High-Resolution Mapping of Vegetation, Elevation, Salinity and Bathymetry to Advance Coastal Habitat Management in Georgia* [Final Status Report].

Alper, J. (1992). Everglades Rebound From Andrew. *Science*, *257*(5078), 1852–1854. https://doi.org/10.1126/science.257.5078.1852

Andreatta, D., Gianelle, D., Scotton, M., & Dalponte, M. (2022). Estimating grassland vegetation cover with remote sensing: A comparison between Landsat-8, Sentinel-2 and

PlanetScope imagery. Ecological Indicators, 141, 109102. https://doi.org/10.1016/j.ecolind.2022.109102

Anisfeld, S. C., & Benoit, G. (1997). Impacts of Flow Restrictions on Salt Marshes: An Instance of Acidification. *Environmental Science & Technology*, *31*(6), 1650–1657. https://doi.org/10.1021/es960490o

Baden, S. P., Loo, L.-O., Pihl, L., & Rosenberg, R. (1990). Effects of eutrophication on benthic communities including fish: Swedish west coast. *AMBIO: A Journal of the Human Environment*.

Baldwin, A. H. (2004). Restoring complex vegetation in urban settings: The case of tidal freshwater marshes. *Urban Ecosystems*, *7*(2), 125–137. https://doi.org/10.1023/B:UECO.0000036265.86125.34

Barendregt, A. (2016). Tidal Freshwater Wetlands, the Fresh Dimension of the Estuary. In C. M. Finlayson, G. R. Milton, R. C. Prentice, & N. C. Davidson (Eds.), *The Wetland Book: II: Distribution, Description and Conservation* (pp. 1–14). Springer Netherlands. https://doi.org/10.1007/978-94-007-6173-5_103-2

Barendregt, A., & Swarth, C. W. (2013). Tidal Freshwater Wetlands: Variation and Changes. *Estuaries and Coasts*, *36*(3), 445–456. https://doi.org/10.1007/s12237-013-9626-z

Belluco, E., Camuffo, M., Ferrari, S., Modenese, L., Silvestri, S., Marani, A., & Marani, M. (2006). Mapping salt-marsh vegetation by multispectral and hyperspectral remote sensing. *Remote Sensing of Environment*, *105*(1), 54–67. https://doi.org/10.1016/j.rse.2006.06.006

Boström, C., Pittman, S., Simenstad, C., & Kneib, R. (2011). Seascape ecology of coastal biogenic habitats: Advances, gaps, and challenges. *Marine Ecology Progress Series*, *427*, 191–217. https://doi.org/10.3354/meps09051

Boyd, J., & Banzhaf, S. (2007). What Are Ecosystem Services? *Ecological Economics*, *63*(2–3), 616–626. https://doi.org/10.1016/j.ecolecon.2007.01.002

Burns, C. J., Alber, M., & Alexander, C. R. (2021). Historical changes in the vegetated area of salt marshes. *Estuaries and Coasts*, *44*(1), 162–177. https://doi.org/10.1007/s12237-020-00781-6

Cahoon, D. R., Day Jr., J. W., & Reed, D. J. (1999). The influence of surface and shallow subsurface soil processes on wetland elevation: A synthesis. *Current Topics in Wetland Biogeochemistry*, *3*, 72–88. USGS Publications Warehouse.

Campbell, A., & Wang, Y. (2019). High Spatial Resolution Remote Sensing for Salt Marsh Mapping and Change Analysis at Fire Island National Seashore. *Remote Sensing*, *11*(9), 1107. https://doi.org/10.3390/rs11091107

Charles, H., & Dukes, J. S. (2009). Effects of warming and altered precipitation on plant and nutrient dynamics of a New England salt marsh. *Ecological Applications*, *19*(7), 1758–1773. https://doi.org/10.1890/08-0172.1

Cheng, Y., Vrieling, A., Fava, F., Meroni, M., Marshall, M., & Gachoki, S. (2020). Phenology of short vegetation cycles in a Kenyan rangeland from PlanetScope and Sentinel-2. Remote Sensing of Environment, 248, 112004. https://doi.org/10.1016/j.rse.2020.112004

Chintapenta, L. K., Ommanney, K. I., & Ozbay, G. (2022). Presence and Plant Uptake of Heavy Metals in Tidal Marsh Wetland Soils. *Frontiers in Public Health*, *10*, 821892. https://doi.org/10.3389/fpubh.2022.821892

Colodey, A. G., & Wells, P. G. (1992). Effects of pulp and paper mill effluents on estuarine and marine ecosystems in Canada: A review. *JOURNAL OF AQUATIC ECOSYSTEM HEALTH*, *1*(3), 201–226. https://doi.org/10.1007/BF00044716

Correll, M. D., Hantson, W., Hodgman, T. P., Cline, B. B., Elphick, C. S., Gregory Shriver, W., Tymkiw, E. L., & Olsen, B. J. (2019). Fine-Scale Mapping of Coastal Plant Communities in the Northeastern USA. *Wetlands*, *39*(1), 17–28. https://doi.org/10.1007/s13157-018-1028-3

Cowardin, L. M., Carter, V., Golet, F. C., & LaRoe, E. T. (1979). *Classification of wetlands and deepwater habitats of the United States* (Report No. 79/31; FWS/OBS). USGS Publications Warehouse. http://pubs.er.usgs.gov/publication/2000109

Craft, C., Clough, J., Ehman, J., Joye, S., Park, R., Pennings, S., Guo, H., & Machmuller, M. (2009). Forecasting the effects of accelerated sea-level rise on tidal marsh ecosystem services. *Frontiers in Ecology and the Environment*, *7*(2), 73–78. https://doi.org/10.1890/070219

Crooks, S., Herr, D., Tamelander, J., Laffoley, D., & Vandever, J. (2011). Mitigating climate change through restoration and management of coastal wetlands and near-shore marine ecosystems: Challenges and opportunities. *Environment Department Papers,* 121(121).

Crosby, S. C., Sax, D. F., Palmer, M. E., Booth, H. S., Deegan, L. A., Bertness, M. D., & Leslie, H. M. (2016). Salt marsh persistence is threatened by predicted sea-level rise. *Estuarine, Coastal and Shelf Science*, *181*, 93–99. https://doi.org/10.1016/j.ecss.2016.08.018

Dick, S. E., & Johnson, M. D. (2000). The Smell of Money: The Pulp and Paper-Making Industry in Savannah, 1931-1947. *The Georgia Historical Quarterly*, *84*(2), 308–323.

Duarte, C. M., Dennison, W. C., Orth, R. J. W., & Carruthers, T. J. B. (2008). The charisma of coastal ecosystems: *Addressing the imbalance. Estuaries and Coasts*, 31(2), 233– 238. https://doi.org/10.1007/s12237-008-9038-7

Ehrenfeld, J. G. (2000). Evaluating wetlands within an urban context. *Ecological Engineering*, *15*(3–4), 253–265. https://doi.org/10.1016/S0925-8574(00)00080-X

Etheridge, J. (2013). Quantifying the water quality benefits ofa constructed brackish marsh and tidal stream system usingcontinuous water quality and flow monitoring. *PhD. Dissertation*, 512.

Fagherazzi, S., FitzGerald, D. M., Fulweiler, R. W., Hughes, Z., Wiberg, P. L., McGlathery, K. J., Morris, J. T., Tolhurst, T. J., Deegan, L. A., Johnson, D. S., Lesser, J. S., & Nelson, J. A. (2022). Ecogeomorphology of Salt Marshes. In *Treatise on Geomorphology* (pp. 445–464). Elsevier. https://doi.org/10.1016/B978-0-12-818234-5.00194-2

Feagin, R. A., Lozada-Bernard, S. M., Ravens, T. M., Möller, I., Yeager, K. M., & Baird, A. H. (2009). Does vegetation prevent wave erosion of salt marsh edges? *Proceedings of the National Academy of Sciences*, *106*(25), 10109–10113. https://doi.org/10.1073/pnas.0901297106

Fisher, B., Turner, R. K., & Morling, P. (2009). Defining and classifying ecosystem services for decision making. *Ecological Economics*, *68*(3), 643–653. https://doi.org/10.1016/j.ecolecon.2008.09.014

Gedan, K. B., Kirwan, M. L., Wolanski, E., Barbier, E. B., & Silliman, B. R. (2011). The present and future role of coastal wetland vegetation in protecting shorelines: Answering recent challenges to the paradigm. *Climatic Change*, *106*(1), 7–29. https://doi.org/10.1007/s10584-010-0003-7

Gedan, K. B., & Silliman, B. R. (2009). Patterns of salt marsh loss within coastal regions of North America: Presettlement to present. *Human Impacts on Salt Marshes: A Global Perspective*, 253–266.

Gedan, K. B., Silliman, B. R., & Bertness, M. D. (2009). Centuries of Human-Driven Change in Salt Marsh Ecosystems. *Annual Review of Marine Science*, *1*(1), 117–141. https://doi.org/10.1146/annurev.marine.010908.163930

Georgia Department of Natural Resources (n.d.) Salt marsh. https://coastalgadnr.org/salt-marsh

Gilby, B. L., Weinstein, M. P., Baker, R., Cebrian, J., Alford, S. B., Chelsky, A., Colombano, D., Connolly, R. M., Currin, C. A., Feller, I. C., Frank, A., Goeke, J. A., Goodridge Gaines, L. A., Hardcastle, F. E., Henderson, C. J., Martin, C. W., McDonald, A. E., Morrison, B. H., Olds, A. D., … Ziegler, S. L. (2021). Human actions alter tidal marsh seascapes and the provision of ecosystem services. *Estuaries and Coasts*, *44*(6), 1628–1636. https://doi.org/10.1007/s12237-020-00830-0

Gönnert, G., Dube, S., Murty, T. S., & Siefert, W. (2001). Global storm surges: Theory, observations and applications. *Kuste*, 581–623.

Greenberg, R., Maldonado, J. E., Droege, S., & McDONALD, M. V. (2006). Tidal marshes: A global perspective on the evolution and conservation of their terrestrial vertebrates. *BioScience*, *56*(8), 675. https://doi.org/10.1641/0006-3568(2006)56[675:TMAGPO]2.0.CO;2

Hardy, R. D., & Hauer, M. E. (2018). Social vulnerability projections improve sea-level rise risk assessments. *Applied Geography*, *91*, 10–20. https://doi.org/10.1016/j.apgeog.2017.12.019

Herbert, E. R., Schubauer-Berigan, J., & Craft, C. B. (2018). Differential effects of chronic and acute simulated seawater intrusion on tidal freshwater marsh carbon cycling. *Biogeochemistry*, *138*(2), 137–154. https://doi.org/10.1007/s10533-018-0436-z

Hladik, C., & Alber, M. (2014). Classification of salt marsh vegetation using edaphic and remote sensing-derived variables. *Estuarine, Coastal and Shelf Science*, *141*, 47–57. https://doi.org/10.1016/j.ecss.2014.01.011

Hladik, C., Schalles, J., & Alber, M. (2013). Salt marsh elevation and habitat mapping using hyperspectral and LIDAR data. *Remote Sensing of Environment*, *139*, 318–330. https://doi.org/10.1016/j.rse.2013.08.003

Järup, L. (2003). Hazards of heavy metal contamination. *British Medical Bulletin*, *68*(1), 167–182. https://doi.org/10.1093/bmb/ldg032

Jolley, G. J., Khalaf, C., Michaud, G. L., & Belleville, D. (2020). The economic contribution of logging, forestry, pulp & paper mills, and paper products: A 50-state analysis. *Forest Policy and Economics*, *115*, 102140. https://doi.org/10.1016/j.forpol.2020.102140

Kc, B., Shepherd, J. M., & Gaither, C. J. (2015). Climate change vulnerability assessment in Georgia. *Applied Geography*, *62*, 62–74. https://doi.org/10.1016/j.apgeog.2015.04.007

Kirwan, M. L., Guntenspergen, G. R., D'Alpaos, A., Morris, J. T., Mudd, S. M., & Temmerman, S. (2010). Limits on the adaptability of coastal marshes to rising sea level: Ecomorphic limits to wetland survival. *Geophysical Research Letters*, *37*(23), n/a-n/a. https://doi.org/10.1029/2010GL045489

Kirwan, M. L., & Mudd, S. M. (2012). Response of salt-marsh carbon accumulation to climate change. *Nature*, *489*(7417), 550–553. https://doi.org/10.1038/nature11440

Lin, H., Chen, M., Lu, G., Zhu, Q., Gong, J., You, X., Wen, Y., Xu, B., & Hu, M. (2013). Virtual Geographic Environments (VGEs): A New Generation of Geographic Analysis Tool. *Earth-Science Reviews*, *126*, 74–84. https://doi.org/10.1016/j.earscirev.2013.08.001

Loomis, M. J., & Craft, C. B. (2010). Carbon sequestration and nutrient (nitrogen, phosphorus) accumulation in river-dominated tidal marshes, Georgia, USA. *Soil Science Society of America Journal*, *74*(3), 1028–1036. https://doi.org/10.2136/sssaj2009.0171

Mazzocco, V., Hasan, T., Trandafir, S., & Uchida, E. (2022). Economic value of salt marshes under uncertainty of sea level rise: A case study of the Narragansett Bay. *Coastal Management*, *50*(4), 306–324. https://doi.org/10.1080/08920753.2022.2078174

Mcowen, C., Weatherdon, L., Bochove, J.-W., Sullivan, E., Blyth, S., Zockler, C., Stanwell-Smith, D., Kingston, N., Martin, C., Spalding, M., & Fletcher, S. (2017). A global map of saltmarshes. *Biodiversity Data Journal*, *5*, e11764. https://doi.org/10.3897/BDJ.5.e11764

Miller, G. J., Morris, J. T., & Wang, C. (2019). Estimating Aboveground Biomass and Its Spatial Distribution in Coastal Wetlands Utilizing Planet Multispectral Imagery. Remote Sensing, 11(17), 2020. https://doi.org/10.3390/rs11172020

Mo, Y., Kearney, M. S., & Turner, R. E. (2020). The resilience of coastal marshes to hurricanes: The potential impact of excess nutrients. *Environment International*, *138*, 105409. https://doi.org/10.1016/j.envint.2019.105409

Möller, I., Kudella, M., Rupprecht, F., Spencer, T., Paul, M., van Wesenbeeck, B. K., Wolters, G., Jensen, K., Bouma, T. J., Miranda-Lange, M., & Schimmels, S. (2014). Wave attenuation over coastal salt marshes under storm surge conditions. *Nature Geoscience*, *7*(10), 727–731. https://doi.org/10.1038/ngeo2251

Moorhead, K. K., & Brinson, M. M. (1995). Response of Wetlands to Rising Sea Level in the Lower Coastal Plain of North Carolina. *Ecological Applications*, *5*(1), 261–271. https://doi.org/10.2307/1942068

Moorman, M. C., Ladin, Z. S., Tsai, E., Smith, A., Bessler, A., Richter, J., Harrison, R., Van Druten, B., Stanton, W., Hayes, C., Harris, B. W., Hoff, M., Sasser, C., Wells, D. M., Tupacz, J., & Rankin, N. (2023). Will They Stay or Will They Go—Understanding South Atlantic Coastal Wetland Transformation in Response to Sea-Level Rise. *Estuaries and Coasts*. https://doi.org/10.1007/s12237-023-01225-7

Morris, J. T., Sundareshwar, P. V., Nietch, C. T., Kjerfve, B., & Cahoon, D. R. (2002). Responses of coastal wetlands to rising sea level. *Ecology*, *83*(10), 2869–2877. https://doi.org/10.1890/0012-9658(2002)083[2869:ROCWTR]2.0.CO;2

Mudereri, B. T., Dube, T., Adel-Rahman, E. M., Niassy, S., Kimathi, E., Khan, Z., & Landmann, T. (2019). A Comparative Analysis of PlanetScope and Senintel-2 Space-borne Sensor in Mapping Striga Weed using Guided Regularised Random Forest Classifcation Ensemble. *The International Archives of the Photogrammetry, Remote Sensing and Spatial Information Sciences*, *XLII-2/W13*, 701–708. https://doi.org/10.5194/isprs-archives-XLII-2-W13-701-2019

Murray, N. J., Worthington, T. A., Bunting, P., Duce, S., Hagger, V., Lovelock, C. E., Lucas, R., Saunders, M. I., Sheaves, M., Spalding, M., Waltham, N. J., & Lyons, M. B. (2022). High-resolution mapping of losses and gains of Earth's tidal wetlands. *Science*, *376*(6594), 744–749.

Narron, C. R., O'Connell, J. L., Mishra, D. R., Cotten, D. L., Hawman, P. A., & Mao, L. (2022). Flooding in Landsat across tidal systems (FLATS): An index for intermittent tidal

filtering and frequency detection in salt marsh environments. Ecological Indicators, 141, 109045. https://doi.org/10.1016/j.ecolind.2022.109045

Neubauer, S. C. (2013). Ecosystem Responses of a Tidal Freshwater Marsh Experiencing Saltwater Intrusion and Altered Hydrology. *Estuaries and Coasts*, *36*(3), 491–507. https://doi.org/10.1007/s12237-011-9455-x

Neubauer, S. C., & Craft, C. B. (n.d.). *GLOBAL CHANGE AND TIDAL FRESHWATER WETLANDS: SCENARIOS AND IMPACTS*.

Neyland, R. (2007). The Effects of Hurricane Rita on the Aquatic Vascular Flora in a Large Fresh-Water Marsh in Cameron Parish, Louisiana. *Castanea*, *72*(1), 1–7. https://doi.org/10.2179/0008-7475(2007)72[1:TEOHRO]2.0.CO;2

Nitze, I., Schulthess, U., & Asche, H. (2012). A Comparison of Machine Learning Algothrims Random Forest, Artifical Neural Network, and Support Vector Machine to Maximum Likelihood for Supervised Crop Type Classification. *GEOBIA*, 6.

National Oceanic and Atmospheric Administration (NOAA). Total Economy of Coastal Areas Data. Based on data from the Bureau of Labor Statistics and the Bureau of Economic Analysis. Charleston, SC: NOAA Office for Coastal Management.

O'Donnell, J. P. R., & Schalles, J. F. (2016). Examination of Abiotic Drivers and Their Influence on Spartina alterniflora Biomass over a Twenty-Eight Year Period Using Landsat 5 TM Satellite Imagery of the Central Georgia Coast. *Remote Sensing*, *8*(6), 477. https://doi.org/10.3390/rs8060477

Odum, W. E. (1988). Comparative ecology of tidal freshwater and salt marshes. *Annual Review of Ecology and Systematics*, *19*(1), 147–176. https://doi.org/10.1146/annurev.es.19.110188.001051

Olaniran, A., Balgobind, A., & Pillay, B. (2013). Bioavailability of Heavy Metals in Soil: Impact on Microbial Biodegradation of Organic Compounds and Possible Improvement Strategies. *International Journal of Molecular Sciences*, *14*(5), 10197–10228. https://doi.org/10.3390/ijms140510197

Ozesmi, S. L., & Bauer, M. E. (2002). Satellite remote sensing of wetlands. *Wetlands Ecology and Management*, *10*, 22.

Palomo, L., Meile, C., & Joye, S. B. (2013). Drought impacts on biogeochemistry and microbial processes in salt marsh sediments: A flow-through reactor approach. *Biogeochemistry*, *112*(1–3), 389–407. https://doi.org/10.1007/s10533-012-9734-z

Panno, S. V., Nuzzo, V. A., Cartwright, K., Hensel, B. R., & Krapac, I. G. (1999). Impact of urban development on the chemical composition of ground water in a fen-wetland complex. *Wetlands*, *19*(1), 236–245. https://doi.org/10.1007/BF03161753

Planet, 2021a. Planet Imagery Product Specification–June 2021. Planet Labs, Inc., San Francisco, CA, USA. Available online: https://assets.planet.com/docs/Planet_ PSScene_Imagery_Product_Spec_June_2021.pdf. (Accessed 23 December 2021).

Purnamasari, E., Kamal, M., & Wicaksono, P. (2021). Comparison of vegetation indices for estimating above-ground mangrove carbon stocks using PlanetScope image. Regional Studies in Marine Science, 44, 101730. https://doi.org/10.1016/j.rsma.2021.101730

Reed, D. J. (1995). The response of coastal marshes to sea-level rise: Survival or submergence? *Earth Surface Processes and Landforms*, *20*(1), 39–48. https://doi.org/10.1002/esp.3290200105

Reimold, R. J., Gallagher, J. L., & Thompson, D. E. (1973). Remote sensing of tidal marsh. Photogrammetric Engineering and Remote Sensing, 39,477–488.

Reinelt, L., Horner, R., & Azous, A. (1998). Impacts of urbanization on palustrine (depressional freshwater) wetlands—Research and management in the Puget Sound region. *Urban Ecosystems*, *2*(4), 219–236. https://doi.org/10.1023/A:1009532605918

Saintilan, N., Wilson, N. C., Rogers, K., Rajkaran, A., & Krauss, K. W. (2014). Mangrove expansion and salt marsh decline at mangrove poleward limits. *Global Change Biology*, *20*(1), 147–157. https://doi.org/10.1111/gcb.12341

Schaefer, S. C., & Alber, M. (2007). Temperature controls a latitudinal gradient in the proportion of watershed nitrogen exported to coastal ecosystems. *Biogeochemistry*, *85*(3), 333–346. https://doi.org/10.1007/s10533-007-9144-9

Seabrook, C. (2006). Tidal Marshes. In *New Georgia Encyclopedia*. Retrieved Mar 4, 2022, from https://www.georgiaencyclopedia.org/articles/geography-environment/tidal-marshes/.

Shepard, C. C., Crain, C. M., & Beck, M. W. (2011). The protective role of coastal marshes: A systematic review and meta-analysis. *PLoS ONE*, *6*(11), e27374. https://doi.org/10.1371/journal.pone.0027374

Shi, Y., Huang, W., Ye, H., Ruan, C., Xing, N., Geng, Y., Dong, Y., & Peng, D. (2018). Partial Least Square Discriminant Analysis Based on Normalized Two-Stage Vegetation Indices for Mapping Damage from Rice Diseases Using PlanetScope Datasets. Sensors, 18(6), 1901. https://doi.org/10.3390/s18061901

Shiau, Y.-J., Burchell, M. R., Krauss, K. W., Broome, S. W., & Birgand, F. (2019). Carbon storage potential in a recently created brackish marsh in eastern North Carolina, USA. *Ecological Engineering*, *127*, 579–588. https://doi.org/10.1016/j.ecoleng.2018.09.007

Shoko, C., & Mutanga, O. (2017). Examining the strength of the newly-launched Sentinel 2 MSI sensor in detecting and discriminating subtle differences between C3 and C4 grass species. *ISPRS Journal of Photogrammetry and Remote Sensing*, *129*, 32–40. https://doi.org/10.1016/j.isprsjprs.2017.04.016

Silvestri, S., Defina, A., & Marani, M. (2005). Tidal regime, salinity and salt marsh plant zonation. *Estuarine, Coastal and Shelf Science*, *62*(1), 119–130. https://doi.org/10.1016/j.ecss.2004.08.010

Solohin, E., Widney, S. E., & Craft, C. B. (2020). Declines in plant productivity drive loss of soil elevation in a tidal freshwater marsh exposed to saltwater intrusion. *Ecology*, *101*(12). https://doi.org/10.1002/ecy.3148

Sweet, W. V., Hamlington, B. D., Kopp, R. E., Weaver, C. P., Barnard, D., Brooks, W., Craghan, M., Dusek, G., Frederikse, T., Garner, G., Genz, A. S., Krasting, J. P., Larour, E., Marcy, D., Marra, J. J., Obeysekera, J., Osler, M., Pendleton, M., Roman, D., … Zuzak, C. (2022). Global and Regional Sea Level Rise Scenarios for the United States: Up dated Mean Projections and Extreme Water Level Probabilities Along U.S. Coastlines. *NOAA Technical Report NOS 01*, 111.

Thomas, R. F., Kingsford, R. T., Lu, Y., Cox, S. J., Sims, N. C., & Hunter, S. J. (2015). Mapping inundation in the heterogeneous floodplain wetlands of the Macquarie Marshes, using Landsat Thematic Mapper. *Journal of Hydrology*, *524*, 194–213. https://doi.org/10.1016/j.jhydrol.2015.02.029

Tong, F., Jaramillo, P., & Azevedo, I. M. L. (2015). Comparison of Life Cycle Greenhouse Gases from Natural Gas Pathways for Light-Duty Vehicles. *Energy & Fuels*, *29*(9), 6008–6018. https://doi.org/10.1021/acs.energyfuels.5b01063

Tortajada, C., Landry, C., Rodriguez, E. M., Meinzen-Dick, R., Moellendorf, S., Porras, I., Ratner, B., Shea, A., Swallow, B., Thomich, T., & Voutchkov, N. (1990). *Freshwater ecosystem services*. 43.

van Eerdt, M. M. (1985). The influence of vegetation on erosion and accretion in salt marshes of the Oosterschelde, The Netherlands. *Vegetatio*, *62*(1), 367–373. https://doi.org/10.1007/BF00044763

Vitousek, P. M., Aber, J. D., Howarth, R. W., Likens, G. E., Matson, P. A., Schindler, D. W., Schlesinger, W. H., & Tilman, D. G. (1997). Human alteration of the global nitrogen cycle: Sources and consequences. *Ecological Applications*, *7*(3), 737–750. https://doi.org/10.1890/1051-0761(1997)007[0737:HAOTGN]2.0.CO;2

Wiegert, R., & Freeman, B. (1990). Tidal salt marshes of the southeastern Atlantic coast: A community profile. *Biological Report*, *85*(7.29), 70. https://doi.org/10.2172/5032823

Wieski, K., Guo, H., Craft, C., & Pennings, S. (n.d.). *Ecosystem Functions of Tidal Fresh, Brackish, and salt Marshes on the Georgia Coast*. Retrieved October 18, 2021.

Woolf, W., & Kundell, J. (1990). Georgia wetlands: Values, trends, and legal status. *MERCER LAW REVIEW*, *41*, 53.

Zhang, C., Denka, S., & Mishra, D. R. (2018). Mapping freshwater marsh species in the wetlands of Lake Okeechobee using very high-resolution aerial photography and lidar data. *International Journal of Remote Sensing*, *39*(17), 5600–5618. https://doi.org/10.1080/01431161.2018.1455242

1.8 Tables and Figures

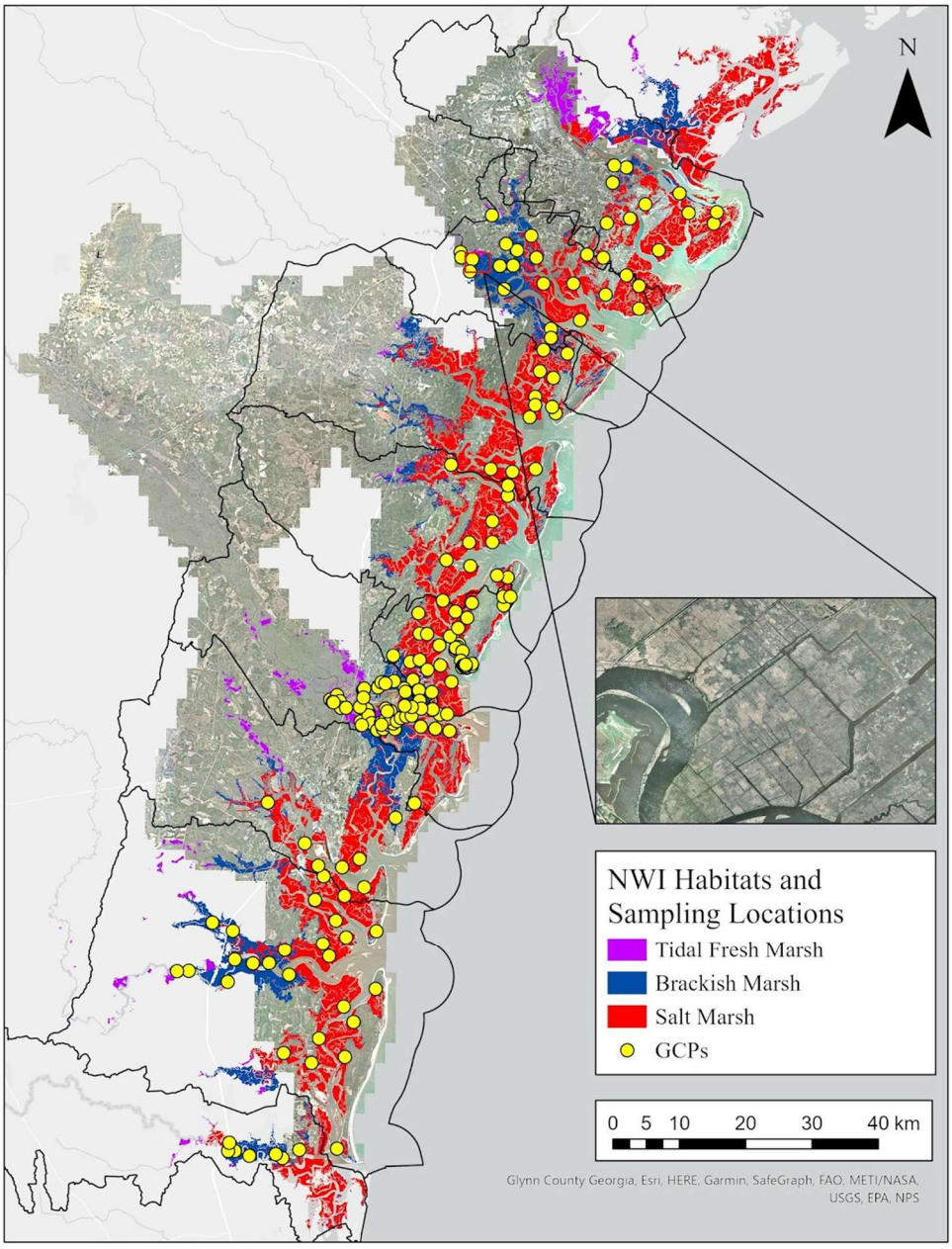

Figure 1.1 The study area (black outline representing HUCs) and field sampling locations (yellow circles) along the Georgia coast. The National Wetlands Inventory (NWI) habitat classes are also shown. The inset map shows one of our field sampling locations using high resolution (0.15 m) 2017 aerial imagery.

Table 1.1 A list of common ground cover species found during the Summer of 2022 field survey. Species are written with their common name along with which habitat type (salt brackish, or tidal fresh) in which they are found and the unique species code. These species are the basis for class assignments in Chapters 2 and 3. Within salt marshes, the dominant macrophyte is *Spartina alterniflora*, in brackish *Juncus roemerianus,* and in tidal freshwater marshes, *Zizaniopsis miliacea*.

Dominant Plant Type	Code	Common Name	NWI
Batis maritima	BAMA	Saltwort (Combined with MM)	Salt
Borrichia frutescens	BOFR	Sea Oxeye (Combined with MM)	Salt
Cladium jamaicense	CLJA	Sawgrass	Tidal Fresh
Forest	FORE	Forest	Upland
Distichlis spicata	DISP	Desert Saltgrass	Salt
Intertidal Mud/Creek Bank Mud	MUD	Intertidal Mud/Creek Bank Mud	All Habitats
Juncus roemerianus	JURO	Black Needlerush	Salt, Brackish
Marsh Meadow	MM	Marsh Meadow (SS, SAVI, BAMA, BOFR, DISP)	Salt
Salicornia virginica	SAVI	Pickleweed (Combined with MM)	Salt
Salt Pan	SALT	Salt Pan	Salt, Brackish
Sand/Beach	SAND	Sand/Beach	Salt, Brackish, Tidal Fresh
Schoenoplectus americanus	SCAM	Threesquare Bullrush	Brackish
Schoenoplectus tabernaemontani	SCTA	Softstem Bullrush	Brackish, Tidal Fresh
SHELL	SHELL	SHELL	Salt, Brackish, Tidal Fresh
Spartina alterniflora (Short)	SS	Smooth Cordgrass (Short)	Salt
Spartina alterniflora (Medium)	SM	Smooth Cordgrass (Medium)	Salt
Spartina alterniflora (Tall)	ST	Smooth Cordgrass (Tall)	Salt
Spartina cynosuroides	SPCY	Big Cordgrass	Brackish, Tidal Fresh
Zizaniopsis miliacea	ZIMI	Giant Cutgrass	Tidal Fresh

CHAPTER 2

CLASSIFICATION SALT, BRACKISH, AND TIDAL FRESH MARSHES OF GEORGIA USING HIGH-RESOLUTION AERIAL IMAGERY AND MACHINE LEARNING

2.1 Introduction

Tidal marshes are susceptible to many different threats such as sea level rise (Burns et al., 2021; Solohin et al., 2020), drought (Neubauer & Craft, 2009; Palomo et al., 2013), coastal development (Baldwin, 2004; Greenberg et al., 2006), and large-scale disturbance events (Mo et al., 2020). These threats can cause a variety of issues such as the reduction of marsh biomass (Mo et al., 2020; O'Donnell & Schalles, 2016) and the altering of natural biogeochemical processes (Palomo et al., 2013), which both cause a reduction in the ecosystem services that each of these marshes provides. This chapter details our efforts to classify the tidal marshes of the Georgia coast, USA using high-spatial resolution aerial orthorectified imagery, vegetation indices, a digital elevation model (DEM), and the National Wetlands Inventory (NWI) using a random forest classifier. We especially wanted to put an emphasis on tidal freshwater marsh classification and extent as these areas have historically been understudied (Barendregt & Swarth, 2013). These classification maps allow conservationists, government agencies, and scientists to study, teach and make important policy and management decisions about these ecosystems and scale-up ecosystem services (Macintyre et al., 2020).

Aerial imagery has been widely used in the classification of tidal marshes using a variety of classification techniques (probabilities, machine learning and deep learning) and a wide array

of predictor variables (DEM, NWI, texture, etc.) (Alexander & Hladik, 2015; Campbell & Wang, 2019; Correll et al., 2019; Hladik & Alber, 2014; Morgan et al., 2022; Zhang et al., 2018). The accuracies of these studies vary greatly depending on the predictor variables and the physical location of the study. A study in Florida was able to successfully map freshwater marsh species using high resolution aerial orthoimagery, DEM, and texture features but found one of the most important variables to be the DEM using the random forest classification method (Zhang et al., 2018). For the coast of Georgia, previous studies have been able to produce an overall accuracy of 90% for both salt and brackish marshes (Alexander & Hladik 2015). Alexander and Hladik (2015) used aerial orthoimagery, DEM, NWI, and vegetation indices while finding similar results to Zhang et al. (2018), in that the DEM proved to be the most important predictor variable. In order to keep continuity for classifications along the Georgia coast, this study will be done using similar methodologies and classes to that of Alexander and Hladik (2015). The study in this chapter does improve upon the 2015 classification by adding tidal freshwater marshes and by not grouping as many classes creating a more detailed and updated coast-wide classification.

2.2 Methods

2.2.1 Aerial Orthorectified Imagery and Other Data Sources

This study used multiple sources of remotely sensed imagery (Table 2.1). Multispectral aerial orthorectified imagery was obtained as part of the NOAA Coastal Georgia Imagery project (Office for Coastal Management, 2023) which was acquired between February 25, 2019, and March 13, 2019, and required nine flights for the collection of the entire coast (Atlantic, 2019). Imagery are freely available through the NOAA: Data Access Viewer (https://coast.noaa.gov/dataviewer). The aerial survey was targeted to be flown during low tide and cloud-free conditions. The 8-bit radiometric resolution imagery were collected with an

UltraCam Eagle digital aerial camera that has four bands in blue, green, red, and near-infrared (NIR) spectral regions with a spatial resolution of 15cm (vexcel-imaging.com). The reported horizontal accuracy was 0.37 m at the 90% circular error confidence level (Office for Coastal Management, 2023). These data were collected in the state plane coordinate system, North American Datum (NAD) 1983, Georgia East (EPSG: 26966) with units of US Survey feet. Imagery were converted to the Universal Transverse Mercator (UTM) zone 17 North, NAD 1983 (National Spatial Reference System of 2011) (EPSG: 6346) coordinate system with units of meters. This imagery came preprocessed using the Aerial Triangulation module using SimActive Correlator 3D by Atlantic Inc to create the othromosaiced product (Atlantic, 2019). Once the preprocessing was completed, the imagery had a horizontal root mean square error (RMSEx) of 0.182 m and a RMSEy of 0.124 m (Atlantic, 2019). Imagery from Camden County, Georgia was not collected as part of the Coastal Georgia Imagery aerial survey, and imagery from the National Agriculture Imagery Program (NAIP) was used to fill in the missing data gaps (US Department of Agriculture, 2008). NAIP imagery is freely available high-resolution spatial aerial imagery that is flown by the United States Department of Agriculture (USDA) during leaf-off conditions but is not tide-controlled (https://www.usgs.gov/centers/eros/science/). NAIP 2021 imagery was captured between October 7, 2021 – January 13, 2022, with 60-cm spatial resolution and at a relatively low tide condition based on exposed features known to be visible during lower tide conditions. NAIP imagery has a horizontal accuracy of +/- 4 with their 60-cm imagery and was downloaded in the Universal Transverse Mercator (UTM) zone 17 North, NAD 1983 (National Spatial Reference System of 2011) (EPSG: 6346) coordinate system with units of meters from the NOAA Data Access Viewer (coast.noaa.gov). The imagery was processed using Xpro orthorectification software to correct and orthorectify the imagery (OCM Partners, 2022).

This high-resolution imagery was used because of the high-spatial resolution and similar band combinations to that of the UltraCam Eagle, allowing for similar viewing and vegetation indices to be collected. For this study, all of the imagery were resampled to a 1 m spatial resolution. This was achieved by using ArcGIS Pro 3.0 and the resample tool. Within this tool, the cell size was set to a 1 m spatial resolution with all images being snapped to the DEM. The resampling technique was then set to the nearest neighbor in order to try and reduce the changing of pixel values (Lillesand et al., 2015)

The NAIP and UltraCam Eagle's high spatial resolution, in combination with ground reference data, allowing for the identification of tidal marshes vegetation at the species-level. The Coastal Georgia and Camden County NAIP datasets remained at their original resolutions of 0.15 m and 0.60 m, respectively, for interpretation and delineation of regions of interest (ROIs) but were then scaled to a common 1-m resolution for all classifications. The data was then split into the hydrological unit's code level 10 (HUC10). HUCs are delineated by the United States Geological Survey (USGS) based on hydrological features (USGS citation). These features can be broken into different levels (2, 4, 6, 8,10, and 12) where the lower numbers represent larger areas such as a basin, and the higher values represent smaller areas such as watersheds (level 10) and subbasins (level 12).

In addition to the high-resolution imagery, elevation information, and the National Wetlands Inventory (NWI) were used as predictor rasters in the classification. Due to the flooding and salinity tolerance on species distribution, elevation data collected using light detection and ranging (LiDAR)-derived DEM was used in tidal marsh classification (Alexander & Hladik, 2015; Hladik et al., 2013). The Lidar-derived DEM was obtained as part of the USGS Georgia statewide LiDAR survey was acquired using the NOAA: Data Access Viewer

(https://coast.noaa.gov/dataviewer) and was not corrected for vegetation bias (Hladik & Alber, 2012). All LIDAR data were collected between November 27, 2018, and April 24, 2019. The data were collected in the North American Datum (NAD) (2011) (ESPG: 6350) with the units of meters in the horizontal. In the vertical, the data were collected in the North American Vertical Datum (NADV) (1988) (ESPG: 5703) in meters GEOID 12B.The USGS reported a non-vegetated and vegetated accuracy of 7.2 cm and 18.69 cm RMSE at the 95th percentile, respectively, with an estimated point spacing of 0.5 m (OCM Partners, 2023). The NWI was downloaded from the United States Fish and Wildlife Service (USFWS) for the state of Georgia. When collected, the data were in the North American Datum (NAD) (1983) (EPSG: 6269). All of the data was then reprojected in the coordinate system Universal Transverse Mercator (UTM) zone 17 North, NAD 1983 (National Spatial Reference System of 2011) Georgia East (EPSG: 6346) coordinate system with a spatial resolution of 1 m to keep coordinate systems and spatial resolution consistent with the orthoimagery.

From the orthoimagery, vegetation indices were generated to aid in vegetation delineation (Alexander & Hladik, 2015). In order to determine which vegetation indices, I would use in my classification, I calculated 12 different indices and used variable importance from a random forest classification in R to determine which vegetation indices contributed most to the classification. Of those 12, half were chosen to be used as predictor variables in the final classification. Vegetation indices used were the Enhanced Vegetation Index (EVI) (Huete et al., 2002), Green Normalized Difference Vegetation Index (GNDVI) (Gitelson et al., 1996), Modified Soil-Adjusted Vegetation Index (MSAVI) (Qi et al., 1994), Modified Soil Ratio (MSR) (Chen, 1996), Normalized Difference Vegetation Index (NDVI) (Rouse et al., 1974), and Renormalized Difference Vegetation Index (RDVI) (Roujean & Breon, 1995). The vegetation

indices were used to aid in the separation of different vegetation species. This was especially true for the three height classes (short, medium, tall) of *Spartina alterniflora* as they are spectrally similar (Hladik et al., 2013). These marsh macrophytes are also influenced by elevation. For example, tall *S. alterniflora* is often found near the low creek bank edge in the low marsh, at a lower elevation, while the short S. alterniflora is often found at higher elevations in the high marsh (Wiegert, & Freeman, 1990). The NWI was also used to aid in the classification by providing the general marsh habitat (i.e., regularly-flood salt marsh, irregularly flooded brackish marsh, and tidal freshwater marsh)

2.2.2 Ground Reference Data

The inputs into the random forest classifier were the 1 m aerial imagery, DEM, NWI, and vegetation indices. The DEM, while being used in the model, is also being used to create a mask for the upland (using an elevation cutoff above 2.5 m) and water (elevation cuttoff below -0.8m) which removed most of the upland area and all of the water. The upland and water masks were then applied to all of the imagery in order to maintain the same extent which is required of the random forest classifier. This, along with the digitization of regions of interest (ROIs) were performed in ArcGIS Pro 3.0.0 (ESRI) using field data. These data were collected in the summer of 2022 using a Trimble 12 real time kinematic (RTK) GPS. In total, 811 ground control points were collected with species-level vegetation composition. These ROIs were split into 80 percent training and 20 percent validation using Google Colab (https://colab.research.google.com/). Once split, the ROIs were converted into point data to use in the random forest.

In total, 13 habitat classes were used in the high-resolution orthoimagery classification of Georgia salt, brackish, and tidal fresh marshes based on their spectral separability: *Cladium jamaicense*, intertidal mud, *Juncus roemerianus*, marsh meadow (which consisted of *Batis*

maritima, *Borrichia frutescens*, *Distichlis spicata*, and *Salicornia virginica*), high reflectance areas (salt pans, urban, shells, and beaches), *Schoenoplectus americanus*/*tabernaemontani*, S. alterniflora (Short, medium and tall), *Spartina cynosuroides*, trees (tidal forest and upland vegetation), and *Zizaniopsis miliacea* (Table 2.4). An additional class called submerged vegetation was included due to some of the aerial imagery being flooded during collection in the Ossabaw, Wassaw, St. Catherine's, and Sapelo HUCs. This class was composed largely of tall and medium *S. alterniflora* and was used to maintain relatively accurate extent information for each of the different marsh types. Note that all of the 13 classes were not present in each HUC that was classified. HUC units were classified separately and mosaiced together following post-classification procedures. In order to calculate the final overall accuracy, each class had to be given a unique value using the "reclassify" tool in ArcGIS Pro. Once these values were assigned, the mosaic tool was used to combine the classifications, and the merge tool to combine all ROI point data. Values were then extracted from the final classification using the "extract multi values from points" tool and then inputted into R in order to obtain the final results.

In order to determine differences in elevation at the species-level from the RTK survey, a Kruskal-Wallis test was run to determine differences between elevation among the different groups. If it was found to be significant, a post hoc Dunn's Test which is a pairwise comparison test to determine which group's elevations are statistically significant. Other summary statistics were also used to speak more broadly on differences in elevation between species and all statistical analysis was completed using R Studio. Significance was determined at the *p*-value level of 0.05.

2.2.3 Image Classification

This project used a supervised machine learning classifier called random forest (Breiman, 2001). These supervised classifications simply mean that it requires user input to train the model and in the case of this study, in the form of ROIs differentiating vegetation (Table 2.2). The random forest classifier works by producing decision trees that are individually based on a subset of the input training data. The final classification decision for each pixel is reached by taking the outputs from individual decision trees and assigning the majority class. This project used the *randomForest* package in R (Liaw & Wiener, 2001). The classification used the following raster predictor variables: 4-band aerial imagery, six vegetation indices (EVI, GNDVI, MSAVI, MSR, NDVI, RDVI), a DEM, and the NWI (Table 2.1). When setting the parameters of the random forest, it was set to produce 1000 trees which produced three variables being tried at each of the splits. The primary outputs of the random forest classification were an internal accuracy assessment using out-of-bag error, variable importance, and the classified raster. An additional accuracy assessment was performed using the reserved, external validation data. These are described in more detail below.

Once the classification was complete, pixel aggregation was implemented in order to remove the "salt and pepper" appearance. This was conducted in ArcGIS Pro using the majority filter tool where the 4 orthogonal cells are used to determine the value of the center cell (ESRI, Redlands). Once this was performed, the accuracy assessment was performed using the withheld 20% ROIs and the addition of the field collect ground reference points (Figure 2.1).

2.2.4 Accuracy Assessment and Variable Importance

Multiple calculations were performed after pixel aggregation in order to assess the accuracy of the Random Forest classification. Following the class aggregation, a confusion matrix was constructed in which the overall accuracy, producer's accuracy, user's accuracy, and

errors of omission and commission (Congalton, 1991) were calculated using the reserved (20%) validation ground control points. Along with this, the out-of-bag error was used as a quick assessment of model performance when determining the appropriate input variables, hyperparameters, and classes. The out-of-bag error is an internal estimate of the model's performance that is calculated using data that are not part of the bootstrapping method which involves taking repeated samples that are similar to the original dataset and running statistics to assess uncertainty. Another metric examined was variable importance which was constructed by calculating the mean decrease in accuracy (MDA), calculated by estimating the decrease in prediction error if a variable is removed from the classification (Breiman, 2001). Variable importance aided in the selection of predictor variables. In order to quantify variable importance, the mean MDA and rank values were averaged for each one of the HUC unit classifications. The final ranking was assigned based on the final mean rank.

2.3. Results

2.3.1 Ground Reference Data

As a part of the field sampling conducted in the Summer of 2022, RTK ground control points were collected and then summarized for the different classes as well as the different tidal marsh habitat types (salt, brackish, and tidal freshwater) (Table 2.3). Overall, many species that share the same habitat did not have significantly different RTK elevations (Table 2.4). *S. alterniflora* (short) and *S. alterniflora* (medium) are very close to the same elevation only being separated by 0.0037 m ($p = 1.00$) while the tall form is seen at a much lower mean elevation of 0.5912. which is a difference of 0.2653 m ($p = <0.0001$ for both forms) (Table 2.4). Other classes within the same habitat vary quite a bit such as *Z. miliacea* (0.7778 m) and *C. jamaicense* (0.9710 m) which is a difference of 0.1932 m ($p = 1.00$) (Table 2.4). Most species within the

same habitat type had a mean average elevation difference of at least 0.02 m (Table 2.4). It is important to note that some of the sample sizes are small within each class, but some were fixed when combining classes such as *S. americanus* (N = 23) and *S. tabernaemontani* (N = 8). Other small classes included salt pan (N = 11) and shell (N = 15) but were also combined to create the high reflectance ground cover class. Once combined, most classes had a sample size over 38 with the exception of *C. jamaicense* which has a small sample of 4 due to the species' small geographic extent in Georgia. Along with these general summary statistics, we found a significant difference in vegetation groups elevations using the Kruskal-Wallis test ($\chi^2 = 220.56$; df = 10; $p = 2.2e^{-16}$). Confirming this test significance, we moved to conduct a post hoc pairwise comparison Dunn's test. The Dunn's Test showed significant differences in marsh meadow and all other classes with the exception of *C. jamaicense* and the high reflectance class. Tall *Spartina alterniflora* showed a similar pattern with having significance in all classes with the exception of *C. jamaicense* and *Z. miliacea* (Figure 2.4).

2.3.2 Image Classification and Accuracy Assessment

The overall accuracy of the mosaiced Georgia coast orthoimagery and NAIP classification was 86.3% with individual class accuracies ranging from 98.3% for *J. roemerianus* to 43.4% for *S. cynosuroides* (Table 2.5), when assessed using the reserved external 20% validation ROIs. Most of the classes performed well with the exception of *S. cynosuroides* which was misclassified with *J. roemerianus* 34.3% of the time (Table 2.5). This caused a low producer accuracy of 43.4% but a relatively high user accuracy of 71.9% (Table 2.6). The three height forms of *S. alterniflora* accuracies ranged in class accuracy from 66.9% and 76.3% (Table 2.5). Within the individual classes, the different forms of *S. alterniflora* were often confused with each other. For example, *S. alterniflora* (short) was misclassified with *S. alterniflora* (medium)

25.6% of the time and *S. alterniflora* (medium) was confused with *S. alterniflora* (short) 12.4% of the time (Table 2.5). Other species that were commonly misclassified when found in the same HUC were *C. jamaicense* and *Z. miliacea* with *C. jamaicense* being misclassified 10.9% as *Z. miliacea*. Many of the misclassifications appear to correspond with lower spectral separability values (Table 2.7). For example, the medium form of *S. alternilfora* had a value (out of 2) of 0.749 and 0.805 when comparing the short and tall form respectively. While this did not have a value of 1.8 or greater, it is important to separate these classes ecologically as they have different levels of productivity and allow for the observation of small changes within the salt marshes. Another class that was misclassified, *C. jamaicense* and *Z. miliacea,* have a class separability of 0.596 (Table 2.7). While this is a very low spectral separability, other predictor variables such as elevation. These were important to keep as the goal of this study was to create an accurate and detailed tidal freshwater marsh classification. C. jamaicense, while only found in the St Andrew's and Cumberland sounds, appeared to be an abundant and important species to separate from the tidal freshwater marsh coast-wide dominant Z. miliacea. While spectrally similar, some classes may have differences in elevation that would allow for these species to be accurately mapped such as *Z. miliacea* (0.78m) and *C. jamaicense* (0.97 m).

When examining the classification, species distribution appears to correspond with expected spatial patterns and field observations. For example, *S. alterniflora* (tall) is often found near the creek edges and banks at lower elevations (0.5912 ± 0.2628 m), whereas *S. alterniflora* (medium) can be found mostly in the mid marsh (0.8565 ± 0.1796 m). *S. alterniflora* (short) (0.8528 ± 0.1146 m) and marsh meadow (a high marsh class) can be mainly found at higher elevations with the mean elevation of marsh meadow being 1.0630 ± 0.1156 m which is the highest mean elevation for all species (Table 2.4). Moving upstream to brackish marsh, a mixture

of *J. roemerianus*, *S. cynosuroides,* and *S. alterniflora* can be found where it transitions to mostly *J. roemerianus.* For three of the watersheds (Ossabaw, Altamaha, and Satilla), marshes transition to small extents of tidal freshwater marsh species such as *Z. miliacea* and *C. jamaicense* (only found in the Satilla watershed). Within these three watersheds, the distribution of tidal marsh types is not equal across the three watersheds (Table 2.8, Figure 2.2). The Ossabaw watershed has three times the amount of tidal fresh marshes (29.259 km^2) compared to the other HUCS (Table 2.8). The Altamaha and Satilla had 10.223 km^2 and 14.405 km^2 respectively. This is also the case for St Andrew's Sound as it has the highest amount of both salt and brackish water due to the overall size of the HUC unit itself. Proportionality, Sapelo Sound contained the most *S. alterniflora* species with over 50% of the area being classified as such and Cumberland having the largest proportion of *J. roemerianus.* The high reflectance (which includes urban areas and salt pans) and tree classes can both be seen in the marsh but often on the border of the high marsh species. These values were not included when calculating the total or proportional amount of salt, brackish, and tidal freshwater marshes (Table 2.8). *S. alterniflora* (medium) made up the largest area of the marsh species with an area of 593.6 km^2 excluding the submerged vegetation (Table 2.8). When the submerged vegetation is included in this value, *S. alterniflora* (medium) makes up an area of 665.9 km^2. If just examining the marsh species (excluding trees, high reflectance, and mud), the three height classes of *S. alterniflora*, with the addition of the submerged class, make up 66.1% of the tidal marshes. The main brackish marsh species, *J. roemerianus* makes up 19.1% of the total area and the tidal freshwater marsh species *Z. miliacea* makes up 3.1%. Of the entire image, when excluding non-marsh classes, typical salt marsh species make up 67.8%, brackish marshes 28.7%, and tidal freshwater marshes 3.5%.

2.3.3 Variable Importance

In order to determine the most important predictor variables, the mean decrease in accuracy was ranked in each watershed and the ranks were averaged across all of the watersheds (Table 2.9). DEM elevation, NWI, and the orthoimagery blue band were the three most important variables in tidal marsh mapping out of the 12 predictor variables selected (Table 2.9). The most important vegetation indices included EVI (mean rank of 4) and GNDVI (mean rank of 5) (Table 2.9). The variables with the lowest mean decrease in accuracy included MSR (mean rank of 12), NDVI (mean rank of 11), and a tie between the orthoimagery red band and RDV (mean rank of 10) (Table 2.9).

2.4 Discussion

2.4.1 Ground Reference Data

The lack of significant differences found between plant species elevation, may be partially related to the lack of points in some of the ground cover classes (Table 2.3). Once significance was determined with the Kruskal-Wallis test, Dunn's test was performed to determines the significance between different classes based on the elevation of ground reference data (Table 2.4). Table 2.4 shows that there are only two main ground cover classes, marsh meadow and *Spartina alterniflora* (tall), that are significantly different from all other ground covers. The medium and short forms of *Spartina alterniflora* show differences with other ground cover classes but not with each other which has been well documented in other studies (Hladik et al., 2013). The classes with fewer training and validation data had no statistical differences between other classes, possibly indicating there was an insufficient number of sampling points. This is especially true for *C. jamaicense* which was only found in one HUC and *S. americanus*

and *S. tabernaemontani* which was only found in three of the HUCs. Since both of these were not extensively sampled, it may have led to a wide array of elevation values which in turn would lead to some uncertainty. While the elevations may not have been separable between all species, the number and variety of predictor variable inputs may have allowed for accurate classification results. For example, both *Cladium jamaicense* and *Schoenoplectus americanus* and *S. tabernaemontani* were found to be spectrally different (Table 2.7). Additionally, other inputs such as the NWI may have accounted for the differences in habitat type (Table 2.1).

2.4.2 Image Classification and Accuracy Assessment

This study, to the authors' knowledge, is the most detailed attempt to use machine learning to classify the Georgia coast's tidal fresh, brackish, and salt marshes at a 1 m spatial resolution using orthoimagery, DEMs, NWI, and six vegetation indices (Table 2.1). We mapped 12 different cover classes (Figure 2.2) at the species-level using the random forest classifier with an overall accuracy of 86.3% (Table 2.4).

Other studies mapping tidal marshes obtained accuracies between 80 percent and 95 percent depending on the predictor variables used and geographic region (Campbell & Wang, 2019; Morgan et al., 2022; Thomas et al., 2015; Zhang et al., 2018). In a study most similar to the current project, Alexander and Hladik (2015) used orthoimagery, DEMs, NWI, and vegetation indices to map Georgia salt and brackish marshes with an overall accuracy of 90%. Our classification (Figure 3.2) expands on Alexander and Hladik (2015) by adding four species-level classes, separating *J. roemerianus/Shoenoplectus sp.* and *S. cynosuroides/S. tabernaemontari* into their own classes. Our classification also expanded the study domain to include tidal freshwater marsh classes. While tidal freshwater marshes make up a small extent of the coast, they provide numerous ecosystem services such as carbon sequestration, water quality

maintenance, flood and erosion control (Woolf & Kundell, 1990), and nutrient cycling (Tortajada et al., 1990). Class accuracies in Alexander and Hladik (2015) were similar except for S. *alterniflora* (tall), which had the lowest class producer's accuracy of 55% and was often misclassified with *S. alterniflora* (medium) (30%) and *J. roemerianus/Schoenoplectus spp.* (10%). In comparison to Alexander and Hladik (2015), our classification was able to classify S. alterniflora (tall) with a class accuracy of 72.3%, misclassified as *S. alterniflora* (medium) (11.9%) and *S. cynosuroides* (4.8%). Zhang et al. (2018) used high-resolution orthoimagery (30.48 cm) and DEMs to separate salt and freshwater marshes and to map nine freshwater marsh cover classes in Florida using various machine learning classifiers such as support vector machine, random forest, and artificial neural network. Classes included in Zang et al. (2018) (*C. jamaicense, Typha spp.,* S*alix caroliniana, Spartina bakeri, Polygonum spp., Phragmites austrakis,* Graminoid and swamp shrubland) were generally not comparable to the classes mapped in this study. Using the random forest classification, Zhang et al (2018) were able to produce an overall accuracy of 85.3% with all class accuracies performing over 75.8%. In this study, they found that the addition of spatial texture features was important and that a multi-temporal dataset could have been used to improve the overall accuracy of our study. Using broader land use and land cover classes in South Carolina, Morgan et al. (2022) mapped marsh, forest, urban, agriculture, and bare ground and compared machine learning and deep learning techniques using spectral bands from NAIP imagery. While using broad classes, bare ground was often misclassified as urban areas and parts of the marsh being misclassified as urban which could be due to salt pans and other highly reflective areas in marshes. The random forest classification had an overall accuracy of 76.4% which the authors said could be improved upon by using elevation data and spectral indices (Morgan et al., 2022).

In this study, one of the primary misclassifications was between the different forms of *S. alterniflora* which are most easily confused with each other. This has also been found across the other studies mentioned previously in which Alexander and Hladik (20 15) had a 55% accuracy for tall *S. alterniflora* (medium) which was confused 30% of the time with *S. alterniflora* (medium). This can also be seen in the short form where it was confused 15% of the time with the medium form of S. alterniflora. While the tall and short class of S. alterniflora have lower accuracies, misclassified pixels commonly stayed within the S. alterniflora species which reiterates the idea of the “Spartina Problem" (Hladik et al., 2013). There were also misclassifications among *S. cynosuroides* and *J. roemerianus* which could be due to a low spectral separability (0.902) and occupying similar habitats (Table 2.7) Their elevation may have also contributed to the misclassification as their mean elevation based on ground reference data differed by 0.0433 m and was not significantly different between the two species (Table 2.4). Their occupation of similar regions possibly contributed the most to confusion between classes. While the elevation between the two is only slightly different, it only requires a few centimeters to determine inundation frequency (Callaway et al., 1990; Silvestri et al., 2005; Suchrow and Jensen, 2010). Hladik et al. (2013) showed the importance of adding a DEM to their classification in order to classify marsh species based on height. Zhang et al. (2018) used different iterations of their classification in which the addition of a DEM improved the classification by 5.3% compared to just using aerial imagery and texture and by 20.2% when just using aerial imagery in freshwater marsh species.

We examined river discharge rates to better understand how freshwater inputs an effect on tidal marsh distributions may have, as river discharge has been found to have a positive relationship with tidal marsh extent (Rabalais & Turner, 2001). An increase in river discharge

can bring vital nutrients and higher sedimentation rates, which can influence tidal marsh health and extent (Rabalais & Turner, 2001; Cahhon et al., 1999; Schile et al., 2014). Another study found that freshwater tidal marshes respond positively with a 75% increase in net ecosystem productions while seeing a negative impact when these systems are exposed to salt water with a decrease of 55% in net ecosystem productions (Neubauer, 2013). When the areas experienced both the saline and freshwater treatment, no difference was found from the control.

We plotted river discharge from 1930 until 2022 using data from USGS river monitoring stations (Figures 2.5, 2.6, and 2.7). The Altamaha had the highest discharge with an average of 372.27 m^3/s (station 02226000). In the last year, the discharge of the river was 267.94 m^3/s which is still the highest of the rivers. The Ogeechee is the second highest with a few of 62.03 and within 2022 had the lowest discharge of 44.34 m^3/s (station 02202680). The lowest long-term flow rate but the second highest in 2022 was the Satilla with a discharge of 61.37 m^3/s and 48.17 m^3/s (station 0226362). Based on the values alone, it suggests that there are other mechanisms at work as one of the lowest extents had the highest discharge rate (Figure 2.7 and Table 2.8). These systems are also influenced by ocean tides which vary based on the location and which could also affect tidal freshwater marsh extent (Barendregt & Swarth, 2013). Tidal freshwater marshes, as well as other marshes, need freshwater flushing events but the river output also provides high sediment loads, vital nutrients, and other suspended matter (Barendregt & Swath, 2013). Other information that needs to be included to better understand tidal freshwater marsh extents would include the above metrics.

2.4.3 Variable Importance

As mentioned above, the most important predictor variables based on the mean decrease in accuracy were: (1) DEM, (2) NWI, and (3) Blue reflectance band. These results were

consistent with other studies using high-resolution aerial orthoimagery (Alexander & Hladik, 2015; Zhang et al., 2018). Elevation plays a large role in the distribution of tidal marsh species due to the hydrology of the area (Callaway et al., 1990; Silvestri et al., 2005; Suchrow and Jensen, 2010). Thus, DEM elevation plays a significant role in accurate classification. Of note, spectral bands that are typically important in vegetation classification such as the red and near-infrared bands, appear to make little impact on the classification based on variable importance (Table 2.9). Some of this may be attributed to the imagery not being atmospherically corrected. The atmospheric process considers atmospheric interference to give an accurate radiance or surface reflectance value (Emberton et al., 2015). Since this was not completed, and the pixel values were only as a digital number, the random forest classification may be required to use other means in order to delineate different vegetation species. This potentially explains the lack of importance in the different spectral bands and vegetation indices although more exploration is needed.

2.4.4 Significance and Future Work

With this classification, there are many potential uses across the Georgia coast. High resolution imagery can be used to better understand ecosystem services, as different plant communities contribute to different ecosystem services. Deverel et al, (2016), used similar vegetation maps to assess different ecosystem services such as carbon storage and flood regulation. These vegetation maps can also be used to conduct time change analysis to understand long-term changes in marshes and relate changes in species composition and marsh extent to anthropogenic land use and land cover change (Deverel et al, 2016; Mukhopadhyay et al., 2018). Future work could use this imagery to scale above and below ground biomass and be used in a long term analysis to explain losses and gains based on environmental factors (McKee

et al., 2007; O'Connel et al., 2021 The advantage of using high-resolution aerial orthoimagery compared to lower resolution imagery, is that the smaller pixel sizes reduce the mixed pixel effects that can be seen when using lower spatial resolution data but does not eliminate these issues (Ozesmi & Bauer, 2002).

2.5 Conclusion

This study shows that an accurate coast-wide classification using 4-band high resolution ortho imagery is possible across salt, brackish, and tidal freshwater marshes. We were able to map 12 different marsh and upland classes with an overall accuracy of 86.3%. This classification was able to add upon existing classifications by providing more detailed classes and adding tidal freshwater marshes to the classification. With these known tidal marsh extents, ecosystem services can now be scaled and applied to the entire coast. Other studies can include time change analysis to see how vegetation has changed within the tidal marshes of Georgia. This will also hopefully promote the continued aerial monitoring of the Georgia coast.

2.6 References

Alexander, C. R., & Hladik, C. (2015). High-Resolution Mapping of Vegetation, Elevation, Salinity and Bathymetry to Advance Coastal Habitat Management in Georgia [Final Status Report].

Atlantic. (2019). NOAA Coastal Georgia Imagery Project Report (No. 17079; p. 32).

Baldwin, A. H. (2004). Restoring complex vegetation in urban settings: The case of tidal freshwater marshes. Urban Ecosystems, 7(2), 125–137. https://doi.org/10.1023/B:UECO.0000036265.86125.34

Barendregt, A., & Swarth, C. W. (2013). Tidal Freshwater Wetlands: Variation and Changes. Estuaries and Coasts, 36(3), 445–456. https://doi.org/10.1007/s12237-013-9626-z

Breiman, L. (2001). Random Forests. Machine Learning, 45, 5–32.

Burns, C. J., Alber, M., & Alexander, C. R. (2021). Historical changes in the vegetated area of salt marshes. Estuaries and Coasts, 44(1), 162–177. https://doi.org/10.1007/s12237-020-00781-6

Callaway, R. M., Jones, S., Ferren Jr., W. R., & Parikh, A. (1990). Ecology of a mediterranean-climate estuarine wetland at Carpinteria, California: Plant distributions and soil salinity in the upper marsh. *Canadian Journal of Botany*, *68*(5), 1139–1146. https://doi.org/10.1139/b90-144

Campbell, A., & Wang, Y. (2019). High Spatial Resolution Remote Sensing for Salt Marsh Mapping and Change Analysis at Fire Island National Seashore. Remote Sensing, 11(9), 1107. https://doi.org/10.3390/rs11091107

Chen, J. M. (1996). Evaluation of Vegetation Indices and a Modified Simple Ratio for Boreal Applications. Canadian Journal of Remote Sensing, 22(3), 229–242. https://doi.org/10.1080/07038992.1996.10855178

Congalton, R. G. (1991). A review of assessing the accuracy of classifications of remotely sensed data. Remote Sensing of Environment, 37(1), 35–46. https://doi.org/10.1016/0034-4257(91)90048-B

Deverel, S. J., Ingrum, T., & Leighton, D. (2016). Present-day oxidative subsidence of organic soils and mitigation in the Sacramento-San Joaquin Delta, California, USA. *Hydrogeology Journal*, *24*(3), 569–586. https://doi.org/10.1007/s10040-016-1391-1

Emberton, S., Chittka, L., Cavallaro, A., & Wang, M. (2015). Sensor Capability and Atmospheric Correction in Ocean Colour Remote Sensing. *Remote Sensing*, *8*(1), 1. https://doi.org/10.3390/rs8010001

Gitelson, A. A., Kaufman, Y. J., & Merzlyak, M. N. (1996). Use of a green channel in remote sensing of global vegetation from EOS-MODIS. Remote Sensing of Environment, 58(3), 289–298. https://doi.org/10.1016/S0034-4257(96)00072-7

Greenberg, R., Maldonado, J. E., Droege, S., & McDONALD, M. V. (2006). Tidal marshes: A global perspective on the evolution and conservation of their terrestrial vertebrates. BioScience, 56(8), 675. https://doi.org/10.1641/0006-3568(2006)56[675:TMAGPO]2.0.CO;2

Hladik, C., & Alber, M. (2012). Accuracy assessment and correction of a LIDAR-derived salt marsh digital elevation model. Remote Sensing of Environment, 121, 224–235. https://doi.org/10.1016/j.rse.2012.01.018

Hladik, C., Schalles, J., & Alber, M. (2013). Salt marsh elevation and habitat mapping using hyperspectral and LIDAR data. Remote Sensing of Environment, 139, 318–330. https://doi.org/10.1016/j.rse.2013.08.003

Huete, A., Didan, K., Miura, T., Rodriguez, E. P., Gao, X., & Ferreira, L. G. (2002). Overview of the radiometric and biophysical performance of the MODIS vegetation indices. Remote Sensing of Environment, 83(1–2), 195–213. https://doi.org/10.1016/S0034-4257(02)00096-2

Liaw, A., & Wiener, M. (2001). Classification and Regression by RandomForest. R News, 2, 18–22.

Lillesand, T. M., Kiefer, R. W., & Chipman, J. W. (2015). Remote sensing and image interpretation (7th ed.). Wiley.

Macintyre, P., van Niekerk, A., & Mucina, L. (2020). Efficacy of multi-season Sentinel-2 imagery for compositional vegetation classification. International Journal of Applied Earth Observation and Geoinformation, 85, 101980. https://doi.org/10.1016/j.jag.2019.101980

McKee, K. L., Cahoon, D. R., & Feller, I. C. (2007). Caribbean mangroves adjust to rising sea level through biotic controls on change in soil elevation. *Global Ecology and Biogeography*, *16*(5), 545–556. https://doi.org/10.1111/j.1466-8238.2007.00317.x

Mo, Y., Kearney, M. S., & Turner, R. E. (2020). The resilience of coastal marshes to hurricanes: The potential impact of excess nutrients. Environment International, 138, 105409. https://doi.org/10.1016/j.envint.2019.105409

Morgan, G. R., Wang, C., Li, Z., Schill, S. R., & Morgan, D. R. (2022). Deep Learning of High-Resolution Aerial Imagery for Coastal Marsh Change Detection: A Comparative Study. ISPRS International Journal of Geo-Information, 11(2), 100. https://doi.org/10.3390/ijgi11020100

Mukhopadhyay, A., Hornby, D. D., Hutton, C. W., Lázár, A. N., Amoako Johnson, F., & Ghosh, T. (2018). Land Cover and Land Use Analysis in Coastal Bangladesh. In R. J. Nicholls, C. W. Hutton, W. N. Adger, S. E. Hanson, Md. M. Rahman, & M. Salehin (Eds.), *Ecosystem Services for Well-Being in Deltas* (pp. 367–381). Springer International Publishing. https://doi.org/10.1007/978-3-319-71093-8_20

Neubauer, S. C., & Craft, C. B. (2009). Global change and tidal freshwater wetlands: Scenarios and impacts. In Tidal Freshwater Wetlands. Margraf Publishers GmbH.

OCM Partners. (2022). OCM Partners, 2023: 2021 Georgia NAIP 4-Band 8 Bit Imagery from 2021-10-05 to 2022-10-55. NOAA National Centers for Environmental Information, https://www.fisheries.noaa.gov/inport/item/68396.

OCM Partners, 2023: 2018 - 2019 USGS Lidar: GA Statewide from 2010-06-15 to 2010-08-15. NOAA National Centers for Environmental Information, https://www.fisheries.noaa.gov/inport/item/67264.

O'Connell, J. L., Mishra, D. R., Alber, M., & Byrd, K. B. (2021). BERM: A Belowground Ecosystem Resiliency Model for estimating Spartina alterniflora belowground biomass. New Phytologist, 232(1), 425–439. https://doi.org/10.1111/nph.17607

O'Donnell, J., & Schalles, J. (2016). Examination of abiotic drivers and their influence on Spartina alterniflora biomass over a twenty-eight year period using Landsat 5 TM satellite imagery of the central Georgia coast. Remote Sensing, 8(6), 477. https://doi.org/10.3390/rs8060477

Office for Coastal Management, 2023: 2018 Coastal Georgia 4-Band 8 Bit Imagery from 2010-06-15 to 2010-08-15. NOAA National Centers for Environmental Information, https://www.fisheries.noaa.gov/inport/item/55001.

Ozesmi, S. L., & Bauer, M. E. (2002). Satellite remote sensing of wetlands. Wetlands Ecology and Management, 10, 22.

Palomo, L., Meile, C., & Joye, S. B. (2013). Drought impacts on biogeochemistry and microbial processes in salt marsh sediments: A flow-through reactor approach. Biogeochemistry, 112(1–3), 389–407. https://doi.org/10.1007/s10533-012-9734-z

Qi, J., Chehbouni, A., Huete, A. R., Kerr, Y. H., & Sorooshian, S. (1994). A modified soil adjusted vegetation index. Remote Sensing of Environment, 48(2), 119–126. https://doi.org/10.1016/0034-4257(94)90134-1

Rabalais, N. N., & Turner, R. E. (2001). Hypoxia in the northern Gulf of Mexico: Description, causes and change. In N. N. Rabalais & R. E. Turner (Eds.), *Coastal and Estuarine Studies* (Vol. 58, pp. 1–36). American Geophysical Union. https://doi.org/10.1029/CE058p0001

Roujean, J.-L., & Breon, F.-M. (1995). Estimating PAR absorbed by vegetation from bidirectional reflectance measurements. Remote Sensing of Environment, 51(3), 375–384. https://doi.org/10.1016/0034-4257(94)00114-3

Rouse, J. W., Haas, R. H., Schell, J. A., & Deering, D. W. (1974). Monitoring vegetation systems in the Great Plains with ERTS. NASA Spec. Publ, 351(1), 309.

Schile, L. M., Callaway, J. C., Morris, J. T., Stralberg, D., Parker, V. T., & Kelly, M. (2014). Modeling Tidal Marsh Distribution with Sea-Level Rise: Evaluating the Role of

Vegetation, Sediment, and Upland Habitat in Marsh Resiliency. *PLoS ONE*, *9*(2), e88760. https://doi.org/10.1371/journal.pone.0088760

Silvestri, S., Defina, A., & Marani, M. (2005). Tidal regime, salinity and salt marsh plant zonation. *Estuarine, Coastal and Shelf Science*, *62*(1), 119–130. https://doi.org/10.1016/j.ecss.2004.08.010

Solohin, E., Widney, S. E., & Craft, C. B. (2020). Declines in plant productivity drive loss of soil elevation in a tidal freshwater marsh exposed to saltwater intrusion. Ecology, 101(12). https://doi.org/10.1002/ecy.3148

Suchrow, S., & Jensen, K. (2010). Plant Species Responses to an Elevational Gradient in German North Sea Salt Marshes. *Wetlands*, *30*(4), 735–746. https://doi.org/10.1007/s13157-010-0073-3

Thomas, R. F., Kingsford, R. T., Lu, Y., Cox, S. J., Sims, N. C., & Hunter, S. J. (2015). Mapping inundation in the heterogeneous floodplain wetlands of the Macquarie Marshes, using Landsat Thematic Mapper. *Journal of Hydrology*, *524*, 194–213. https://doi.org/10.1016/j.jhydrol.2015.02.029

U.S. Geological Survey. (2018, May 10). Hydrological Unit Maps. https://www.usgs.gov/tools/hydrologic-unit-maps.

Wiegert, R., & Freeman, B. (1990). Tidal salt marshes of the southeastern Atlantic coast: A community profile. Biological Report, 85(7.29), 70. https://doi.org/10.2172/5032823

Zhang, C., Denka, S., & Mishra, D. R. (2018). Mapping freshwater marsh species in the wetlands of Lake Okeechobee using very high-resolution aerial photography and lidar data. *International Journal of Remote Sensing*, *39*(17), 5600–5618. https://doi.org/10.1080/01431161.2018.1455242

2.7 Tables and Figures

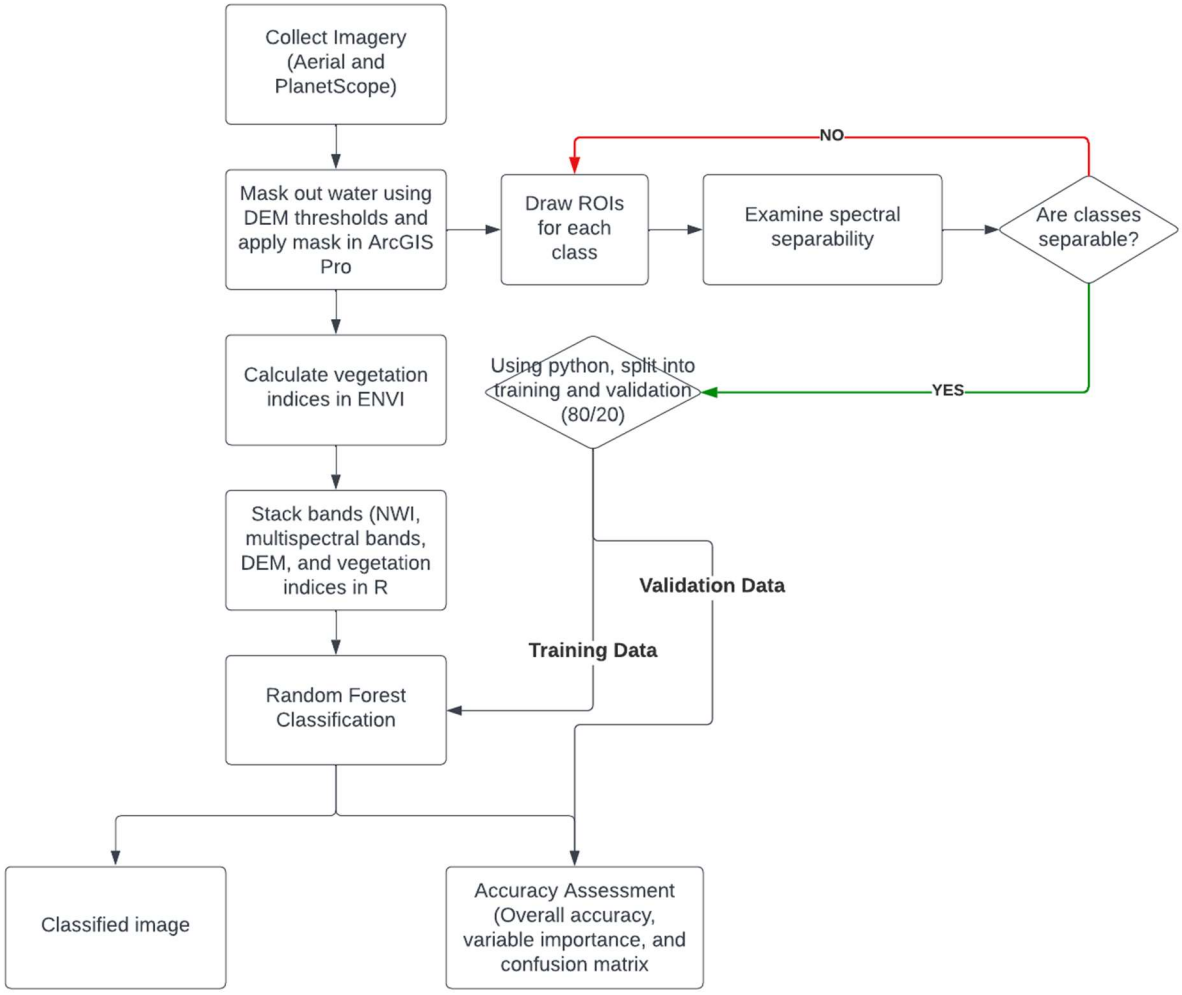

Figure 2.1 Workflow of our random forest classification of the aerial orthoimagery.

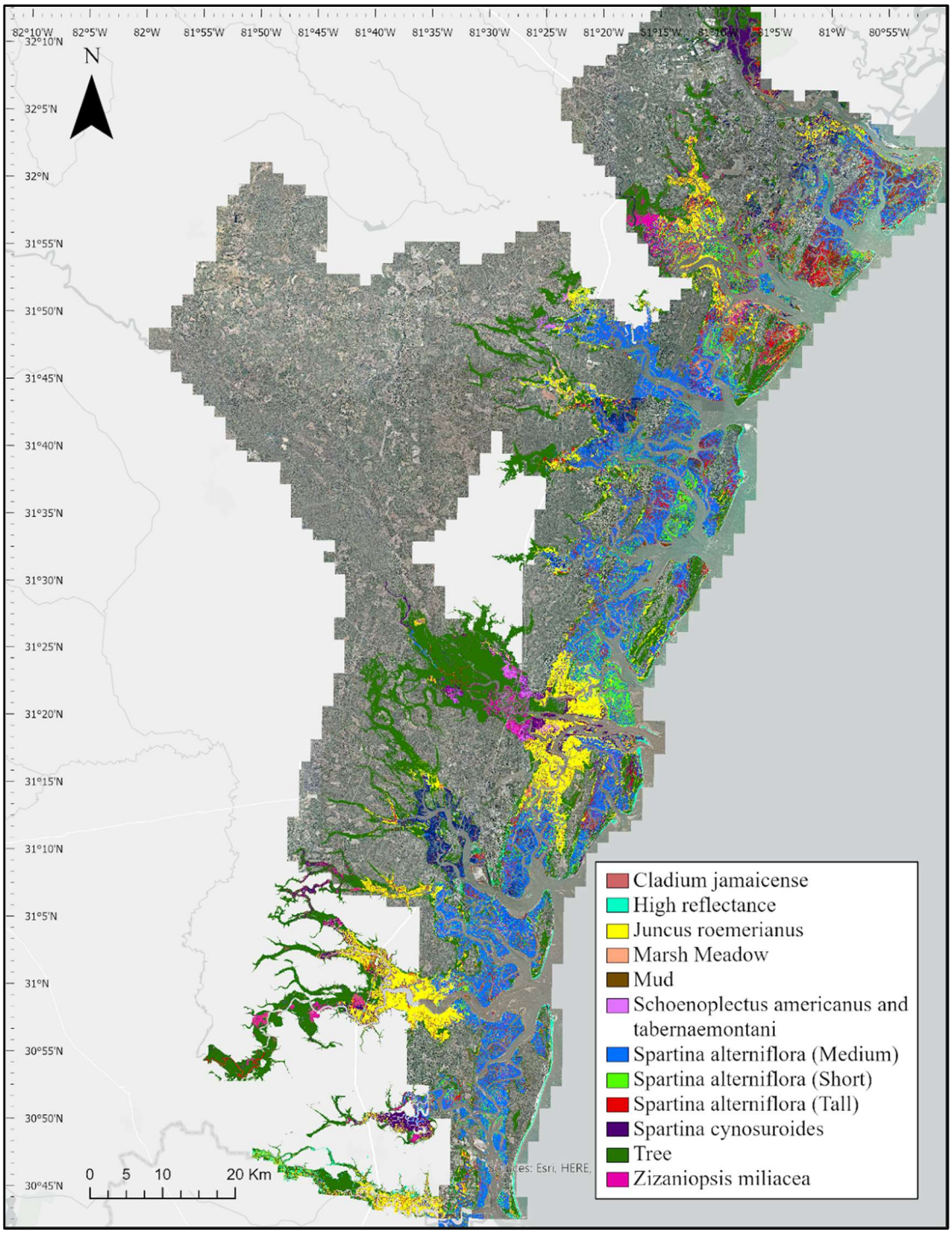

Figure 2.2 Final random forest classified imagery for the Georgia coast using 1 m aerial orthoimagery with 12 different dominant classes. The overall classification was 86.3%. The classified image was smoothed using a majority filter in ArcGIS Pro prior to the final accuracy assessment.

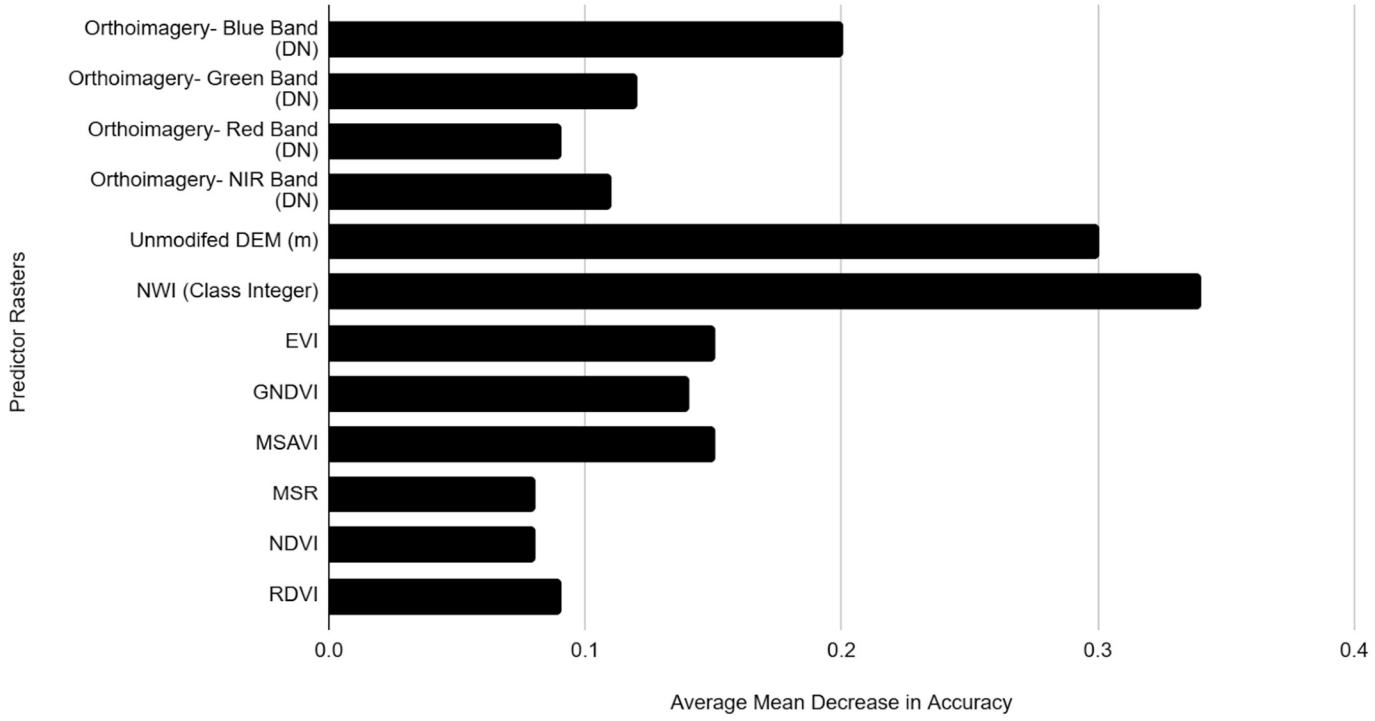

Figure 2.3 The average mean decrease in accuracy that was averaged per HUC unit for each of the predictor variables and then given a rank which was based on the mean rank. The most important predictors of the classification included a NIW, DEM, and the Orthoimagery blue band.

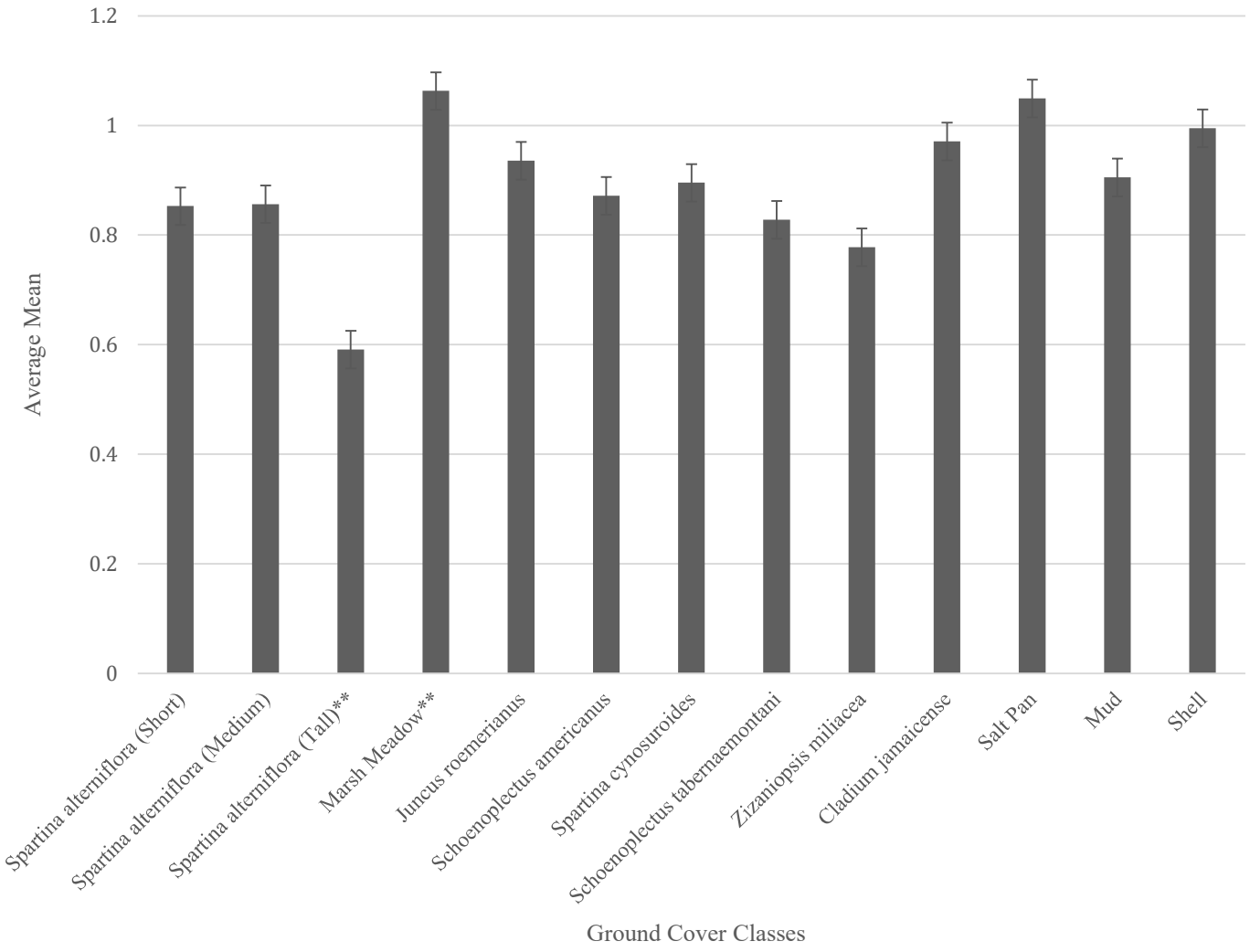

Figure 2.4 The average mean of the different ground cover classes using RTK points with standard error bars. The "**" next to the ground cover classes represents classes that were statistically different from most or all the other ground cover species.

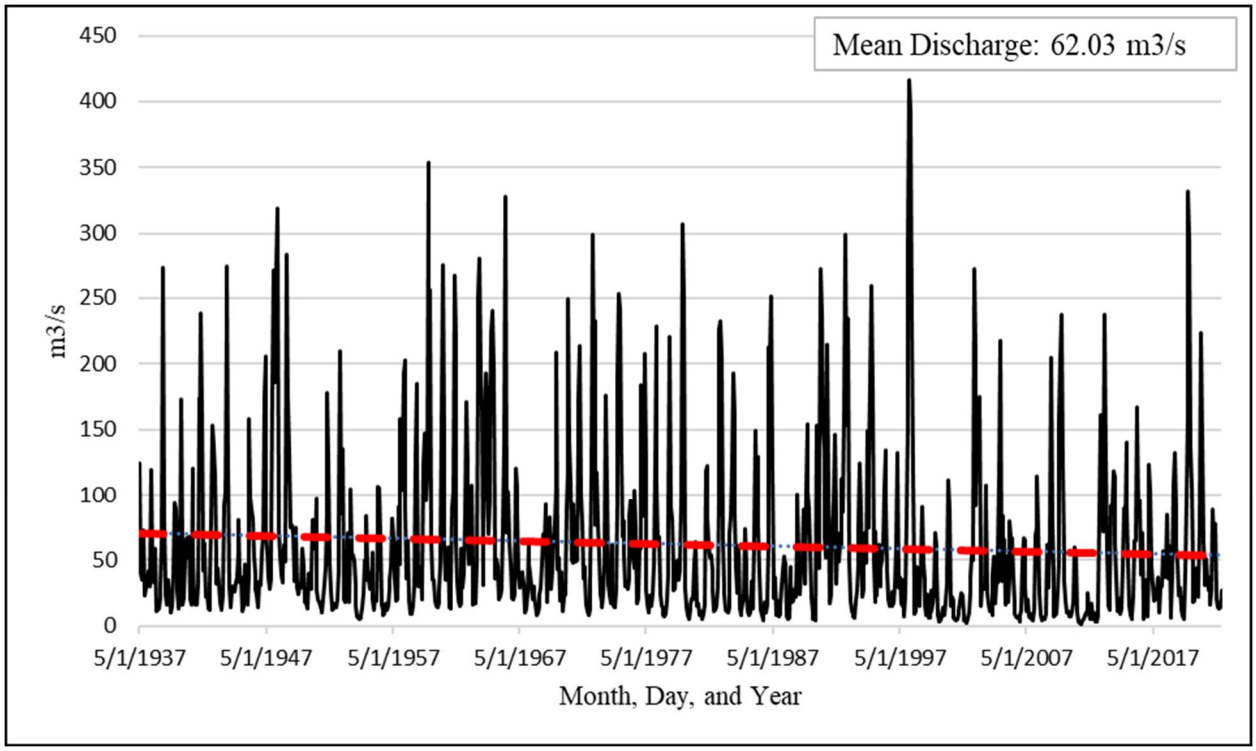

Figure 2.5 The discharge rate over an 85-year period for the Ogeechee River. The mean average water discharge rate is 62.02 m^3s (station 02202680).

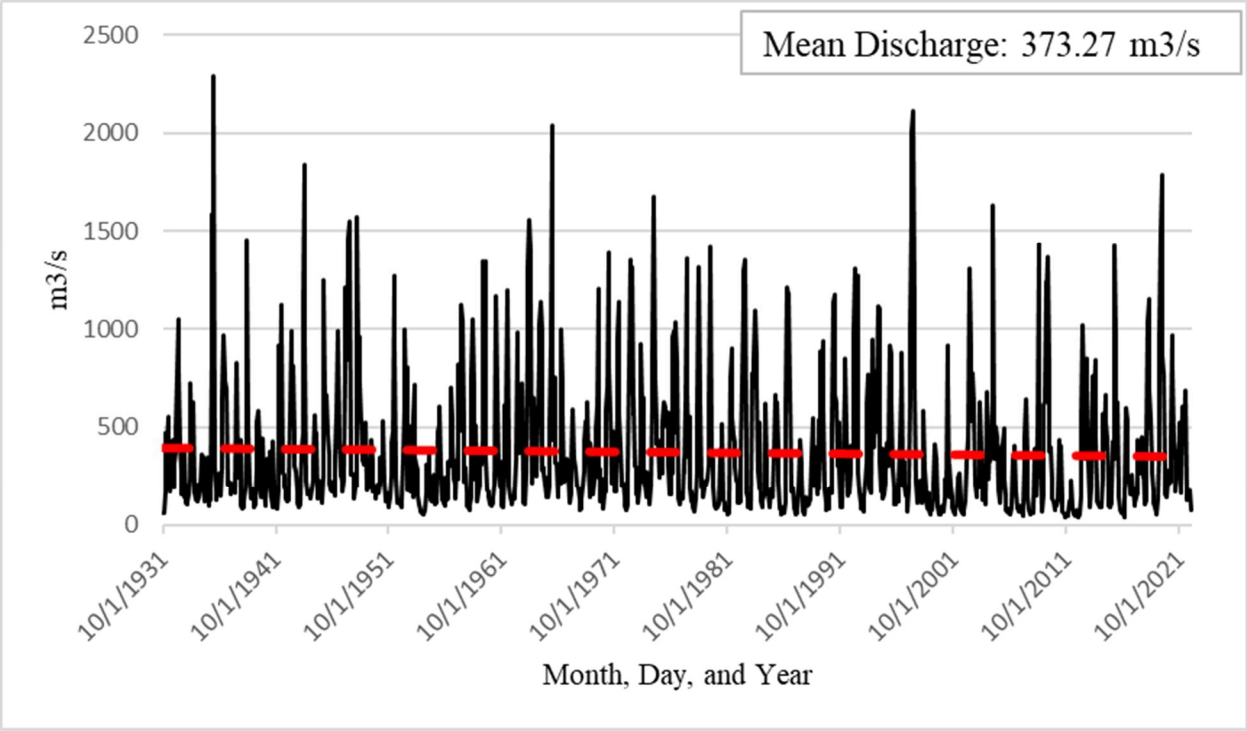

Figure 2.6 The discharge rate over a 92-year period for the Altamaha River. The mean average water discharge rate is 373.27 m^3s (station 02226000).

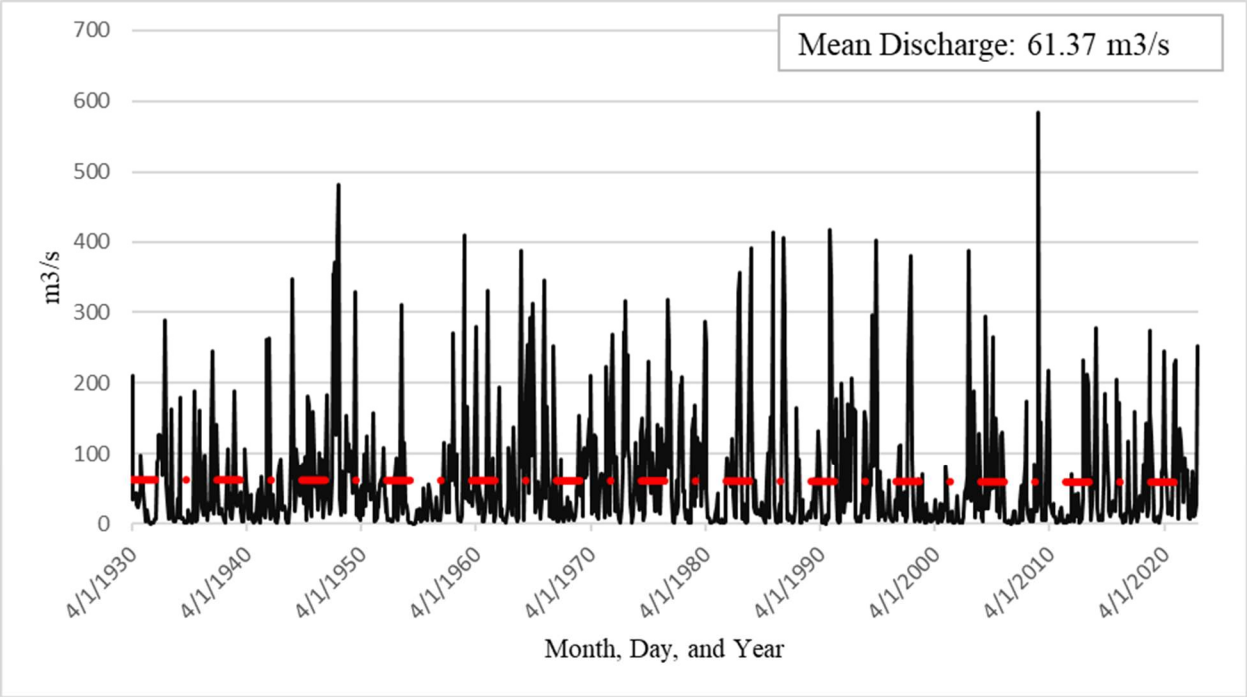

Figure 2.7 The discharge rate over a 93-year period for the Satilla River. The mean average water discharge rate is 61.37 m3s (station 0226362).

Table 2.1 Names and information of the predictor variables used in the random forest classification. All predictor variables were projected to Universal Transverse Mercator (UTM) zone 17 North, NAD 1983 (National Spatial Reference System of 2011) (EPSG: 26917) with a 1-meter spatial resolution. The inputs included all aerial and NAIP spectral bands, National Wetland Inventory (NWI) digital elevation model (DEM), enhanced vegetation index (EVI), green normalized difference vegetation index (GNDVI), modified soil adjusted vegetation index (MSAVI), modified simple ratio (MSR), normalized difference vegetation index, renormalized difference vegetation index (RDVI).

Predictor Rasters	Description	Spatial Resolution	Purpose	References	Data Source
Orthoimagery-Band 1	Blue	0.15 m	Vegetation classification.	Office for Coastal Management, 2023	NOAA
Orthoimagery-Band 2	Green	0.15 m	Vegetation classification.	Office for Coastal Management, 2023	NOAA
Orthoimagery-Band 3	Red	0.15 m	Vegetation classification.	Office for Coastal Management, 2023	NOAA
Orthoimagery-Band 4	NIR	0.15 m	Vegetation classification.	Office for Coastal Management, 2023	NOAA
NAIP Imagery	4 band imagery	0.6 m	Vegetation classification.	USDA FSA, 2019	USDA
Unmodifed DEM (m)	Elevation in meters	1 m	Vegetation classification.	USGS, 2019	USGS
NWI (Class Integer)	Habitat classes	1 m	Used to fill in missing data in aerial imagery.	USFWS, 2018	USFWS
EVI	$2.5 * \frac{B4 - B3}{B4 + 2.5 * B3 - 7.5 + B1 + 1}$	1 m	Accounts for atmospheric conditions, canopy background, and soil reflectance.	Huete et al., 2002	Derived from orthoimagery
GNDVI	$\frac{B4 - B2}{B4 + B2}$	1 m	Highlights vegetation greenness and denseness	Gitelson et al., 1996	Derived from orthoimagery
MSAVI	$\frac{2}{2} * B4 + 1 - \sqrt{(2 * B4 + 1)^2 - 8 * (B4 -}$	1 m	Accounts for soil background reflectance	Qi et al., 1994	Derived from orthoimagery

MSR	$\frac{\frac{B4}{B3}-1}{\sqrt{\frac{B4}{B3}+1}}$	1 m	Sensitive to biophysical parameters	Chen, 1996	Derived from orthoimagery
NDVI	$\frac{B4-B3}{B4+B3}$	1 m	Presence, health, and greenness of vegetation	Rouse et al., 1974	Derived from orthoimagery
RDVI	$\frac{B4-B3}{\sqrt{B4+B3}}$	1 m	Renormalization to enhance sensitivity to vegetation changes	Roujean & Breon, 1995	Derived from orthoimagery

Table 2.2 Training and validation data for the aerial orthoimagery random forest classification based on ground reference data and visual interpretation of high spatial resolution orthoimagery.

Habitat Class	Training Pixels	Training Polygons	Validation Pixels	Validation Polygons
All Coastal Huc's	**1,343,039**	**2,073**	**349,528**	**514**
Dominant Class				
Cladium jamaicense	881	6	293	2
High Reflectance	104,899	168	30,986	40
Juncus roemerianus	237,768	251	73,364	63
Marsh Meadow	54,180	143	16,596	38
Mud	62,691	133	7,506	31
Schoenoplectus americanus and *tabernaemontani*	23,639	48	6,753	13
Spartina alterniflora (Medium)	130,489	258	37,782	66
Spartina alterniflora (Short)	99,471	221	25,549	58
Spartina alterniflora (Tall)	61,574	403	9,507	93
Spartina cynosuroides	52,045	161	11,635	41
Submerged	43,700	88	8,852	22
Tree	340,774	124	96,908	31
Zizaniopsis miliacea	130,928	69	23,797	16
Altamaha Sound	**271,446**	**237**	**94,820**	**58**
Dominant Class				
High Reflectance	29,137	19	17,695	5
Juncus roemerianus	51,265	23	12,226	5
Marsh Meadow	2,765	18	609	4
Mud	8,538	15	1,359	3
Schoenoplectus americanus and *tabernaemontani*	21,581	30	6,058	8
Spartina alterniflora (Medium)	4,930	16	2,785	4
Spartina alterniflora (Short)	2,179	16	408	4
Spartina alterniflora (Tall)	4,389	27	681	7
Spartina cynosuroides	32,547	40	6,576	10
Tree	86,624	6	36,719	2
Zizaniopsis miliacea	27,491	27	9,704	6
Cumberland Sound	**41,942**	**101**	**7,340**	**25**
Dominant Class				
High Reflectance	2,383	9	1,774	3
Juncus roemerianus	17,346	20	2,992	5
Mud	741	10	370	2

Spartina alterniflora (Medium)	3,598	10	816	3
Spartina alterniflora (Short)	1,405	5	309	1
Spartina alterniflora (Tall)	1,591	29	620	7
Spartina cynosuroides	433	12	280	3
Tree	14,445	6	179	1
Doboy Sound	**281,023**	**226**	**73,885**	**61**
Dominant Class				
High Reflectance	12,763	21	500	4
Juncus roemerianus	41,204	27	28,529	10
Marsh Meadow	17,622	17	5,427	7
Mud	8,193	11	162	3
Spartina alterniflora (Medium)	25,056	58	6,648	16
Spartina alterniflora (Short)	29,850	46	3,205	8
Spartina alterniflora (Tall)	4,188	29	838	8
Tree	142,147	17	28,576	5
Ossabaw Sound	**248,894**	**317**	**55,484**	**80**
Dominant Class				
High Reflectance	8,787	19	1,524	5
Juncus roemerianus	55,413	44	11,090	11
Marsh Meadow	13,341	17	6,412	4
Mud	1,928	15	427	4
Spartina alterniflora (Medium)	8,523	34	3,094	9
Spartina alterniflora (Short)	16,000	36	2,501	9
Spartina alterniflora (Tall)	9,611	65	2,148	16
Spartina cynosuroides	2,459	20	3,384	5
Submerged	12,615	26	525	6
Tree	21,199	16	10,819	5
Zizaniopsis miliacea	99,018	25	13,560	6
Sapelo Sound	**81,666**	**196**	**17,599**	**52**
Dominant Class				
High Reflectance	4,608	16	1,230	4
Juncus roemerianus	18,061	19	5,338	5
Marsh Meadow	9,436	17	1,208	5
Mud	3,381	17	495	5
Spartina alterniflora (Medium)	14,945	37	3,117	8
Spartina alterniflora (Short)	15,628	26	2,811	7
Spartina alterniflora (Tall)	1,824	34	486	9
Submerged	6,651	19	724	5

Tree	7,132	11	2,190	4
St. Andrew's Sound	**134,978**	**178**	**33,322**	**45**
Dominant Class				
Cladium jamaicense	881	6	293	2
High Reflectance	12,929	12	628	3
Juncus roemerianus	35,847	20	10,198	5
Marsh Meadow	622	6	555	2
Mud	9,440	13	888	3
Spartina alterniflora (Medium)	48,104	42	11,220	11
Spartina alterniflora (Short)	8,244	18	4,662	4
Spartina alterniflora (Tall)	3,331	25	621	6
Spartina cynosuroides	5,961	11	600	3
Tree	5,200	8	3,124	2
Zizaniopsis miliacea	4,419	17	533	4
St. Catherine's Sound	**133,681**	**286**	**33,366**	**75**
Dominant Class				
High Reflectance	18,065	30	3,119	7
Juncus roemerianus	15,020	33	3,367	8
Marsh Meadow	3,104	32	584	8
Mud	4,583	16	886	4
Schoenoplectus americanus and *tabernaemontani*	2,058	18	695	5
Spartina alterniflora (Medium)	16,372	42	7,835	11
Spartina alterniflora (Short)	13,196	13	4,668	7
Spartina alterniflora (Tall)	5,300	64	733	16
Submerged	8,920	21	1,613	5
Tree	47,063	17	9,866	4
St. Simon's Sound	**104,154**	**281**	**25,352**	**71**
Dominant Class				
High Reflectance	8,627	20	1,150	5
Juncus roemerianus	20,560	39	7,448	10
Marsh Meadow	2,549	16	697	4
Mud	18,450	18	2,235	5
Spartina alterniflora (Medium)	14,769	37	6,389	10
Spartina alterniflora (Short)	11,102	22	1,673	5
Spartina alterniflora (Tall)	2,748	68	474	17
Spartina cynosuroides	1,938	20	327	5
Submerged	10,917	15	2,773	4
Tree	12,494	26	2,186	6

Wassaw Sound	**59,980**	**248**	**17,768**	**46**
Dominant Class				
High Reflectance	7,600	22	3,366	4
Juncus roemerianus	5,970	34	1,746	6
Marsh Meadow	4,741	20	1,104	4
Mud	7,437	18	684	2
Spartina alterniflora (Medium)	11,055	29	2,364	7
Spartina alterniflora (Short)	6,661	27	1,869	5
Spartina alterniflora (Tall)	2,930	45	539	7
Spartina cynosuroides	4,519	23	2,489	6
Submerged	4,597	13	358	3
Tree	4,470	17	3,249	2

Table 2.3 RTK statistics for the different vegetation elevation heights and the three habitat classes (Salt, Brackish, and Fresh).

Species	Min	1st Quartile	Median	Mean	3rd Quartile	Max	SD	SE	N
Dominant Class									
Spartina alterniflora (Short)	0.52400	0.78550	0.86300	0.85280	0.92300	1.26600	0.11456	0.00932	151
Spartina alterniflora (Medium)	0.29200	0.75900	0.87500	0.85650	0.98200	1.25100	0.17963	0.01249	207
Spartina alterniflora (Tall)	0.24300	0.45620	0.62150	0.59120	0.77200	1.01200	0.26275	0.02710	94
Marsh Meadow	0.90900	0.99100	1.03100	1.06300	1.12100	1.50600	0.11564	0.01852	39
Juncus roemerianus	0.56100	0.81900	0.97800	0.93580	1.05300	1.35000	0.17463	0.01851	89
Schoenoplectus americanus	0.58800	0.82000	0.89200	0.87160	0.92950	1.04400	0.12188	0.02541	23
Spartina cynosuroides	0.26000	0.79370	0.96800	0.89550	1.05650	1.22400	0.23033	0.02303	100
Schoenoplectus tabernaemontani	0.54800	0.73850	0.90000	0.82810	0.91300	0.97300	0.14344	0.05071	8
Zizaniopsis miliacea	0.21900	0.75850	0.81100	0.77780	0.89800	1.13700	0.20652	0.03709	31
Cladium jamaicense	0.88000	0.92570	0.98550	0.97100	1.03080	1.03300	0.07418	0.03709	4
Salt Pan	0.86500	0.92050	0.99200	1.04950	1.11200	1.37400	0.17962	0.05416	11
Mud	0.70400	0.74900	0.82300	0.90550	1.02700	1.36200	0.19655	0.05451	13
Shell	0.10100	0.95350	1.13400	0.99490	1.25150	1.42500	0.43095	0.11127	15
Habitat Class									
Salt	0.24300	0.73900	0.86900	0.84360	0.98250	1.50600	0.22880	0.00996	528
Brackish	0.06100	0.78400	0.95000	0.89030	1.03800	1.36200	0.22278	0.01571	201
Fresh	0.21900	0.79850	0.89500	0.85820	0.94350	1.22400	0.18021	0.02027	79

Table 2.4 Values from the post hoc pairwise comparison Dunn's Test examining statistical differences in the elevation between different ground cover classes from RTK data. The boxes shaded in gray are values that meet the less than 0.05 p value threshold.

Ground Cover Classes	*Cladium jamaicense*	High Reflectance	*Juncus roemerianus*	Marsh Meadow	Mud	*Schoenoplectus americanus* and *tabernaemontani*	*Spartina alterniflora* (Medium)	*Spartina alterniflora* (Short)	*Spartina alterniflora* (Tall)	*Spartina cynosuroides*	*Zizaniopsis miliacea*
Cladium jamaicense	-	-	-	-	-	-	-	-	-	-	-
High Reflectance	1.000	-	-	-	-	-	-	-	-	-	-
Juncus roemerianus	1.000	1.000	-	-	-	-	-	-	-	-	-
Marsh Meadow	1.000	1.000	0.0040	-	-	-	-	-	-	-	-
Mud	1.000	1.000	1.000	0.0163	-	-	-	-	-	-	-
Schoenoplectus americanus and *tabernaemontani*	1.000	0.0460	1.000	<0.0001	1.000	-	-	-	-	-	-
Spartina alterniflora (Medium)	1.000	0.0013	0.0240	<0.0001	1.000	1.000	-	-	-	-	-
Spartina alterniflora (Short)	1.000	<0.0001	0.0020	<0.0001	1.000	1.000	1.000	-	-	-	-
Spartina alterniflora (Tall)	0.536	<0.0001	<0.0001	<0.0001	0.0135	0.0004	<0.0001	<0.0001	-	-	-
Spartina cynosuroides	1.000	0.650	1.000	<0.0001	1.000	1.000	0.319	0.0365	<0.0001	-	-
Zizaniopsis miliacea	1.000	<0.0001	0.0017	<0.0001	1.000	1.000	1.000	1.000	0.1370	0.0134	-

Table 2.5 Random Forest classification confusion matrix for the twelve tidal marsh dominant classes. The rows represent the image data (the classified pixel) while the columns represent the reference data (what the pixel is based on reference data). The shaded cells represent the classification accuracy for each of the classes which is equivalent to the producer's accuracy.

	Ground Referenced												
Classified	*Cladium jamaicense*	High Reflectance	*Juncus roemerianus*	Marsh Meadow	Mud	*Schoenoplectus americanus* and *tabernaemontani*	*Spartina alterniflora* (Medium)	*Spartina alterniflora* (Short)	*Spartina alterniflora* (Tall)	*Spartina cynosuroides*	Submerged	Tree	*Zizaniopsis miliacea*
Cladium jamaicense	0.730	0.000	0.000	0.000	0.000	0.000	0.000	0.000	0.000	0.000	0.000	0.000	0.000
High Reflectance	0.000	0.983	0.004	0.096	0.140	0.002	0.006	0.004	0.002	0.343	0.000	0.009	0.005
Juncus roemerianus	0.000	0.004	0.907	0.030	0.000	0.022	0.048	0.001	0.035	0.047	0.000	0.012	0.001
Marsh Meadow	0.000	0.005	0.010	0.825	0.005	0.021	0.021	0.059	0.006	0.001	0.000	0.003	0.003
Mud	0.000	0.000	0.000	0.000	0.811	0.000	0.006	0.002	0.025	0.000	0.018	0.000	0.000
Schoenoplectus americanus and *tabernaemontani*	0.000	0.000	0.018	0.011	0.000	0.896	0.000	0.000	0.000	0.101	0.000	0.000	0.009
Spartina alterniflora (Medium)	0.000	0.000	0.020	0.006	0.007	0.002	0.763	0.256	0.119	0.049	0.017	0.000	0.002
Spartina alterniflora (Short)	0.000	0.002	0.003	0.016	0.018	0.000	0.124	0.669	0.038	0.006	0.000	0.000	0.006
Spartina alterniflora (Tall)	0.000	0.001	0.007	0.009	0.016	0.001	0.030	0.005	0.723	0.014	0.003	0.000	0.002
Spartina cynosuroides	0.000	0.000	0.026	0.002	0.002	0.018	0.002	0.002	0.048	0.434	0.000	0.000	0.007
Submerged	0.000	0.000	0.000	0.000	0.000	0.000	0.001	0.002	0.000	0.000	0.962	0.000	0.000
Tree	0.161	0.003	0.004	0.003	0.000	0.002	0.000	0.000	0.002	0.000	0.000	0.976	0.081
Zizaniopsis miliacea	0.109	0.000	0.000	0.002	0.000	0.037	0.000	0.000	0.001	0.005	0.000	0.000	0.885
Overall Accuracy: 0.863													

Table 2.6 Random Forest error matrix for the twelve tidal marsh dominant classes. The producer's accuracy is the probability of correctly classified pixels while user's accuracy is the probability that the predicted value is that class. The error of omission is a measure of false negatives while the error of commission is a measure of false positives.

Dominant Class	Producer Accuracy	User Accuracy	Error of Omission	Error of Commission
Cladium jamaicense	0.730	1.000	0.270	0.000
High Reflectance	0.983	0.655	0.017	0.345
Juncus roemerianus	0.907	0.939	0.093	0.061
Marsh Meadow	0.825	0.776	0.175	0.224
Mud	0.811	0.848	0.189	0.152
Schoenoplectus americanus and *tabernaemontani*	0.896	0.430	0.104	0.570
Spartina alterniflora (Medium)	0.763	0.770	0.237	0.230
Spartina alterniflora (Short)	0.669	0.702	0.331	0.298
Spartina alterniflora (Tall)	0.723	0.700	0.277	0.300
Spartina cynosuroides	0.434	0.719	0.566	0.281
Submerged	0.962	0.989	0.038	0.011
Tree	0.976	0.972	0.024	0.028
Zizaniopsis miliacea	0.885	0.986	0.115	0.014

Table 2.7 Averaged spectral separability across the three different watersheds. The Jeffries-Matusita distance was used in order to determine the average difference between all classes using ENVI 5.6.1 spectral separability tool. Any value above 1.8 is to be considered spectrally different while the lower values represent classes that are not as spectrally separable.

Dominant Class	*Cladium jamaicense*	High Reflectance	*Juncus roemerianus*	Marsh Meadow	Mud	*Schoenoplectus americanus* and *tabernaemontani*	*Spartina alterniflora* (Medium)	*Spartina alterniflora* (Short)	*Spartina alterniflora* (Tall)	*Spartina cynosuroides*	Submerged	Tree	*Zizaniopsis miliacea*
Cladium jamaicense	-	-	-	-	-	-	-	-	-	-	-	-	-
High Reflectance	1.654	-	-	-	-	-	-	-	-	-	-	-	-
Juncus roemerianus	1.267	1.840	-	-	-	-	-	-	-	-	-	-	-
Marsh Meadow	1.747	1.648	1.315		-	-	-	-	-	-	-	-	-
Mud	1.938	1.706	1.918	1.542	-	-	-	-	-	-	-	-	-
Schoenoplectus americanus and *tabernaemontani*	-	1.603	0.856	1.214	1.716	-	-	-	-	-	-	-	-
Spartina alterniflora (Medium)	1.756	1.856	1.017	1.446	1.663	1.680	-	-	-	-	-	-	-
Spartina alterniflora (Short)	1.726	1.762	1.337	1.129	1.419	1.455	0.749	-	-	-	-	-	-
Spartina alterniflora (Tall)	1.576	1.850	0.984	1.230	1.737	1.598	0.805	1.249	-	-	-	-	-
Spartina cynosuroides	0.618	1.747	0.902	1.210	1.867	0.358	1.399	1.467	1.147	-	-	-	-
Submerged	-	1.954	1.906	1.747	1.853	2.000	1.730	1.815	1.798	1.949	-	-	-
Tree	1.654	1.840	1.344	1.510	1.879	1.514	1.507	1.656	0.820	1.408	1.960	-	-
Zizaniopsis miliacea	0.596	1.873	1.139	1.499	1.966	1.190	1.208	1.494	1.556	1.196	1.974	1.632	-

Table 2.8 Area coverage (kilometer squared) of the different dominant classes classified using random forest per watershed. The classes were aggregated based on the different NWI habitat class using vegetation. *Juncus roemerianus*, *Spartina cynosuroides, Schoenoplectus americanus/tabernaemontani* were combined to form brackish marsh. The salt marsh was formed by combining short, medium, and tall *Spartina alterniflora*, submerged, and marsh meadow. Tidal freshwater marshes were found to have *Cladium jamaicense* and *Zizaniopsis miliacea*.

Habitat Class	Square Kilometers (km^2)	Proportional Area
All Coastal HUCs	**2,427.349**	**1.000**
Dominant Class		
Cladium jamaicense	6.313	0.003
High Reflectance	35.831	0.015
Juncus roemerianus	295.762	0.122
Marsh Meadow	26.310	0.011
Mud	78.634	0.032
Schoenoplectus americanus and *tabernaemontani*	21.829	0.009
Spartina alterniflora (Medium)	593.595	0.245
Spartina alterniflora (Short)	148.267	0.061
Spartina alterniflora (Tall)	212.138	0.087
Spartina cynosuroides	128.227	0.053
Submerged	72.331	0.030
Tree	760.538	0.313
Zizaniopsis miliacea	47.575	0.020
NWI Habitat Class		
Salt	1052.640	0.434
Brackish	445.818	0.184
Tidal Freshwater	53.888	0.022
Altamaha Sound	**307.962**	**1.000**
Dominant Class		
High Reflectance	4.308	0.014
Juncus roemerianus	38.815	0.126
Marsh Meadow	0.766	0.002
Mud	7.525	0.024
Schoenoplectus americanus and *tabernaemontani*	13.649	0.044
Spartina alterniflora (Medium)	24.841	0.081
Spartina alterniflora (Short)	3.134	0.010

Spartina alterniflora (Tall)	9.190	0.030
Spartina cynosuroides	31.936	0.104
Tree	163.574	0.531
Zizaniopsis miliacea	10.223	0.033
NWI Habitat Class		
Salt	37.931	0.123
Brackish	84.401	0.274
Tidal Freshwater	10.223	0.033
Cumberland Sound	**81.556**	**1.000**
Dominant Class		
High Reflectance	0.762	0.009
Juncus roemerianus	23.005	0.282
Mud	5.076	0.062
Spartina alterniflora (Medium)	11.476	0.141
Spartina alterniflora (Short)	0.986	0.012
Spartina alterniflora (Tall)	4.556	0.056
Spartina cynosuroides	2.408	0.030
Tree	33.286	0.408
NWI Habitat Class		
Salt	17.02	0.21
Brackish	25.41	0.31
Tidal Freshwater	0.00	0.00
Doboy Sound	**141.304**	**1.000**
Dominant Class		
High Reflectance	2.505	0.018
Juncus roemerianus	22.969	0.163
Marsh Meadow	2.137	0.015
Mud	2.798	0.020
Spartina alterniflora (Medium)	53.046	0.375
Spartina alterniflora (Short)	22.915	0.162
Spartina alterniflora (Tall)	12.258	0.087
Tree	22.676	0.160
NWI Habitat Class		
Salt	90.355	0.639
Brackish	22.969	0.163

Tidal Freshwater	0.000	0.000
Ossabaw Sound	**288.993**	**1.000**
Dominant Class		
High Reflectance	4.132	0.014
Juncus roemerianus	38.603	0.134
Marsh Meadow	5.209	0.018
Mud	6.573	0.023
Spartina alterniflora (Medium)	32.733	0.113
Spartina alterniflora (Short)	30.760	0.106
Spartina alterniflora (Tall)	47.185	0.163
Spartina cynosuroides	22.558	0.078
Submerged	2.013	0.007
Tree	69.967	0.242
Zizaniopsis miliacea	29.259	0.101
NWI Habitat Class		
Salt	117.900	0.408
Brackish	61.161	0.212
Tidal Freshwater	29.259	0.101
Sapelo Sound	**230.183**	**1.000**
Dominant Class		
High Reflectance	1.925	0.008
Juncus roemerianus	12.303	0.053
Marsh Meadow	4.306	0.019
Mud	12.272	0.053
Spartina alterniflora (Medium)	93.054	0.404
Spartina alterniflora (Short)	23.226	0.101
Spartina alterniflora (Tall)	21.471	0.093
Submerged	8.389	0.036
Tree	53.237	0.231
NWI Habitat Class		
Salt	150.445	0.654
Brackish	12.303	0.053
Tidal Freshwater	0.000	0.000
St. Andrew's Sound	**527.956**	**1.000**
Dominant Class		
Cladium jamaicense	6.313	0.012

High Reflectance	8.737	0.017
Juncus roemerianus	79.804	0.151
Marsh Meadow	1.124	0.002
Mud	14.649	0.028
Spartina alterniflora (Medium)	140.781	0.267
Spartina alterniflora (Short)	23.575	0.045
Spartina alterniflora (Tall)	34.983	0.066
Spartina cynosuroides	37.804	0.072
Tree	172.093	0.326
Zizaniopsis miliacea	8.093	0.015
NWI Habitat Class		
Salt	200.463	0.380
Brackish	117.608	0.223
Tidal Freshwater	14.405	0.027
St Catherine's Sound	**334.988**	**1.000**
Dominant Class		
High Reflectance	4.166	0.012
Juncus roemerianus	25.384	0.076
Marsh Meadow	5.092	0.015
Mud	9.879	0.029
Schoenoplectus americanus and *tabernaemontani*	8.180	0.024
Spartina alterniflora (Medium)	119.030	0.355
Spartina alterniflora (Short)	21.475	0.064
Spartina alterniflora (Tall)	33.236	0.099
Submerged	14.595	0.044
Tree	93.951	0.280
NWI Habitat Class		
Salt	193.428	0.577
Brackish	33.563	0.100
Tidal Freshwater	0.000	0.000
St. Simon's	**281.430**	**1.000**
Dominant Class		
High Reflectance	5.478	0.019
Juncus roemerianus	37.900	0.135
Marsh Meadow	4.704	0.017
Mud	4.551	0.016

Spartina alterniflora (Medium)	55.382	0.197
Spartina alterniflora (Short)	9.876	0.035
Spartina alterniflora (Tall)	16.823	0.060
Spartina cynosuroides	5.061	0.018
Submerged	32.869	0.117
Tree	108.785	0.387
NWI Habitat Class		
Salt	114.950	0.408
Brackish	42.961	0.153
Tidal Freshwater	0.000	0.000
Wassaw Sound	**232.979**	**1.000**
Dominant Class		
High Reflectance	3.816	0.016
Juncus roemerianus	16.979	0.073
Marsh Meadow	2.971	0.013
Mud	15.309	0.066
Spartina alterniflora (Medium)	63.252	0.271
Spartina alterniflora (Short)	12.320	0.053
Spartina alterniflora (Tall)	32.436	0.139
Spartina cynosuroides	28.461	0.122
Submerged	14.465	0.062
Tree	42.968	0.184
NWI Habitat Class		
Salt	125.445	0.538
Brackish	45.440	0.195
Tidal Freshwater	0.000	0.000

Table 2.9 Mean decrease in random forest accuracy values and overall ranks. Mean decrease in accuracy is a predictor of variable importance with larger decreases in accuracy indicating variables with more importance in the classification. * and ** indicates a tie in overall rank.

Predictor Variable	Mean Values	Overall Mean Rank	Overall Rank
Orthoimagery- Blue Band (DN)	0.20	3.56	3
Orthoimagery- Green Band (DN)	0.12	6.78	7
**Orthoimagery- Red Band (DN)	0.09	9.22	9
Orthoimagery- NIR Band (DN)	0.11	7.56	8
Unmodifed DEM (m)	0.30	2.44	1
NWI (Class Integer)	0.34	2.89	2
EVI	0.15	5.22	4
*GNDVI	0.14	5.44	5
*MSAVI	0.15	5.44	5
MSR	0.08	10.22	12
NDVI	0.08	10.00	11
**RDVI	0.09	9.22	9

CHAPTER 3

CLASSIFICATION OF PLANETSCOPE IMAGERY

3.1 Introduction

Tidal marshes are susceptible to many different threats such as sea level rise (Burns et al., 2021; Solohin et al., 2020), drought (Neubauer & Craft, 2009; Palomo et al., 2013), coastal development (Baldwin, 2004; Greenberg et al., 2006), and large-scale disturbance events (Mo et al., 2020). These threats can cause a variety of issues such as the reduction of marsh biomass (Mo et al., 2020; O'Donnell & Schalles, 2016) and the altering of natural biogeochemical processes (Palomo et al., 2013), which both cause a reduction in the ecosystem services that each of these marshes provides.

Understanding these threats and ecosystem services requires the ability to measure changes across space and time. Remote sensing provides many advantages for tidal marsh mapping such as repeat coverage, cost-effectiveness, less time-consuming, and can cover large geographic areas (Ozesmi & Bauer, 2002). While useful, remote sensing does have drawbacks that include mixed or fuzzy pixels and spectral similarities between plants that can occur with lower spatial resolution and lower spectral resolution images leading to the misclassification of species (Ozesmi & Bauer, 2002). Despite these limitations, previous studies have shown that tidal marshes can be accurately classified using high-resolution imagery in addition to an unmodified digital elevation model (DEM) and the National Wetland Inventory (NWI) (Alexander & Hladik, 2015). This study classified salt and brackish marshes along the Georgia coast with high accuracies ranging from 85% to 95% across the coastal counties of Georgia.

Alexander and Hladik (2015) also gave important information about variable importance, showing that the digital elevation model (DEM) was ranked as the most important in differentiating different species.

While aerial imagery does have some advantages in tidal marsh mapping, satellite imagery has long been used to map wetlands (Mahdianpari et al., 2020). The most common satellite used for these studies is the Landsat Mission because of its historical archives although, recent studies have begun to use Sentinel-2 due to its higher spatial resolution (10 m versus 30 m) (Mahdianpari et al., 2020). Mahdianpari et al. (2020) conducted a meta-analysis showing the median accuracy of wetland classification using Landsat to be 85% which is comparable to Sentinel-2 but there does appear to be some difference between the satellites. Both Landsat and Sentinel-2 are government-owned satellites which means that these provide freely available data.

In contrast to national organizations, commercial satellites owned by private companies are typically not free to the user. These satellites typically have a higher spatial resolution than others but are less commonly used due to the high cost to the user (Mahdianpari et al., 2020). McCarthy et al. (2015) used Maxar Technologies' WorldView satellite multispectral bands to identify wetlands in the Tampa Bay watershed. The WorldView imagery had a 2m spatial resolution and performed with an overall accuracy that was 36% higher than the Landsat classification. Another study conducted by Campbell and Wang (2019) used WorldView 2, WorldView 3, and LiDAR-derived digital elevation models (DEM) to map 10 salt marsh classes in the Fire Island national Seashore in New York, with an overall accuracy of 92.75%. A moderate class accuracy of 79.8% was achieved for the *S. alterniflora* class which was often misclassified as patchy *S. alterniflora*. Campbell and Wang (2019) also compared classifications using National Agriculture Image Program (NAIP) imagery to those from satellite imagery to

test the accuracy in tidal marsh mapping. They found high-resolution satellite data provided a higher classification accuracy (92.75%) when compared to high-resolution high NAIP imagery (85%).

RapidEye is a commercial satellite constellation that is owned by Planet Inc. (Planet Team, 2017). RapidEye had five bands in the blue, green, red, red edge, and near-infrared regions of the electromagnetic spectrum. Deventer et al. (2019), used RapidEye to map and classify different wetland vegetation such as *Acrostichum aureum L.* (Mangrove fern), *Acacia kosiensis* (Dune sweet thorn); East coast dune forest, *Ficus trichopoda* (swamp fig), *Hibiscus tilleaceus* (lagoon hibiscus), coastal lowland forest, mangrove forests, *Phragmites australis/mauritanus* (reeds), and seasonal wetlands using a random forest classifier and multitemporal seasonal imagery in South Africa. RapidEye produced an overall accuracy of 87% when using all bands, indices, and seasonal imagery with the most important band being the red edge band. (Deventer et al., 2019). While this satellite constellation has been decommissioned, Planet Inc. has a newer microsatellite constellation called PlanetScope (Planet Labs, 2017). PlanetScope is unique in that it is a constellation of over 200 satellites allowing for frequent revisit times of around 1 day and is managed and run by Planet Inc.

PlanetScope has not been extensively used to map and classify tidal marshes. The lack of more extensive research in tidal marshes may be potentially contributed to the newness of this satellite constellation, as it has only been operating since 2016. It has been most often used in crop studies. The 4-band imagery (blue, green, red, near infrared (NIR)) has been shown to map crops accurately using the random forest classifier with a high degree of accuracy (Anul Haq, 2022). Anul Haq (2022), used PlanetScope's 3 m, 4 band satellites to monitor and map agricultural vegetation. They also used PlanetScope's high revisit time of one day to conduct a

time series analysis using NDVI to monitor vegetation health. PlanetScope has been used in marshes to accurately predict above-ground biomass of *S. alterniflora* at North Inlet, in Georgetown, South Carolina (Miller et al., 2019). Normalized difference vegetation index (NDVI), soil adjusted vegetation index (SAVI), modified soil adjusted vegetation index (MSAVI), renormalized difference vegetation index (RDVI), green normalized vegetation index (GNDVI), and visible difference vegetation index (VDVI) were used to help obtain a regression model in order to predict biomass values. The best model was obtained through using MSAVI and VDVI which obtained a root mean square error of 223.38 g/m² and a Wilmott's index of agreement of 0.74. They then scaled this across the study area and showed a total estimated biomass of 2423 Mg (Miller et al., 2019). In 2022, Planet Lab Inc. announced the release of their 8-band product, adding coastal blue, green I, yellow, and red-edge bands. Thus far the 8-band PlanetScope product has not been used to study tidal marsh vegetation at the time of this writing. Due to the lack of literature in this space, this chapter focuses on our efforts to use and compare 4-band and 8-band PlanetScope imagery using the *randomForest* package in R to map Georgia tidal marshes, with a focus on freshwater tidal marshes. This was done to determine if the additional spectral bands and the ability to calculate more vegetation indices lead to a more accurate classification.

3.2 Methodology

3.2.1 Study Area

This study included the three main hydrologic units (HUCs) at a level 10 scale (USGS, 2021) along the coast of Georgia which encompass the three largest rivers along the east coast of Georgia, USA (UTM Zone 17N) which include the Ogeechee, Altamaha, and the Satilla rivers

(Figure 1). The Ogeechee River has a drainage area of 8,415 km^2 and a median discharge of 38 m^3s^{-1} (USGS, Gauge: 02202500). The Altamaha River is the largest undammed river on the east coast of the United States and the largest coastal watershed in Georgia with a size of 35,112 km^2 and a median discharge of 238 m^3s^{-1} (USGS, Gauge: 02226160). The Satilla is the southernmost Georgia coastal watershed and the smallest with an area of 7,348 km^2 and a median discharge of 30 m^3s^{-1} (USGS, Gauge: 02228070).

Each of these systems has varying practical salinity unit (PSU) ranges depending on location and freshwater influence, but each has similar community structures in that *Spartina alterniflora* dominates the salt marshes (17 - 31 PSU) in its three forms short (<0.5 m), medium (0.5 m to 1 m) and tall (> 1m) (Reimold, Gallagher, & Thompson, 1973); *Spartina cynosuroides and Juncus roemerianus* dominate the brackish marshes (4.5 - 24 PSU), and *Zizaniopsis miliacea* dominates the tidal freshwater marshes (0.1 - 12 PSU) (Loomis and Craft, 2009; Wieski et al., 2010).. While these are the dominant species, there were others that were included in our classification of this chapter when present which included: C*ladium jamaicense,* marsh meadow (*Batis maritima*, *Borrichia frutescens*, *Distichlis spicata*, and *Salicornia virginica*), *Panicum virgatum*, *Schoenoplectus americanus*, *Schoenoplectus tabernaemontani*, *Schoenoplectus spp*., and other non-marsh classes such as high reflectance, mud, and trees (Table 1). In total, 13 habitat classes were used in the current analysis. Note that not all classes were present in each watershed.

3.2.2 PlanetScope Satellite Imagery and Other Data Sources

As in Chapter Two (section 2.2.1), this study used multiple sources of remotely sensed imagery to classify salt, brackish, and tidal fresh marshes. This study uses light detection and

ranging (LiDAR)-derived DEMs, the National Wetlands Inventory (NWI), and 6 to 9 vegetation indices for inputs in the random forest classification (Table 3.1). All products maintained the Universal Transverse Mercator (UTM) zone 17 North, NAD 1983 coordinate system (National Spatial Reference System of 2011) (EPSG: 6346) (Table 3.1). The DEM, and NWI were resampled from 1 meter to 3 meters horizontal spatial resolution to match the resolution of the 4- and 8-band PlanetScope imagery.

Training and validation data were generated using ground reference information described in Chapter Two (section 2.2.2). Regions of interest (ROIs) were digitized using ground reference data and high-resolution aerial imagery. The ROIS were resampled to match the 3m resolution of PlanetScope 4- and 8-band data and then were assessed to make sure the ROIs still represented the correct ground cover class. If PlanetScope imagery pixels did not represent the same class as that of the aerial imagery, the ROI would be deleted and a new ROI would be drawn to represent the correct class. This was done in order to try and maintain consistent results between the aerial and PlanetScope classifications for comparison later. The ROIs were split 80/20 between training and external validation data.

Through a National Science Foundation (NSF) grant for the Georgia Coastal Ecosystems Long Term Ecological Research (LTER) site, I have been given access to Planet Commercial Imagery as part of NASA's Commercial Smallsat Data Acquisition (CSDA) Program. PlanetScope 4- and 8-band data for all watersheds were collected on June 23, 2022, during low tide and cloud-free conditions. The images were collected between 15:10 UTC and 15:54 UTC when the tide conditions were 0.155 m - 0.405 m at the Fort Pulaski tide gauge (8670870) and 0.011 m - 0.066 m at the Fernandina Beach tide gauge (8720030). The imagery was acquired in the World Geodetic System 1984 (WGS 84) (EPSG: 3395) but was reprojected to the Universal

Transverse Mercator (UTM) zone 17 North, NAD 1983 (National Spatial Reference System of 2011) (EPSG: 6346) coordinate system. All products were delivered as PlanetScope's level 3B orthorectified surface reflectance product which has an experimental root mean square error (RMSE) of 4.80 m from their SuperDove satellites (PSB.SD) (Dobrinic, 2018). The 4-band product was delivered with the following band designations: blue (490 nm), green (565 nm), red (665 nm), and NIR (865 nm). The 8-band imagery was delivered with the same bands and the addition of a coastal blue (443 nm), green I (531), yellow (610 nm), and red edge (705 nm) (Table 3.1). These products came as eight different tiles and were mosaiced in ArcGIS Pro. The mosaic products were then clipped to the appropriate HUCs (Ogeechee, Altamaha, and Satilla) for classification.

In addition to the spectral bands, DEM, and NWI, various vegetation indices were calculated at the 3 m spatial resolution (Hladik & Alber, 2012). The nine vegetation indices included the enhanced vegetation index (EVI) (Huete et al., 2002), green normalized difference vegetation index (GNDVI) (Gitelson et al., 1996), modified soil-adjusted vegetation index (MSAVI) (Qi et al., 1994), modified simple ratio (MSR) (Chen, 1996), normalized difference vegetation index (NDVI) (Rouse et al., 1974), and the renormalized difference vegetation index (RDVI) (Roujean & Breon, 1995) for both the 4- and 8-band imagery. Due to the increase in spectral resolution with the 8-band product, three additional vegetation indices were included in order to examine the effectiveness of the red edge band which included the Red Edge Normalized Difference Vegetation Index (RENDVI) (Sims & Gamon, 2002), the Red Edge Chlorophyll Index (CI Red Edge) (Gitelson, Gritz †, et al., 2003; Gitelson, Viña, et al., 2003), and Modified Red Edge Normalized Difference Vegetation Index (MRENDVI) (Datt, 1999; Sims & Gamon, 2002).

3.2.3 Image Classification and Accuracy Assessment

As in Chapter 2, this chapter uses the *randomForest* package in R (Liaw & Wiener, 2001). Thirteen predictor rasters were used as inputs in the PlanetScope 4-band random forest classification, and 19 inputs in the 8-band classification. These included the 4-band or 8-band spectral bands, DEM, NWI, and seven or nine vegetation indices which varied depending on the product being classified. The additional spectral bands in the 8-band imagery allowed for more indices to be calculated focusing on the red edge band. All predictor input rasters had a 3 m spatial resolution. Once the classification was completed using the same methodology from Chapter 2 (section 2.2.3), pixel aggregation was used to reduce the "salt and pepper" effect. A confusion matrix was constructed which included the overall accuracy, producer's accuracy, user's accuracy, and errors of omission and commission (Congalton, 1991) using the withheld 20% external validation ROIs and ground control points. Additionally, out-of-bag error generated using *randomForest* was also used as an internal estimate of the model's performance which takes samples that are similar to the original dataset and runs statistics to assess uncertainty. Variable importance was constructed by calculating the mean decrease in accuracy (MDA), calculated by estimating the decrease in prediction error if a variable is removed from the classification (Breiman, 2001). This was used in order to assess the importance of the additional bands and vegetation indices of the 8-band imagery when compared to the 4-band imagery.

3.3 Results

Across the Ogeechee, Altamaha, and Satilla watersheds, overall accuracies ranged from 74.3% to 88.1% depending on the watershed and the number of PlanetScope bands. The 4-band

imagery had lower overall accuracies in all watersheds (Table 3.6) The 8-band imagery had higher overall accuracies across the three watersheds of 86.5% (Ogeechee), 88.1% (Altamaha), and 75.9% (Satilla). There were relatively small differences between the 4- and 8-band classifications of 0.9%, 1.1% and 1.6% for the Ogeechee, Altamaha, and Satilla, respectively (Table 3.6). A similar trend of overall higher 8-band accuracies was also seen in the individual class producer's accuracies (Table 3.7). Many classes only showed a small or no improvement when using the 8-band versus the 4-band imagery. However, for tidal freshwater mapping, the 8-band performed the same (Ogeechee) or better (Altamaha and Satilla) than the 4-band imagery in both identifying species and having low rates of error of omission (false negatives) and errors of commission (false positives) (Table 3.7). When examining species accuracies, *Juncus roemerianus* and *Zizaniopsis miliacea* performed the best while the different classes of *S. alterniflora* performed poorly. In general, there were differences of only 0 percent to 1 percent for the three height classes of *S. alterniflora* (Table 3.6), except for the Satilla watershed. The Satilla classifications showed a high increase between the 4 and 8-band imagery for the short form of S. alterniflora (6.5%)

The different forms of *Spartina alterniflora* had poor spectral separability ranging from 0.513 to 1.158 (on a scale of 2.0) in the 4-band and 0.798 to 1.52 in the 8-band product (Table 3.5). These measurements come from ENVI 5.6.1 Spectral Separability tool which uses Jeffries-Matusita distance which uses probability distributions to obtain the average distance between distributions (Richards, 2013).

Variable importance is an important metric in which the mean decrease in accuracy was used across the different watersheds and then ranked and averaged to better understand the band importance between the 4-band and 8-band product. Based on watershed variable importance

ranks and averages, the most important bands for the 4-band classification included MSR, NDVI, and NWI in descending order (Table 3.4). The predictor bands with the highest variable importance in the 8-band classification were GNDVI, NDVI, and MSR. For the least important inputs, EVI ranked among the lowest for both classifications, while the blue band and DEM for the 4-band, and coastal blue and MRENDVI were least important for the 8-band imagery. Of the red edge band and derived indices, they performed poorly with CI red edge performing the best at rank 14.

Based on visual interpretation, the maps also appear to represent the area based on species distribution patterns and field observations (Figure 3.2). Similar of that to Chapter 2, the different classes of *S. alterniflora* were found in areas closer to the ocean, with tall *S. alterniflora* near creek banks at lower elevations, and medium and short S. alterniflora in the mid and high marsh areas (Wiegert, & Freeman, 1990). Further up the rivers, transitions to brackish marshes made up of *J. roemerianus*, *S. cynosuroides*, and *Schoenoplectus americanus and tabernaemontani* can be found and eventually turn into tidal freshwater marshes made up of *Cladium jamaicense* and *Z. miliacea* and finally transitioning to the tidal forest and upland areas. Based on the classification of herbaceous marsh species, the Satilla watershed made up the largest area of marsh with salt marshes making up 217.82 km^2, brackish 101.25 km^2, and tidal freshwater 20.694 km^2 when using the 8-band classification (Table 3.3). The 4-band classification had a smaller area of overall marshes when compared to 8-band imagery. While the Satilla also had the largest quantity of brackish marshes which was determined by using brackish marsh species such as *Spartina cynosuroides, Juncus roemerianus*, and Schoenoplectus americanus and tabernaemontani. The Ogeechee watershed boasted the most tidal freshwater

marshes, calculated using *Cc jamaicense* and *Z. miliacea,* making up 34.82 km^2, which is 14.06 km^2 more than the next closest (Altamaha at 20.76) (Table 3.3).

3.4 Discussion

In this study, we classified tidal marsh distributions using PlanetScope commercial satellite imagery and random forest machine learning with overall accuracies ranging from 75.0% to 88.1% depending on the location and number of predictor inputs (Table 3.6). This is the first attempt to classify Georgia salt, brackish, and tidal freshwater marsh vegetation using PlanetScope data, and comparing the use of PlanetScope 4-band and 8-band imagery products for tidal marsh mapping. Similar studies have used 4-band aerial imagery at a lower resolution of 4 m for salt and brackish marshes (Alexander & Hladik, 2015). Comparing our results to Alexander and Hladik (2015) for each of the watersheds, the 4-band PlanetScope imagery is fairly comparable within the accuracy per watershed of salt and brackish marshes (Table 3.6). The Alexander & Hladik (2015) classification did not include tidal freshwater marshes, thus our study provides one of the most robust delineations of tidal freshwater marsh distributions.

Alexander and Hladik (2015) and Chapter 2 of this study used similar inputs and found that the DEM and NWI were important inputs, in contrast to our results for the 4- and 8-bandPlanetScope classifications (Table 3.4). The 4-band classification had a higher variable importance for the NWI while the 8-band imagery had a higher variable importance for the vegetation indices. Unlike the classification found in Chapter 2 of this paper, both PlanetScope classifications emphasized the importance of vegetation indices (Table 3.4). One possible reason for this difference in variable importance rankings is that the aerial imagery was not atmospherically corrected as the product did not come as atmospherically corrected and we did

not have the information in which to do complete atmospheric correction (https://www.fisheries.noaa.gov/inport/item/55001). The atmospheric process aims to consider atmospheric interference in order to give an accurate radiance or surface reflectance value (Emberton et al., 2015). Since the data could not be atmospherically corrected, we were unable to obtain surface reflectance data. As the PlanetScope data had been atmospherically corrected, it is possible that the spectral values were a more accurate representation of the ground cover classes. As a result of the data being atmospherically corrected and scaled to surface reflectance, the random forest classification may have relied more on the spectral bands of PlanetScope due to the increase of bands and spectral separability which may have led to the increased importance in vegetation indices. However, this needs to be investigated further in order to have a better understanding of the differences between the aerial and PlanetScope imagery.

Like previous studies and the classification in Chapter 2, the 4-band imagery had difficulties in differentiating the height classes of *the S. alterniflora* in Georgia marshes (Table 3.6) (Alexander & Hladik, 2015; Hladik et al., 2013). It has been found that by using hyperspectral imagery, and multiple inputs this issue can be resolved as these forms are spectrally similar (Artigas & Yang, 2005). However, using the PlanetScope 4- and 8-band imagery along with multiple predictor variables, it was still challenging to differentiate between the different forms (Table 3.6). Although the different forms were difficult to differentiate, if the classes were to just be grouped as *Spartina alterniflora*, similar to that of other species in this study, the class accuracy would be greatly increased. However, the classes were generally comparable to that of Alexander and Hladik (2015) classes were grouped differently.

By using the same training and validation data as the aerial classification in Chapter 2, we also can draw comparisons between aerial and PlanetScope classifications. In examining on a per

class basis, it was found that the 8-band imagery provided small to no improvements in most classes (Table 3.6). However, it did boast an overall increase in two of the three watersheds when compared to the aerial imagery. The 8-band imagery provided greater improvements in almost all classes and provided a higher overall accuracy in two of the three watersheds as well. These differences were minor and cannot be considered to be significant without further investigation. The Ogeechee watershed was found to have the highest overall accuracy for the aerial imagery at 92.91% while the 4- and 8-band imagery was 85.6% and 86.5% respectively. The aerial imagery also had very different variable importance variables as the DEM, NWI, and blue band were found to be the most important. While other studies do not often use NWI, elevation appears to have a greater variable importance among the high spatial but low spatial resolution imagery (Windle et al., 2023). However, this is also across the entire coast and flown at a different time than when the PlanetScope classification was acquired. Significant flooding in the aerial imagery could also explain the differences as the PlanetScope was acquired during low tide conditions and during a different time of year which could cause phenological differences. This is one of the main advantages of PlanetScope when compared to aerial imagery as it can provide high-resolution imagery on a daily basis. Because of this, imagery can be collected at different tide heights and collect imagery more frequently. This reduces a lot of the issues that were seen in some of the aerial imagery as there was significant flooding.

3.5 Conclusion

The advantages of PlanetScope when compared to other sources of imagery, is the high spatial resolution and frequent revisit times of nearly 1 day. This allows for more chances to capture imagery during the right conditions which is an issue found in Chapter 2 of this paper. The 8-band PlanetScope product has also been shown to increase the overall accuracy of the

imagery but only by 0.9 – 1.6% in tidal marsh mapping. Depending on the product available to the user, the 4-band imagery is sufficient to conduct tidal marsh studies. This study produced accuracies of 85.6%, 87.0% and 74.6% across the Ogeechee, Altamaha, and Satilla watersheds using 4-band PlanetScope data and 86.5%, 88.1%, and 75.9% using the 8-band product across 12 different ground cover classes. Future studies could promote the automation or more frequent monitoring of Georgia tidal marshes.

3.6 References

Alber, M., & Sheldon, J. E. (1999). Use of a data-specific method to examine variability in the flushing time of Georgia estuaries. *Estuarine, Coastal and Shelf Science*, *49*(4), 469–482. https://doi.org/10.1006/ecss.1999.0515

Alexander, C. R., & Hladik, C. (2015). *High-Resolution Mapping of Vegetation, Elevation, Salinity and Bathymetry to Advance Coastal Habitat Management in Georgia* [Final Status Report].

Anul Haq, M. (2022). Planetscope Nanosatellites Image Classification Using Machine Learning. *Computer Systems Science and Engineering*, *42*(3), 1031–1046. https://doi.org/10.32604/csse.2022.023221

Artigas, F. J., & Yang, J. S. (2005). Hyperspectral remote sensing of marsh species and plant vigour gradient in the New Jersey Meadowlands. *International Journal of Remote Sensing*, *26*(23), 5209–5220. https://doi.org/10.1080/01431160500218952

Baldwin, A. H. (2004). Restoring complex vegetation in urban settings: The case of tidal freshwater marshes. *Urban Ecosystems*, *7*(2), 125–137. https://doi.org/10.1023/B:UECO.0000036265.86125.34

Breiman, L. (2001). Random Forests. *Machine Learning*, *45*, 5–32.

Burns, C. J., Alber, M., & Alexander, C. R. (2021). Historical changes in the vegetated area of salt marshes. *Estuaries and Coasts*, *44*(1), 162–177. https://doi.org/10.1007/s12237-020-00781-6

Campbell, A., & Wang, Y. (2019). High Spatial Resolution Remote Sensing for Salt Marsh Mapping and Change Analysis at Fire Island National Seashore. *Remote Sensing*, *11*(9), 1107. https://doi.org/10.3390/rs11091107

Chen, J. M. (1996). Evaluation of Vegetation Indices and a Modified Simple Ratio for Boreal Applications. Canadian Journal of Remote Sensing, 22(3), 229–242. https://doi.org/10.1080/07038992.1996.10855178

Congalton, R. G. (1991). A review of assessing the accuracy of classifications of remotely sensed data. *Remote Sensing of Environment*, *37*(1), 35–46. https://doi.org/10.1016/0034-4257(91)90048-B

Datt, B. (1999). A New Reflectance Index for Remote Sensing of Chlorophyll Content in Higher Plants: Tests using Eucalyptus Leaves. *Journal of Plant Physiology*, *154*(1), 30–36. https://doi.org/10.1016/S0176-1617(99)80314-9

van Deventer, H., Cho, M. A., & Mutanga, O. (2019). Multi-season RapidEye imagery improves the classification of wetland and dryland communities in a subtropical coastal region. *ISPRS Journal of Photogrammetry and Remote Sensing*, *157*, 171–187. https://doi.org/10.1016/j.isprsjprs.2019.09.007

Dobrinic, D. (2018, June 20). *Horizontal accuracy assessment of PlanetScope, RapidEye and WorldView-2 satellite imagery*. 18th International Multidisciplinary Scientific GeoConference SGEM2018. https://doi.org/10.5593/sgem2018/2.3/S10.017

Emberton, S., Chittka, L., Cavallaro, A., & Wang, M. (2015). Sensor Capability and Atmospheric Correction in Ocean Colour Remote Sensing. Remote Sensing, 8(1), 1. https://doi.org/10.3390/rs8010001

Gitelson, A. A., Gritz †, Y., & Merzlyak, M. N. (2003). Relationships between leaf chlorophyll content and spectral reflectance and algorithms for non-destructive chlorophyll assessment in higher plant leaves. *Journal of Plant Physiology*, *160*(3), 271–282. https://doi.org/10.1078/0176-1617-00887

Gitelson, A. A., Kaufman, Y. J., & Merzlyak, M. N. (1996). Use of a green channel in remote sensing of global vegetation from EOS-MODIS. *Remote Sensing of Environment*, *58*(3), 289–298. https://doi.org/10.1016/S0034-4257(96)00072-7

Gitelson, A. A., Viña, A., Arkebauer, T. J., Rundquist, D. C., Keydan, G., & Leavitt, B. (2003). Remote estimation of leaf area index and green leaf biomass in maize canopies. *Geophysical Research Letters*, *30*(5). https://doi.org/10.1029/2002GL016450

Greenberg, R., Maldonado, J. E., Droege, S., & McDONALD, M. V. (2006). Tidal marshes: A global perspective on the evolution and conservation of their terrestrial vertebrates. *BioScience*, *56*(8), 675. https://doi.org/10.1641/0006-3568(2006)56[675:TMAGPO]2.0.CO;2

Hladik, C., & Alber, M. (2012). Accuracy assessment and correction of a LIDAR-derived salt marsh digital elevation model. *Remote Sensing of Environment*, *121*, 224–235. https://doi.org/10.1016/j.rse.2012.01.018

Hladik, C., Schalles, J., & Alber, M. (2013). Salt marsh elevation and habitat mapping using hyperspectral and LIDAR data. *Remote Sensing of Environment*, *139*, 318–330. https://doi.org/10.1016/j.rse.2013.08.003

Huete, A., Didan, K., Miura, T., Rodriguez, E. P., Gao, X., & Ferreira, L. G. (2002). Overview of the radiometric and biophysical performance of the MODIS vegetation indices. *Remote Sensing of Environment*, *83*(1–2), 195–213. https://doi.org/10.1016/S0034-4257(02)00096-2

Liaw, A., & Wiener, M. (2001). Classification and Regression by RandomForest. *R News*, *2*, 18–22.

Loomis, M. J., & Craft, C. B. (2010). Carbon sequestration and nutrient (nitrogen, phosphorus) accumulation in river-dominated tidal marshes, Georgia, USA. *Soil Science Society of America Journal*, *74*(3), 1028–1036. https://doi.org/10.2136/sssaj2009.0171

Mahdianpari, M., Granger, J. E., Mohammadimanesh, F., Salehi, B., Brisco, B., Homayouni, S., Gill, E., Huberty, B., & Lang, M. (2020). Meta-Analysis of Wetland Classification Using Remote Sensing: A Systematic Review of a 40-Year Trend in North America. *Remote Sensing*, *12*(11), 1882. https://doi.org/10.3390/rs12111882

McCarthy, M. J., Radabaugh, K. R., Moyer, R. P., & Muller-Karger, F. E. (2018). Enabling efficient, large-scale high-spatial resolution wetland mapping using satellites. *Remote Sensing of Environment*, *208*, 189–201. https://doi.org/10.1016/j.rse.2018.02.021

Miller, G. J., Morris, J. T., & Wang, C. (2019). Estimating Aboveground Biomass and Its Spatial Distribution in Coastal Wetlands Utilizing Planet Multispectral Imagery. *Remote Sensing*, *11*(17), 2020. https://doi.org/10.3390/rs11172020

Mo, Y., Kearney, M. S., & Turner, R. E. (2020). The resilience of coastal marshes to hurricanes: The potential impact of excess nutrients. *Environment International*, *138*, 105409. https://doi.org/10.1016/j.envint.2019.105409

Neubauer, S. C., & Craft, C. B. (2009). Global change and tidal freshwater wetlands: Scenarios and impacts. In *Tidal Freshwater Wetlands*. Margraf Publishers GmbH.

O'Donnell, J., & Schalles, J. (2016). Examination of abiotic drivers and their influence on Spartina alterniflora biomass over a twenty-eight year period using Landsat 5 TM satellite imagery of the central Georgia coast. *Remote Sensing*, *8*(6), 477. https://doi.org/10.3390/rs8060477

Ozesmi, S. L., & Bauer, M. E. (2002). Satellite remote sensing of wetlands. *Wetlands Ecology and Management*, *10*, 22.

Palomo, L., Meile, C., & Joye, S. B. (2013). Drought impacts on biogeochemistry and microbial processes in salt marsh sediments: A flow-through reactor approach. Biogeochemistry, 112(1–3), 389–407. https://doi.org/10.1007/s10533-012-9734-z

Planet Team (2017). Planet Application Program Interface: In Space for Life on Earth. San Francisco, CA. https://api.planet.com

Qi, J., Chehbouni, A., Huete, A. R., Kerr, Y. H., & Sorooshian, S. (1994). A modified soil adjusted vegetation index. *Remote Sensing of Environment*, *48*(2), 119–126. https://doi.org/10.1016/0034-4257(94)90134-1

Reimold, R. J., Gallagher, J. L., & Thompson, D. E. (1973). Remote sensing of tidal marsh. Photogrammetric Engineering and Remote Sensing, 39,477–488.

Richards, J. A. (2013). *Remote Sensing Digital Image Analysis: An Introduction*. Springer Berlin Heidelberg. https://doi.org/10.1007/978-3-642-30062-2

Roujean, J.-L., & Breon, F.-M. (1995). Estimating PAR absorbed by vegetation from bidirectional reflectance measurements. *Remote Sensing of Environment*, *51*(3), 375–384. https://doi.org/10.1016/0034-4257(94)00114-3

Rouse, J. W., Haas, R. H., Schell, J. A., & Deering, D. W. (1974). Monitoring vegetation systems in the Great Plains with ERTS. *NASA Spec. Publ*, *351*(1), 309.

Schaefer, S. C., & Alber, M. (2007). Temperature controls a latitudinal gradient in the proportion of watershed nitrogen exported to coastal ecosystems. *Biogeochemistry*, *85*(3), 333–346. https://doi.org/10.1007/s10533-007-9144-9

Sims, D. A., & Gamon, J. A. (2002). Relationships between leaf pigment content and spectral reflectance across a wide range of species, leaf structures and developmental stages. *Remote Sensing of Environment*, *81*(2), 337–354. https://doi.org/10.1016/S0034-4257(02)00010-X

Solohin, E., Widney, S. E., & Craft, C. B. (2020). Declines in plant productivity drive loss of soil elevation in a tidal freshwater marsh exposed to saltwater intrusion. *Ecology*, *101*(12). https://doi.org/10.1002/ecy.3148

Wiegert, R., & Freeman, B. (1990). Tidal salt marshes of the southeastern Atlantic coast: A community profile. *Biological Report*, *85*(7.29), 70. https://doi.org/10.2172/5032823

Wieski, K., Guo, H., Craft, C., & Pennings, S. (n.d.). *Ecosystem Functions of Tidal Fresh, Brackish, and salt Marshes on the Georgia Coast*. Retrieved October 18, 2021, from

https://mail.google.com/mail/u/0/#inbox/KtbxLrjGQDGShRtnHgKPZbVFQDhnZkcXGq?projector=1&messagePartId=0.1

Windle, A. E., Staver, L. W., Elmore, A. J., Scherer, S., Keller, S., Malmgren, B., & Silsbe, G. M. (2023). Multi-temporal high-resolution marsh vegetation mapping using unoccupied aircraft system remote sensing and machine learning. *Frontiers in Remote Sensing*, *4*, 1140999. https://doi.org/10.3389/frsen.2023.1140999

3.7 Figures and Tables

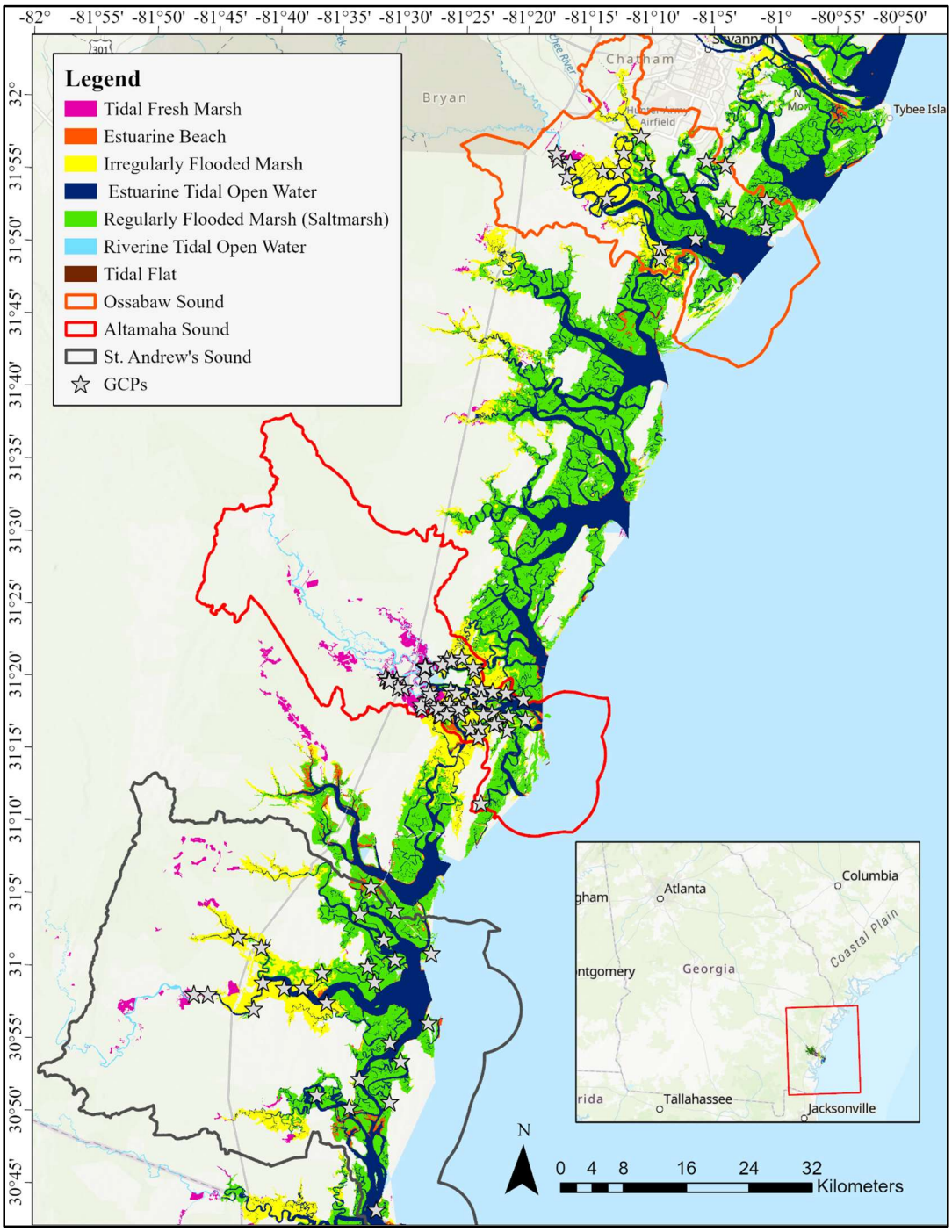

Figure 3.1 Study area of the project which includes the Ogeechee, Altamaha, and Satilla watersheds. The black line represents the extent of each of the HUC units while the red, blue, and purple show the extent of the different tidal marsh habitats based on NWI. Each of the silver stars represent a ground reference point collected in the summer of 2022.

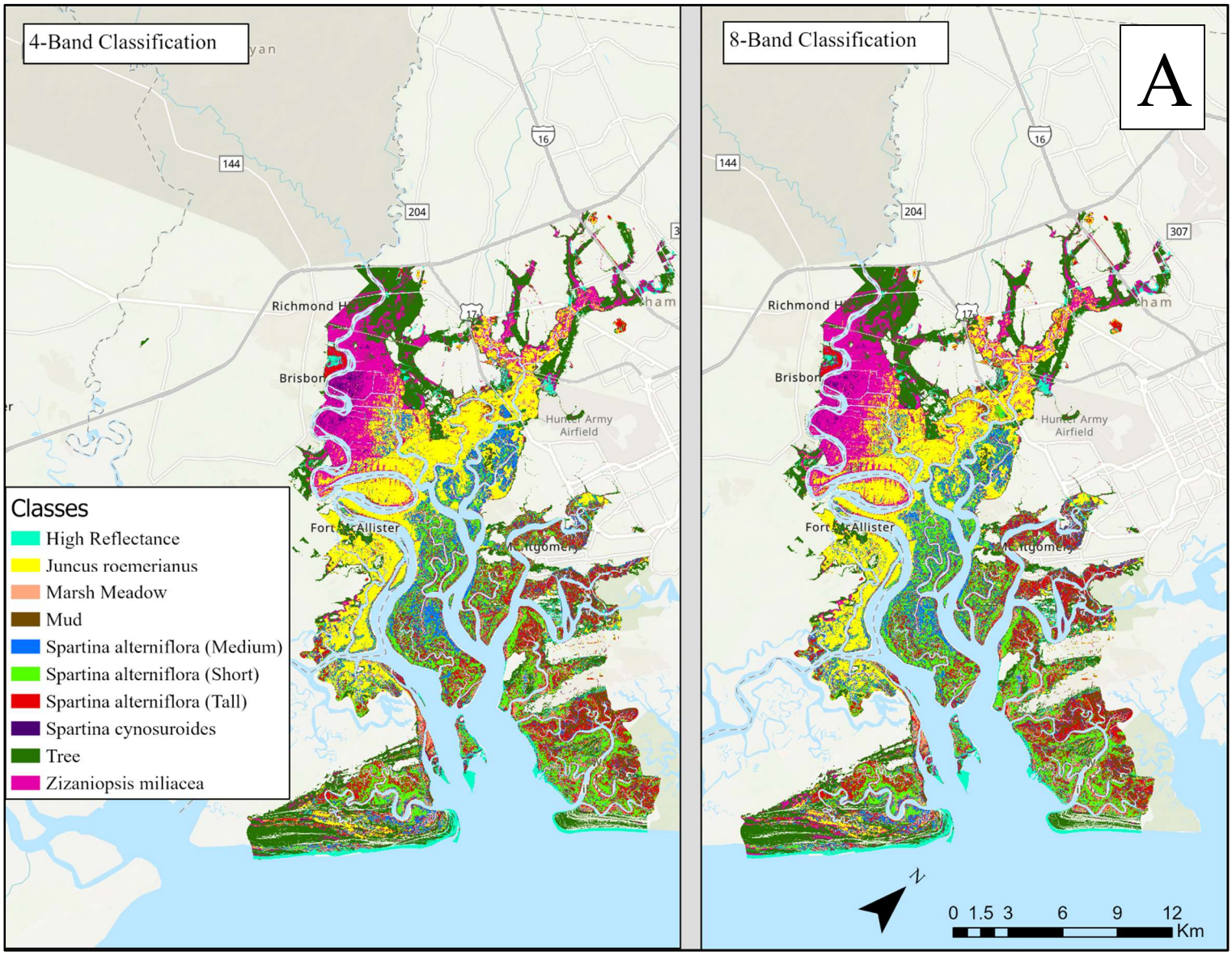
4-Band Classification
8-Band Classification
A
Classes
High Reflectance
Juncus roemerianus
Marsh Meadow
Mud
Spartina alterniflora (Medium)
Spartina alterniflora (Short)
Spartina alterniflora (Tall)
Spartina cynosuroides
Tree
Zizaniopsis miliacea
144
204
16
17
307
Hunter Army Airfield
0 1.5 3 6 9 12
Km

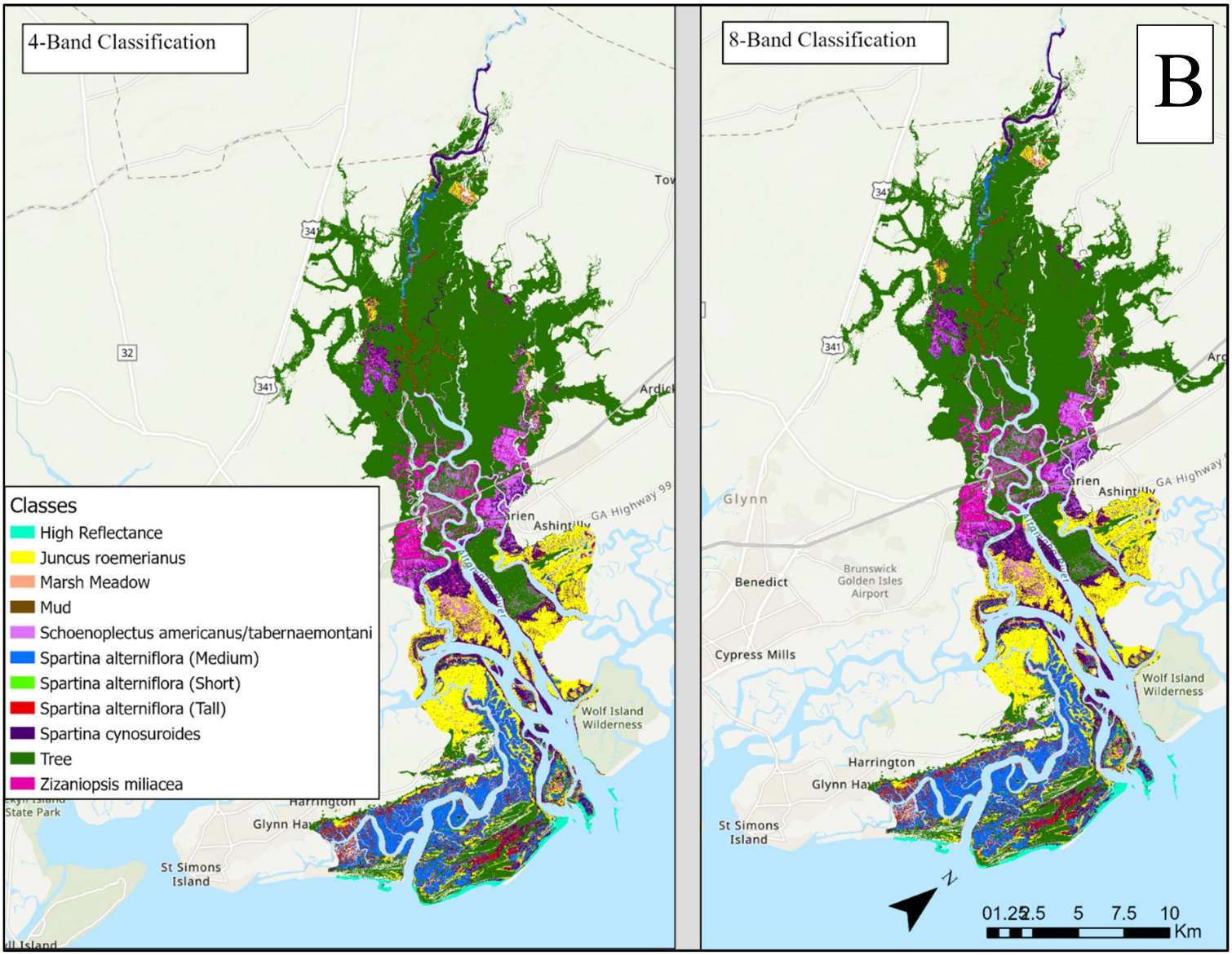
4-Band Classification
8-Band Classification
B
Classes
High Reflectance
Juncus roemerianus
Marsh Meadow
Mud
Schoenoplectus americanus/tabernaemontani
Spartina alterniflora (Medium)
Spartina alterniflora (Short)
Spartina alterniflora (Tall)
Spartina cynosuroides
Tree
Zizaniopsis miliacea
32
341
GA Highway 99
Wolf Island Wilderness
St Simons Island
Glynn
Benedict
Brunswick Golden Isles Airport
Cypress Mills
Harrington
N
0 1.25 2.5 5 7.5 10
Km

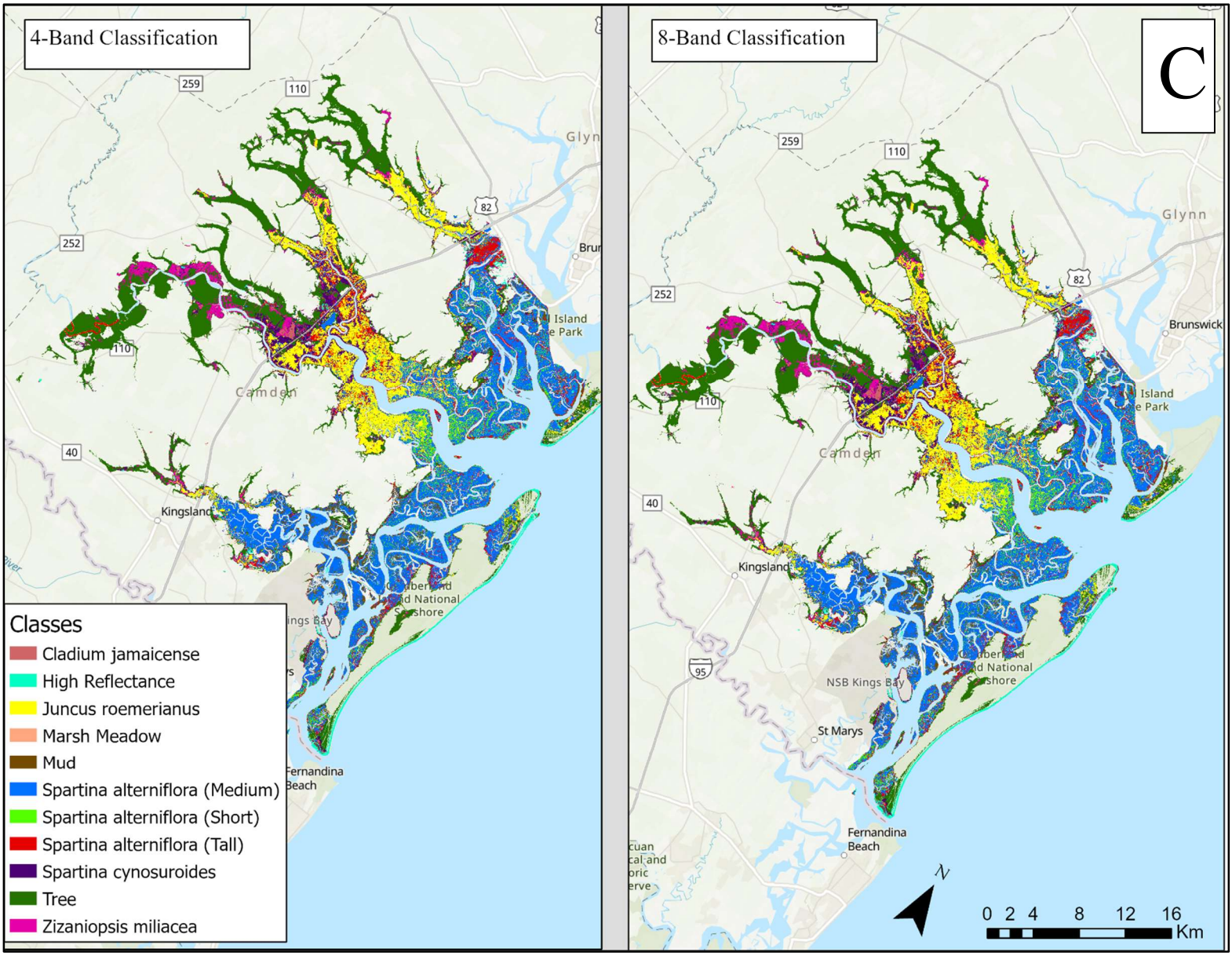

Figure 3.2 Final random forest classified imagery for the three watersheds, Ogeechee, Altamaha, and Satilla with a 3 m spatial resolution. The classified images are also compared with the 4-band classification on the left and the 8-band classification on the right. The overall classifications for the 4-band imagery were 85.6% (Ogeechee), 87.0% (Altamaha), and 74.3% (Satilla) while the 8-band classifications had an overall accuracy of 86.5% (Ogeechee), 88.1% (Altamaha), and 75.9% (Satilla). The classified images were smoothed using a majority filter in ArcGIS Pro prior to the final accuracy assessment. The images are in an order moving south starting with the Ogeechee (A), Altamaha (B), and then the Satilla (C).

Table 3.1 Names and information of the predictor variables used in the random forest classification. All predictor variables were projected to Universal Transverse Mercator (UTM) zone 17 North, NAD 1983 (National Spatial Reference System of 2011) (EPSG: 26917) with a 1-meter spatial resolution. The inputs included all PlanetScope bands, a digital elevation model (DEM), National Wetland Index (NWI), red edge chlorophyll index (CI red edge), enhanced vegetation index (EVI), green normalized difference vegetation index (GNDVI), modified red edge normalized difference vegetation index (MRENDVI), modified soil adjusted vegetation index (MSAVI, modified simple ratio (MSR), normalized difference vegetation index (NDVI), renormalized difference vegetation index, and red edge normalized difference vegetation index (RENDVI).

Predictor Rasters	Description	Spatial Resolution	Purpose	References	Data Source
PlanetScope - Costal Blue	8-band product	3 m	Vegetation classification	Planet, 2023	Planet Inc.
PlanetScope- Blue	4- and 8-band product	3 m	Vegetation classification	Planet, 2024	Planet Inc.
PlanetScope- Green	4- and 8-band product	3 m	Vegetation classification	Planet, 2025	Planet Inc.
PlanetScope- Green I	8-band product	3 m	Vegetation classification	Planet, 2026	Planet Inc.
PlanetScope- Yellow	8-band product	3 m	Vegetation classification	Planet, 2027	Planet Inc.
PlanetScope- Red	4- and 8-band product	3 m	Vegetation classification	Planet, 2028	Planet Inc.
PlanetScope- Red Edge	8-band product	3 m	Vegetation classification	Planet, 2029	Planet Inc.
PlanetScope- NRI	4- and 8-band product	3 m	Vegetation classification	Planet, 2030	Planet Inc.
Unmodifed DEM (m)	Elevation in meters	3 m	Vegetation classification	USGS, 2019	USGS
NWI (Class Integer)	Habitat classes	3 m	Used to separate habitat types	USFWS, 2018	USFWS
CI Red Edge	$\frac{NIR}{Red\ Edge} - 1$	3m	Sensitive to spectral reflectance from vegetation	Gitelson, Gritz †, et al., 2003; Gitelson, Viña, et al., 2003	Derived from PlanetScope
EVI	$2.5 * \frac{B4 - B3}{B4 + 2.5 * B3 - 7.5 * B1 + 1}$	3 m	Accounts for atmospheic conditions, canopy background, and soil reflectance	Huete et al., 2002	Derived from PlanetScope
GNDVI	$\frac{B4 - B2}{B4 + B2}$	3 m	Highlights vegetation greenness and denseness	Gitelson et al., 1996	Derived from PlanetScope
MRENDVI	$\frac{NIR - Red\ Edge}{NIR + Red\ Edge - 2 * Blue}$	3m	Corrects for leaf specular reflection	Datt, 1999; Sims & Gamon, 2002	Derived from PlanetScope
MSAVI	$\frac{2 * B4 + 1 - \sqrt{(2 * B1 + 1)^2 - 8 * (B4 - B3)}}{2}$	3 m	Accounts for soil background reflectance	Qi et al., 1994	Derived from PlanetScope
MSR	$\frac{\frac{B4}{B3} - 1}{\sqrt{\frac{B4}{B3}} + 1}$	3 m	Sensitive to biophysical parameters	Chen, 1996	Derived from PlanetScope
NDVI	$\frac{B4 - B3}{B4 + B3}$	3 m	Presence, health, and greenness of vegetation	Rouse et al., 1974	Derived from PlanetScope
RDVI	$\frac{B4 - B3}{\sqrt{B4 + B3}}$	3 m	Renormalization to enhance sensitivity to vegetation changes	Roujean & Breon, 1995	Derived from PlanetScope
RENDVI	$\frac{NIR - Red\ Edge}{NIR + Red\ Edge}$	3 m	Sensitive to small changes in canopy content and background noise	Sims & Gamon, 2002	Derived from PlanetScope

Table 3.2 Training and validation data the 4- and 8-band PlanetScope imagery for the random forest classification based on ground reference data and visual interpretation of high spatial resolution orthoimagery.

Habitat Class	Training Pixels	Validation Pixels
All Coastal Huc's	**77760**	**22303**
Dominant Class		
Cladium jamaicense	143	33
High Reflectance	6213	2418
Juncus roemerianus	16843	4082
Marsh Meadow	2031	977
Mud	2568	365
Schoenoplectus americanus and *tabernaemontani*	2813	809
Spartina alterniflora (Medium)	7732	2096
Spartina alterniflora (Short)	3327	985
Spartina alterniflora (Tall)	2408	589
Spartina cynosuroides	5313	1095
Tree	13117	5861
Zizaniopsis miliacea	15252	2993
Ossabaw Sound	**26180**	**6892**
Dominant Class		
High Reflectance	967	219
Juncus roemerianus	6155	1433
Marsh Meadow	1484	816
Mud	203	76
Spartina alterniflora (Medium)	912	456
Spartina alterniflora (Short)	1774	382
Spartina alterniflora (Tall)	1052	371
Spartina cynosuroides	270	100
Tree	2352	1327
Zizaniopsis miliacea	11011	1712
Altamaha Sound	**33887**	**11703**
Dominant Class		
High Reflectance	3599	2129
Juncus roemerianus	6258	1521
Marsh Meadow	444	100
Mud	1151	191

Schoenoplectus americanus and *tabernaemontani*	2813	809
Spartina alterniflora (Medium)	706	392
Spartina alterniflora (Short)	336	75
Spartina alterniflora (Tall)	718	148
Spartina cynosuroides	4228	927
Tree	10074	4187
Zizaniopsis miliacea	3560	1224
St. Andrew's Sound	**17693**	**3708**
Dominant Class		
Cladium jamaicense	143	33
High Reflectance	1647	70
Juncus roemerianus	4430	1128
Marsh Meadow	103	61
Mud	1214	98
Spartina alterniflora (Medium)	6114	1248
Spartina alterniflora (Short)	1217	528
Spartina alterniflora (Tall)	638	70
Spartina cynosuroides	815	68
Tree	691	347
Zizaniopsis miliacea	681	57

Table 3.3 Area coverage (kilometer squared) of the different dominant classes classified using random forest per watershed. The classes were aggregated based on the different NWI habitat class using vegetation. *Juncus roemerianus*, *Spartina cynosuroides, Schoenoplectus americanus/tabernaemontani* were combined to form brackish marsh. The salt marsh was formed by combining short, medium, and tall *Spartina alterniflora*, submerged, and marsh meadow. Tidal freshwater marshes were found to have *Cladium jamaicense* and *Zizaniopsis miliacea*.

Habitat Class	Square Kilometers (km^2) (4-Band)	Proportional Area (4-Band)	Square Kilometers (km^2) (8-Band)	Proportional Area (8-Band)
All Coastal HUCs	**1107.500**	**1.000**	**1107.113**	**1.000**
Dominant Class				
Cladium jamaicense	1.705	0.002	2.524	0.002
High Reflectance	29.777	0.027	30.132	0.027
Juncus roemerianus	160.554	0.145	165.265	0.149
Marsh Meadow	13.134	0.012	13.450	0.012
Mud	36.633	0.033	31.004	0.028
Schoenoplectus americanus and *tabernaemontani*	12.428	0.011	11.714	0.011
Spartina alterniflora (Medium)	211.603	0.191	219.392	0.198
Spartina alterniflora (Short)	69.493	0.063	64.096	0.058
Spartina alterniflora (Tall)	85.601	0.077	89.142	0.081
Spartina cynosuroides	57.060	0.052	55.521	0.050
Tree	354.108	0.320	351.133	0.317
Zizaniopsis miliacea	75.404	0.068	73.741	0.067
NWI Habitat Class	**4-Band**	**8-Band**		
Salt	386.080	386.080		
Brackish	232.500	232.500		
Tidal Freshwater	76.265	76.265		
Ossabaw Sound	**289.016172**	**1.000**	**289.075176**	**1.000**
Dominant Class				
High Reflectance	11.404	0.039	12.022	0.042
Juncus roemerianus	52.946	0.183	54.325	0.188
Marsh Meadow	7.417	0.026	7.619	0.026
Mud	8.573	0.030	8.045	0.028
Spartina alterniflora (Medium)	33.510	0.116	32.283	0.112
Spartina alterniflora (Short)	38.145	0.132	37.533	0.130

Spartina alterniflora (Tall)	38.960	0.135	39.690	0.137
Spartina cynosuroides	2.370	0.008	4.145	0.014
Tree	57.531	0.199	58.599	0.203
Zizaniopsis miliacea	38.160	0.132	34.816	0.120

NWI Habitat Class	**4-Band**	**8-Band**
Salt	0.408	117.125
Brackish	0.191	58.470
Tidal Freshwater	0.132	34.816

Altamaha Sound	**305.765991**	**1.000**	**305.574**	**1.000**
Dominant Class				
High Reflectance	5.320	0.017	4.982	0.016
Juncus roemerianus	37.386	0.122	38.822	0.127
Marsh Meadow	4.093	0.013	4.252	0.014
Mud	6.479	0.021	4.554	0.015
Schoenoplectus americanus and *tabernaemontani*	12.428	0.041	11.714	0.038
Spartina alterniflora (Medium)	30.247	0.099	30.281	0.099
Spartina alterniflora (Short)	3.025	0.010	3.222	0.011
Spartina alterniflora (Tall)	10.730	0.035	13.382	0.044
Spartina cynosuroides	23.869	0.078	22.242	0.073
Tree	152.674	0.499	151.370	0.495
Zizaniopsis miliacea	19.515	0.064	20.755	0.068

NWI Habitat Class	**4-Band**	**8-Band**
Salt	0.157	51.137
Brackish	0.241	72.777
Tidal Freshwater	0.064	20.755

St. Andrew's Sound	512.71821	1.000	512.464	1.000
Dominant Class				
Cladium jamaicense	1.705	0.003	2.524	0.005
High Reflectance	13.054	0.025	13.128	0.026
Juncus roemerianus	70.221	0.137	72.118	0.141
Marsh Meadow	1.624	0.003	1.578	0.003
Mud	21.580	0.042	18.406	0.036
Spartina alterniflora (Medium)	147.846	0.288	156.828	0.306
Spartina alterniflora (Short)	28.323	0.055	23.341	0.046
Spartina alterniflora (Tall)	35.911	0.070	36.070	0.070

Spartina cynosuroides	30.821	0.060	29.134	0.057
Tree	143.903	0.281	141.164	0.275
Zizaniopsis miliacea	17.730	0.035	18.171	0.035

NWI Habitat Class	**4-Band**	**8-Band**
Salt	0.417	217.818
Brackish	0.197	101.253
Tidal Freshwater	0.038	20.694

Table 3.4 Mean decrease in random forest accuracy values and overall ranks. The mean decrease in accuracy is a predictor of variable importance with larger decreases in accuracy indicating variables with more importance in the 4-band (A) and 8-band (B) classification. *, **, and *** indicate a tie in overall rank.

A

Predictor Variable	Ogeechee	Ogeechee rank	Altamaha	Altamaha Rank	Satilla	Satilla Rank	Mean Value	Mean Rank	Overall rank
PlanetScope- Blue Band (SR)	0.083	11	0.122	6	0.192	10	0.132	9.00	11
**PlanetScope- Green Band (SR)	0.090	9	0.170	5	0.103	3	0.121	5.67	4
PlanetScope- Red Band (SR)	0.151	5	0.163	7	0.198	7	0.171	6.33	8
PlanetScope- NIR Band (SR)	0.141	7	0.072	11	0.137	2	0.117	6.67	9
Unmodifed DEM (m)	0.084	10	0.077	12	0.227	4	0.129	8.67	10
*NWI (Class Integer)	0.195	1	0.512	1	0.066	12	0.258	4.67	2
EVI	0.033	12	0.122	10	0.070	11	0.075	11.00	12
**GNDVI	0.147	6	0.191	4	0.190	5	0.176	5.00	4
***MSAVI	0.140	8	0.124	9	0.245	1	0.170	6.00	6
MSR	0.193	2	0.216	3	0.122	8	0.177	4.33	1
*NDVI	0.185	3	0.219	2	0.119	9	0.175	4.67	2
***RDVI	0.167	4	0.161	8	0.171	6	0.167	6.00	6

B

Predictor Variable	Ogeechee	Ogeechee rank	Altamaha	Altamaha Rank	Satilla	Satilla Rank	Mean Value	Mean Rank	Overall rank
PlanetScope - Coastal Blue Band (SR)	0.022	19	0.050	16	0.038	19	0.037	18.00	19
****PlanetScope- Blue Band (SR)	0.043	16	0.084	6	0.071	14	0.066	12.00	14
**PlanetScope- Green Band (SR)	0.069	15	0.084	4	0.120	7	0.091	8.67	7
PlanetScope - Green I Band (SR)	0.079	12	0.114	7	0.134	6	0.109	8.33	6
PlanetScope - Yellow Band (SR)	0.128	4	0.102	13	0.086	12	0.105	9.67	9
PlanetScope- Red Band (SR)	0.107	6	0.130	9	0.099	8	0.112	7.67	5
PlanetScope- Red Edge Band (SR)	0.039	17	0.053	12	0.075	13	0.056	14.00	16
***PlanetScope- NIR Band (SR)	0.074	13	0.057	15	0.182	2	0.104	10.00	10
***Unmodifed DEM (m)	0.095	10	0.058	17	0.160	3	0.104	10.00	10
NWI (Class Integer)	0.022	18	0.236	1	0.054	15	0.104	11.33	13
****CI Red Edge	0.100	8	0.066	11	0.050	17	0.072	12.00	14
EVI	0.070	14	0.016	19	0.086	11	0.057	14.67	17
*GNDVI	0.124	5	0.153	5	0.138	4	0.139	4.67	2
MRENDVI	0.095	9	0.033	18	0.039	18	0.056	15.00	18
**MSAVI	0.083	11	0.063	14	0.197	1	0.115	8.67	7
MSR	0.154	2	0.163	2	0.090	9	0.136	4.33	1
*NDVI	0.158	1	0.164	3	0.089	10	0.137	4.67	2
RDVI	0.142	3	0.099	8	0.136	5	0.126	5.33	4
RENDVI	0.102	7	0.064	10	0.053	16	0.073	11.00	12

Table 3.5 Averaged spectral separability across the three different watersheds. The Jeffries-Matusita distance was used in order to determine the average difference between all classes using ENVI 5.6.1 spectral separability tool. Any value above 1.8 is to be considered spectrally different while the lower values represent classes that are not as spectrally separable.

Dominant Class	*Cladium jamaicense*	High Reflectance	*Juncus roemerianus*	Marsh Meadow	Mud	*Schoenoplectus americanus* and *tabernaemontani*	*Spartina alterniflora* (Medium)	*Spartina alterniflora* (Short)	*Spartina alterniflora* (Tall)	*Spartina cynosuroides*	Tree	*Zizaniopsis miliacea*
						4-Band						
Cladium jamaicense												
High Reflectance	1.999											
Juncus roemerianus	2.000	1.963										
Marsh Meadow	1.972	1.901	1.764									
Mud	2.000	1.848	1.903	1.749								
Schoenoplectus americanus and *tabernaemontani*	N/A	1.995	1.995	1.817	2.000							
Spartina alterniflora (Medium)	1.999	1.888	1.499	1.330	1.416	1.917						
Spartina alterniflora (Short)	2.000	1.985	1.582	1.419	1.475	1.802	0.513					
Spartina alterniflora (Tall)	1.999	5.687	1.482	1.145	1.623	1.494	0.944	1.158				
Spartina cynosuroides	1.275	1.695	1.877	1.507	1.999	0.703	1.912	1.898	1.545			
Tree	2.000	1.937	1.993	1.996	1.998	1.964	1.988	1.997	1.933	1.905		
Zizaniopsis miliacea	1.504	1.824	1.878	1.860	1.995	0.752	1.930	1.953	1.682	0.857	1.534	
						8-Band						
Cladium jamaicense												
High Reflectance	2.000											
Juncus roemerianus	2.000	1.979										
Marsh Meadow	1.998	1.935	1.885									
Mud	2.000	1.956	1.924	1.821								
Schoenoplectus americanus and *tabernaemontani*	N/A	2.000	1.883	1.996	2.000							
Spartina alterniflora (Medium)	2.000	1.930	1.652	1.596	1.705	1.983						
Spartina alterniflora (Short)	2.000	1.963	1.768	1.672	1.650	1.955	0.798					
Spartina alterniflora (Tall)	1.986	1.912	1.889	1.483	1.771	1.993	1.262	1.352				
Spartina cynosuroides	1.541	1.990	1.968	1.909	2.000	1.761	1.978	1.972	1.875			
Tree	2.000	1.995	1.997	1.998	2.000	1.997	2.000	2.000	1.965	1.878		
Zizaniopsis miliacea	1.732	1.990	1.947	1.979	2.000	1.002	1.984	1.993	1.952	1.611	1.775	

Table 3.6 Random Forest classification confusion matrix for the Ogeechee (A), Altamaha (B) and Satilla (C). The rows represent the image data (the classified pixel) while the columns represent the reference data (what the pixel is based on reference data). The shaded cells represent the classification accuracy for each of the classes which is equivalent to the producer's accuracy.

A

4-Band Classification											
	Ground reference										
Classified	High Reflectance	Juncus roemerianus	Marsh Meadow	Mud	Schoenoplectus americanus and tabernaemontani	Spartina alterniflora (Medium)	Spartina alterniflora (Short)	Spartina alterniflora (Tall)	Spartina cynosuroides	Tree	Zizaniopsis miliacea
High Reflectance	0.996	0.014	0.688	0.304	0.000	0.000	0.000	0.057	0.088	0.000	0.000
Juncus roemerianus	0.000	0.840	0.000	0.000	0.161	0.000	0.000	0.007	0.085	0.000	0.001
Marsh Meadow	0.001	0.001	0.305	0.000	0.009	0.000	0.000	0.000	0.003	0.000	0.005
Mud	0.000	0.000	0.000	0.669	0.000	0.000	0.095	0.000	0.001	0.000	0.000
Schoenoplectus americanus and tabernaemontani	0.000	0.079	0.000	0.000	0.771	0.000	0.000	0.000	0.077	0.000	0.038
Spartina alterniflora (Medium)	0.003	0.055	0.004	0.000	0.035	0.750	0.524	0.092	0.002	0.000	0.000
Spartina alterniflora (Short)	0.000	0.000	0.000	0.000	0.000	0.196	0.333	0.000	0.000	0.000	0.000
Spartina alterniflora (Tall)	0.001	0.000	0.000	0.028	0.000	0.048	0.048	0.610	0.025	0.001	0.000
Spartina cynosuroides	0.000	0.012	0.004	0.000	0.006	0.006	0.000	0.227	0.607	0.001	0.116
Tree	0.000	0.000	0.000	0.000	0.000	0.000	0.000	0.000	0.001	0.996	0.009
Zizaniopsis miliacea	0.000	0.000	0.000	0.000	0.018	0.000	0.000	0.007	0.113	0.002	0.831
Overall Accuracy: 0.870											
	8-Band Classification										
High Reflectance	0.997	0.000	0.691	0.000	0.000	0.000	0.000	0.156	0.070	0.000	0.000
Juncus roemerianus	0.000	0.863	0.000	0.000	0.192	0.003	0.000	0.011	0.102	0.000	0.001
Marsh Meadow	0.001	0.000	0.295	0.000	0.000	0.000	0.000	0.000	0.000	0.000	0.000
Mud	0.000	0.000	0.000	0.934	0.000	0.000	0.118	0.022	0.001	0.000	0.000
Schoenoplectus americanus and tabernaemontani	0.000	0.057	0.000	0.000	0.777	0.000	0.000	0.000	0.080	0.000	0.033
Spartina alterniflora (Medium)	0.002	0.069	0.003	0.000	0.000	0.755	0.647	0.134	0.000	0.000	0.000
Spartina alterniflora (Short)	0.000	0.000	0.000	0.000	0.000	0.206	0.235	0.000	0.000	0.000	0.000
Spartina alterniflora (Tall)	0.000	0.000	0.006	0.066	0.000	0.036	0.000	0.570	0.014	0.001	0.000
Spartina cynosuroides	0.000	0.010	0.006	0.000	0.016	0.000	0.000	0.102	0.655	0.000	0.104
Tree	0.000	0.000	0.000	0.000	0.000	0.000	0.000	0.000	0.002	0.997	0.006
Zizaniopsis miliacea	0.000	0.001	0.000	0.000	0.016	0.000	0.000	0.005	0.076	0.002	0.856
Overall Accuracy: 0.881											

B

4-Band Classification

Classified	Ground Reference: High Reflectance	Juncus roemerianus	Marsh Meadow	Mud	Spartina alterniflora (Medium)	Spartina alterniflora (Short)	Spartina alterniflora (Tall)	Spartina cynosuroides	Tree	Zizaniopsis miliacea
High Reflectance	0.995	0.008	0.000	0.000	0.012	0.000	0.009	0.000	0.015	0.000
Juncus roemerianus	0.000	0.958	0.143	0.000	0.028	0.002	0.061	0.117	0.000	0.002
Marsh Meadow	0.000	0.002	0.777	0.000	0.056	0.273	0.064	0.039	0.001	0.000
Mud	0.000	0.000	0.000	1.000	0.000	0.000	0.000	0.000	0.000	0.000
Spartina alterniflora (Medium)	0.005	0.002	0.007	0.000	0.681	0.223	0.205	0.000	0.000	0.000
Spartina alterniflora (Short)	0.000	0.021	0.025	0.000	0.093	0.445	0.059	0.000	0.000	0.000
Spartina alterniflora (Tall)	0.000	0.004	0.050	0.000	0.130	0.057	0.580	0.000	0.000	0.002
Spartina cynosuroides	0.000	0.006	0.000	0.000	0.000	0.000	0.021	0.831	0.000	0.011
Tree	0.000	0.000	0.000	0.000	0.000	0.000	0.000	0.000	0.965	0.000
Zizaniopsis miliacea	0.000	0.000	0.000	0.000	0.000	0.000	0.000	0.013	0.019	0.985
Overall Accuracy: 0.856										

8-Band Classification

High Reflectance	0.995	0.008	0.000	0.000	0.012	0.000	0.009	0.000	0.010	0.000
Juncus roemerianus	0.000	0.958	0.143	0.000	0.028	0.002	0.061	0.117	0.000	0.002
Marsh Meadow	0.000	0.002	0.777	0.000	0.056	0.273	0.064	0.039	0.001	0.000
Mud	0.000	0.000	0.000	1.000	0.000	0.000	0.000	0.000	0.000	0.000
Spartina alterniflora (Medium)	0.005	0.002	0.007	0.000	0.681	0.223	0.205	0.000	0.000	0.000
Spartina alterniflora (Short)	0.000	0.021	0.025	0.000	0.093	0.445	0.059	0.000	0.000	0.000
Spartina alterniflora (Tall)	0.000	0.004	0.050	0.000	0.130	0.057	0.580	0.000	0.000	0.002
Spartina cynosuroides	0.000	0.006	0.000	0.000	0.000	0.000	0.021	0.831	0.000	0.011
Tree	0.000	0.000	0.000	0.000	0.000	0.000	0.000	0.000	0.976	0.000
Zizaniopsis miliacea	0.000	0.000	0.000	0.000	0.000	0.000	0.000	0.013	0.013	0.985
Overall Accuracy: 0.865										

C

4-Band Classification

Classified	Ground Reference: Cladium jamaicense	High Reflectance	Juncus roemerianus	Marsh Meadow	Mud	Spartina alterniflora (Medium)	Spartina alterniflora (Short)	Spartina alterniflora (Tall)	Spartina cynosuroides	Tree	Zizaniopsis miliacea
Cladium jamaicense	0.966	0.000	0.000	0.000	0.000	0.000	0.000	0.000	0.000	0.000	0.083
High Reflectance	0.000	1.000	0.000	0.000	0.000	0.000	0.000	0.000	0.000	0.000	0.000
Juncus roemerianus	0.000	0.000	0.934	0.000	0.000	0.054	0.000	0.039	0.739	0.000	0.000
Marsh Meadow	0.000	0.000	0.005	1.000	0.000	0.001	0.017	0.476	0.000	0.000	0.000
Mud	0.000	0.000	0.000	0.000	0.539	0.004	0.006	0.019	0.000	0.000	0.000
Spartina alterniflora (Medium)	0.000	0.000	0.045	0.000	0.000	0.690	0.320	0.087	0.000	0.000	0.000
Spartina alterniflora (Short)	0.000	0.000	0.015	0.000	0.000	0.234	0.652	0.097	0.000	0.000	0.000
Spartina alterniflora (Tall)	0.000	0.000	0.000	0.000	0.462	0.017	0.006	0.252	0.029	0.000	0.000
Spartina cynosuroides	0.000	0.000	0.002	0.000	0.000	0.001	0.000	0.019	0.232	0.000	0.000
Tree	0.000	0.000	0.000	0.000	0.000	0.000	0.000	0.000	0.000	1.000	0.000
Zizaniopsis miliacea	0.035	0.000	0.000	0.000	0.000	0.000	0.000	0.010	0.000	0.000	0.917
Overall Accuracy: 0.743											

8-Band Classification

Cladium jamaicense	0.917	0.000	0.000	0.000	0.000	0.000	0.000	0.000	0.000	0.000	0.000
High Reflectance	0.000	1.000	0.000	0.000	0.000	0.000	0.000	0.000	0.000	0.000	0.000
Juncus roemerianus	0.000	0.000	0.929	0.000	0.000	0.058	0.000	0.212	0.712	0.000	0.000
Marsh Meadow	0.000	0.000	0.006	1.000	0.000	0.001	0.005	0.381	0.000	0.000	0.000
Mud	0.000	0.000	0.000	0.000	0.583	0.003	0.010	0.017	0.000	0.000	0.000
Spartina alterniflora (Medium)	0.000	0.000	0.049	0.000	0.000	0.698	0.263	0.000	0.000	0.000	0.000
Spartina alterniflora (Short)	0.000	0.000	0.014	0.000	0.000	0.221	0.717	0.085	0.000	0.000	0.000
Spartina alterniflora (Tall)	0.000	0.000	0.002	0.000	0.417	0.018	0.005	0.246	0.014	0.000	0.000
Spartina cynosuroides	0.000	0.000	0.000	0.000	0.000	0.001	0.000	0.051	0.274	0.000	0.000
Tree	0.000	0.000	0.000	0.000	0.000	0.000	0.000	0.000	0.000	1.000	0.000
Zizaniopsis miliacea	0.083	0.000	0.000	0.000	0.000	0.000	0.000	0.009	0.000	0.000	1.000
Overall Accuracy: 0.759											

Table 3.7 Random Forest error matrix for the 3 different watersheds where A represents the Ogeechee, B Altamaha, and C Satilla. The producer's accuracy is the probability of correctly classified pixels while the user's accuracy is the probability that the predicted value is that class. The error of omission is a measure of false negatives while the error of commission is a measure of false positives.

A

	Producer Error	User Error	Error of Omission	Error of Commission
4-Band Classification				
High Reflectance	0.995	0.854	0.005	0.146
Juncus roemerianus	0.958	0.890	0.042	0.110
Marsh Meadow	0.776	0.728	0.224	0.272
Mud	1.000	1.000	0.000	0.000
Spartina alterniflora (Medium)	0.681	0.482	0.319	0.518
Spartina alterniflora (Short)	0.445	0.732	0.555	0.268
Spartina alterniflora (Tall)	0.580	0.663	0.420	0.337
Spartina cynosuroides	0.831	0.640	0.169	0.360
Tree	0.965	1.000	0.035	0.000
Zizaniopsis miliacea	0.985	0.989	0.015	0.011
8-Band Classification				
High Reflectance	0.995	0.854	0.005	0.146
Juncus roemerianus	0.958	0.890	0.042	0.110
Marsh Meadow	0.777	0.728	0.224	0.272
Mud	1.000	1.000	0.000	0.000
Spartina alterniflora (Medium)	0.681	0.483	0.319	0.518
Spartina alterniflora (Short)	0.445	0.732	0.555	0.268
Spartina alterniflora (Tall)	0.580	0.663	0.420	0.337
Spartina cynosuroides	0.831	0.640	0.169	0.360
Tree	0.976	1.000	0.024	0.000
Zizaniopsis miliacea	0.985	0.989	0.015	0.011

B

Dominant Class	Producer Error	User Error	Error of Omission	Error of Commission
4-Band Classification				
High Reflectance	0.996	0.824	0.004	0.177
Juncus roemerianus	0.840	0.858	0.160	0.142
Marsh Meadow	0.305	0.830	0.695	0.170
Mud	0.669	0.976	0.332	0.024
Schoenoplectus americanus and *tabernaemontani*	0.771	0.675	0.229	0.325
Spartina alterniflora (Medium)	0.750	0.635	0.250	0.365
Spartina alterniflora (Short)	0.333	0.097	0.667	0.903
Spartina alterniflora (Tall)	0.610	0.610	0.390	0.390
Spartina cynosuroides	0.607	0.776	0.393	0.224
Tree	0.996	0.997	0.004	0.003
Zizaniopsis miliacea	0.831	0.871	0.169	0.129
8-Band Classification				
High Reflectance	0.997	0.840	0.003	0.160
Juncus roemerianus	0.863	0.825	0.138	0.175
Marsh Meadow	0.295	0.990	0.705	0.010
Mud	0.934	0.942	0.066	0.058
Schoenoplectus americanus and *tabernaemontani*	0.777	0.732	0.223	0.268
Spartina alterniflora (Medium)	0.755	0.637	0.246	0.363
Spartina alterniflora (Short)	0.235	0.056	0.765	0.944
Spartina alterniflora (Tall)	0.570	0.721	0.430	0.279
Spartina cynosuroides	0.655	0.801	0.345	0.199
Tree	0.997	0.998	0.003	0.002
Zizaniopsis miliacea	0.856	0.911	0.144	0.089

C

Dominant Class	Producers Accuracy	User Accuracy	Error of Omission	Error of Commission
4-Band Classification				
Cladium jamaicense	0.966	0.849	0.035	0.152
High Reflectance	1.000	1.000	0.000	0.000
Juncus roemerianus	0.934	0.739	0.066	0.262
Marsh Meadow	1.000	0.066	0.000	0.934
Mud	0.539	0.438	0.462	0.563
Spartina alterniflora (Medium)	0.690	0.915	0.310	0.085
Spartina alterniflora (Short)	0.652	0.221	0.348	0.780
Spartina alterniflora (Tall)	0.252	0.377	0.748	0.623
Spartina cynosuroides	0.232	0.927	0.768	0.074
Tree	1.000	1.000	0.000	0.000
Zizaniopsis miliacea	0.917	0.965	0.083	0.035
8-Band Classification				
Cladium jamaicense	0.917	1.000	0.083	0.000
High Reflectance	1.000	1.000	0.000	0.000
Juncus roemerianus	0.929	0.755	0.071	0.245
Marsh Meadow	1.000	0.148	0.000	0.853
Mud	0.583	0.438	0.417	0.563
Spartina alterniflora (Medium)	0.698	0.923	0.302	0.077
Spartina alterniflora (Short)	0.717	0.264	0.284	0.736
Spartina alterniflora (Tall)	0.246	0.420	0.754	0.580
Spartina cynosuroides	0.274	0.882	0.726	0.118
Tree	1.000	1.000	0.000	0.000
Zizaniopsis miliacea	1.000	0.930	0.000	0.070

CHAPTER 4

CONCLUSION

The objective of this study was to map the species distributions of all tidal marshes along the Georgia coast using remote sensing. This was achieved through the following objectives:

1. Creating a coastwide classification of tidal marsh species using high-resolution aerial orthoimagery.
2. Mapping species distribution in the three major tidal freshwater watersheds using a single image of high resolution PlanetScope imagery.

In Chapter 2, we were able to map 12 different upland and marsh classes using high resolution aerial orthoimagery with an overall accuracy of 86.3%. This study improved upon previous studies by providing a more detailed map that included tidal freshwater marshes and had an individual J. roemerianus class. This also demonstrated that a coastwide classification using high-resolution aerial orthoimagery can be achieved using a random forest classifier. This classification was comparable to other studies in similar habitats and locations while incorporating an important, diverse, and biogeochemically active system. With this classification, we were also able to gain a better understanding of the current species distribution of the Georgia coast which will allow for the understanding of current ecological services and the loss or gain of habitat based on previous classifications.

In Chapter 3, we were also able to accurately map the Ogeechee, Altamaha, and Satilla coastal watershed HUCs with an accuracy of 86.5%, 88.1%, and 75.9%, respectively. Depending on the area, we were able to accurately predict the distribution of *Z. miliacea*, the tidal freshwater marshes dominant species, 83.1% to 100% of the time using validation data. This information

allows us to accurately represent the presence of tidal freshwater marshes. With this, we found that the distribution of tidal freshwater marshes comprises 72.6 km2 of the 646.5 km2 of marshes found within these HUCs. Among all the HUCs, tidal marshes make up 53.9 km2 of the 2,427.3 which makes up 11.2% and 2.2% of the areas respectively. This also shows the differences between the aerial and PlanetScope imagery in predicting tidal freshwater marsh extent.

All tidal marshes are threatened by various anthropogenic factors such as pollution, coastal development, and climate change-related factors such as sea level rise, drought, and strengthened tropical events. These systems provide ecosystem services such as habitat and nurseries, carbon sequestration, nutrient cycling, physical coastline protection, and many other biogeochemical processes. Due to these services, it is vital to continue monitoring these systems in order to better understand the changes happening in these marshes over time. In the future, we will refine the classification and potentially rearrange classes to better represent previous studies. This will be done to reduce errors and provide a better understanding of tidal marsh extent.

APPENDIX A: CLASSIFICATIONS AND ACCURACY ASSESSMENT PER HUC USING AERIAL ORTHOIMAGERY

Figure A1. The final random forest classified images for each of the individual HUC units. (A) Wassaw Sound, (B) Ossabaw Sound, (C) St. Catherine's Sound, (D) Sapelo Sound, (E) Doboy Sound, (F) Altamaha Sound, (G) St Simon's Sound, (H) St. Andrew's Sound, (I) Cumberland Sound. The random forest classification included the following predictor rasters: Aerial Orthoimagery bands (blue, green, red, and NIR), DEM, NWI, and 6 vegetation indices that included: EVI, GNDVI, MSAVI, MSR, NDVI, and RDVI. Upon completion of the classification, the images were smoother using the ArcGIS tool majority filter which was set to 4.

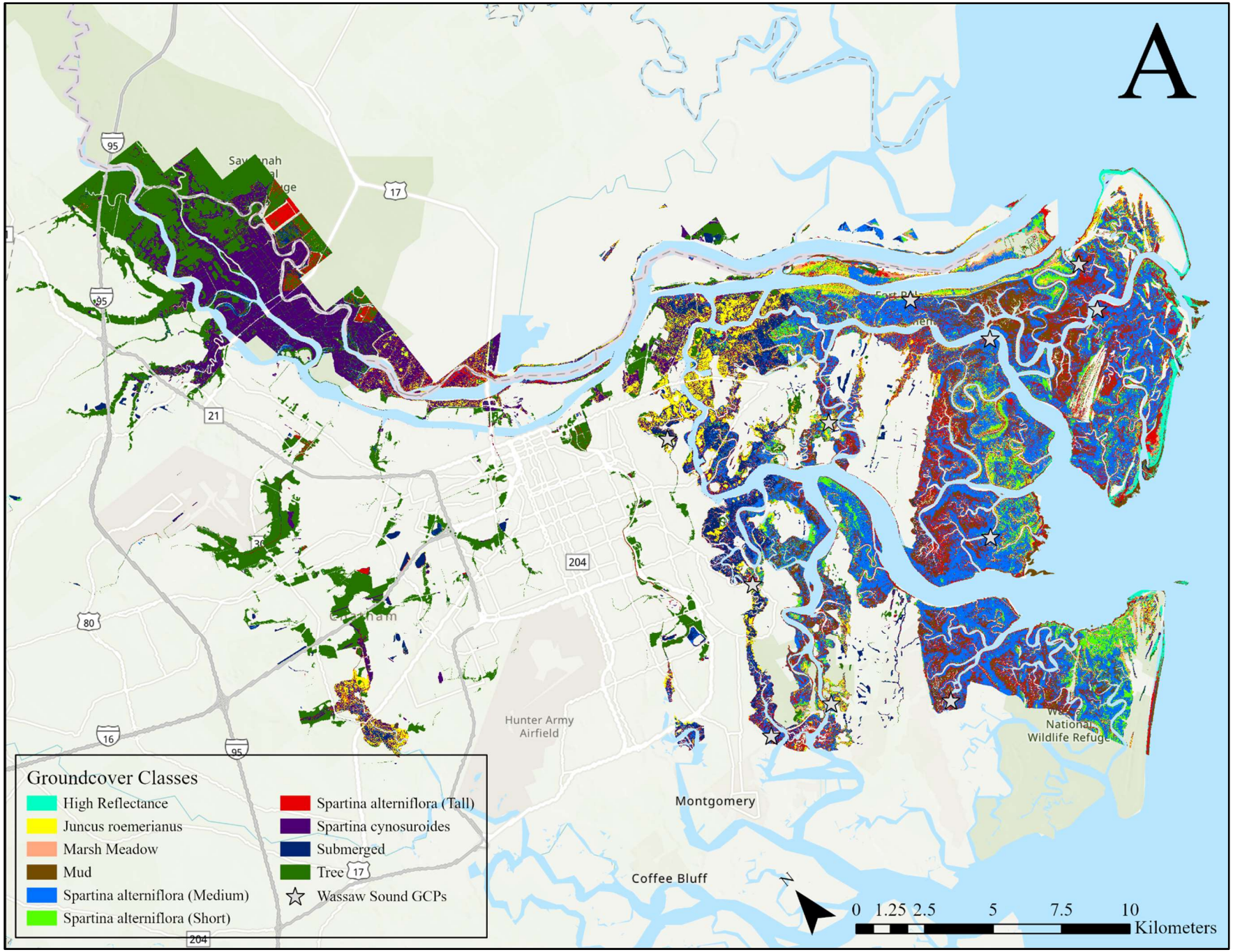
A
Groundcover Classes
High Reflectance
Juncus roemerianus
Marsh Meadow
Mud
Spartina alterniflora (Medium)
Spartina alterniflora (Short)
Spartina alterniflora (Tall)
Spartina cynosuroides
Submerged
Tree
Wassaw Sound GCPs
Hunter Army Airfield
Montgomery
Coffee Bluff
0 1.25 2.5 5 7.5 10
Kilometers

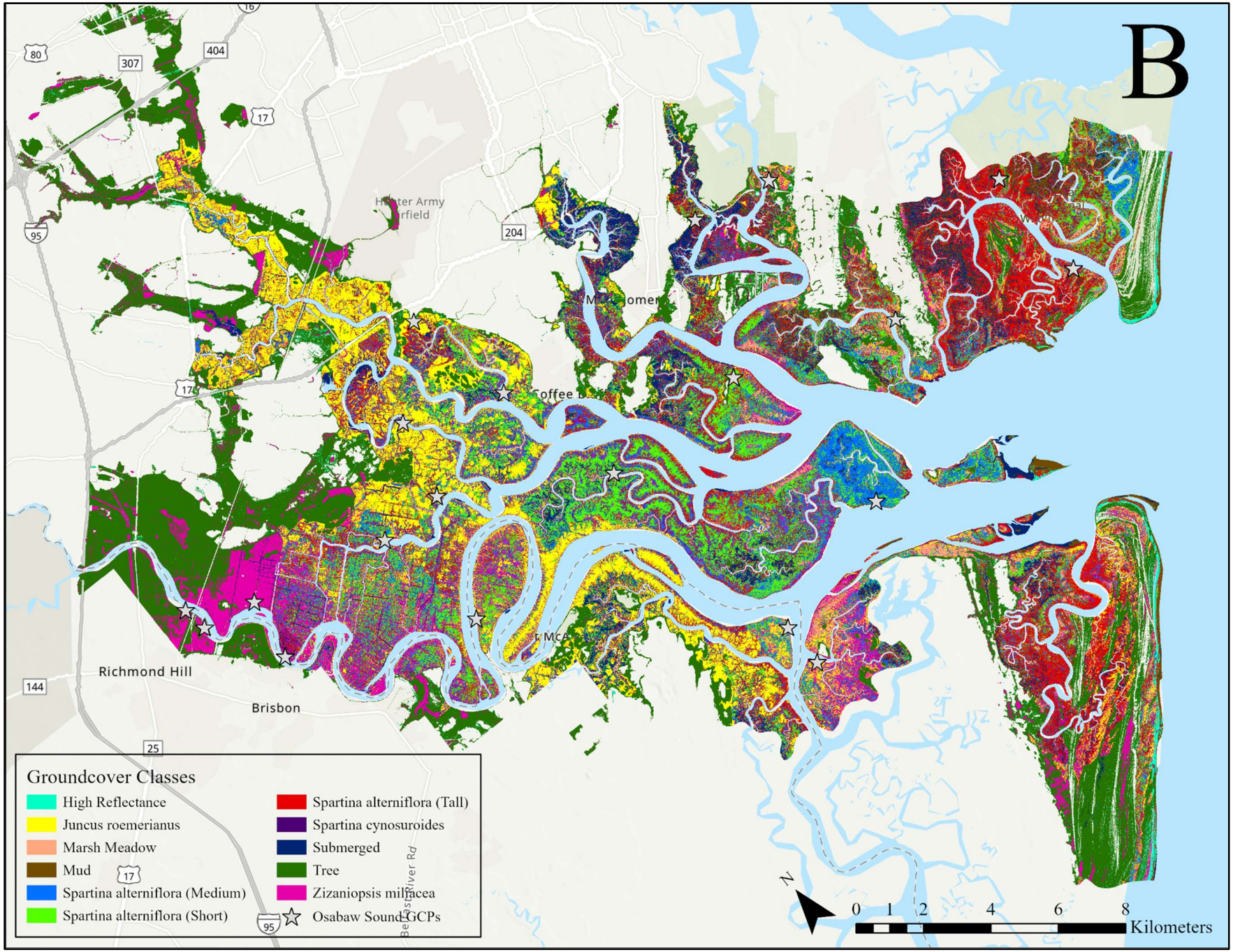
B
Richmond Hill
Brisbon
Groundcover Classes
High Reflectance
Juncus roemerianus
Marsh Meadow
Mud
Spartina alterniflora (Medium)
Spartina alterniflora (Short)
Spartina alterniflora (Tall)
Spartina cynosuroides
Submerged
Tree
Zizaniopsis milliacea
Osabaw Sound GCPs
N
0 1 2 4 6 8
Kilometers

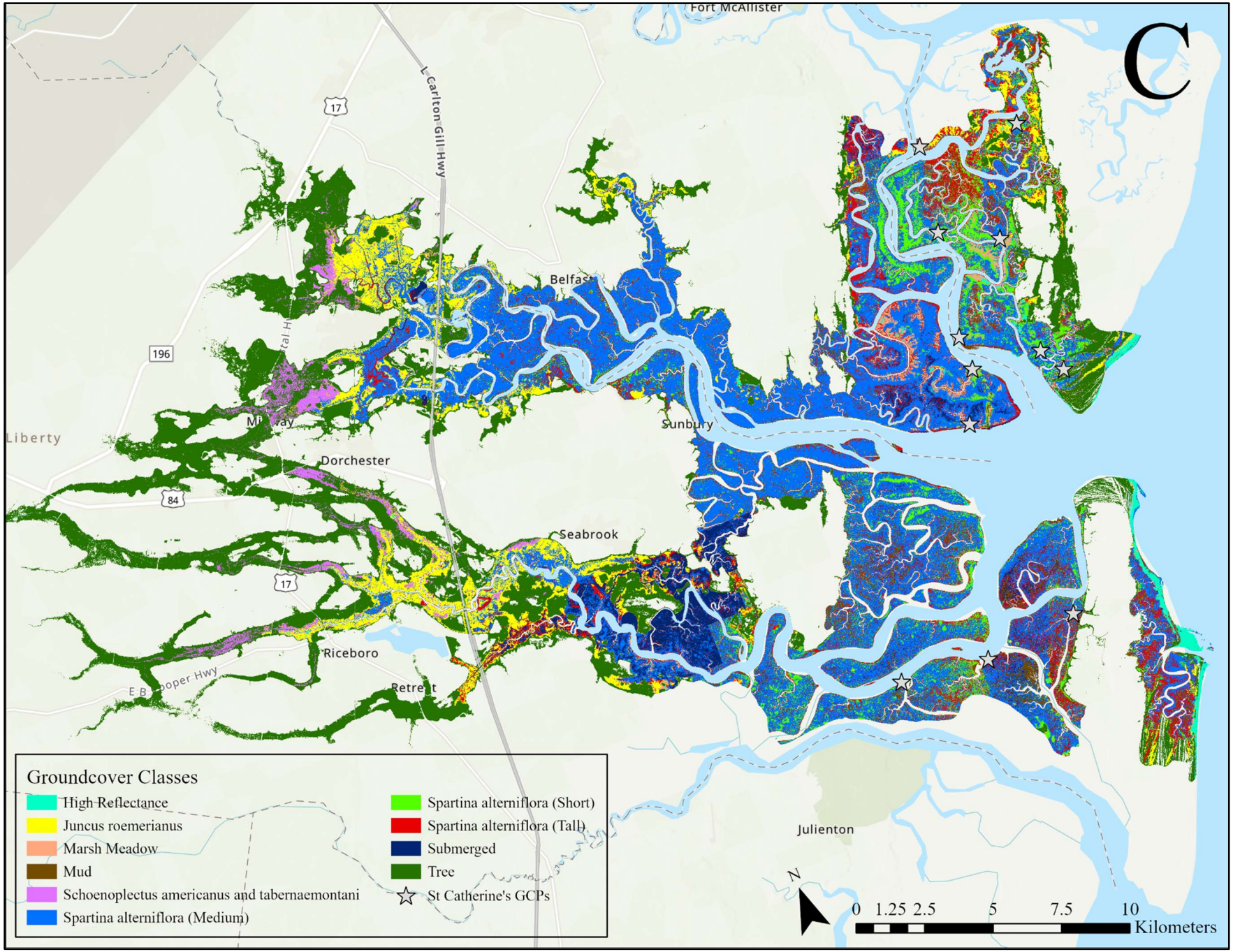
C
Fort McAllister
L Carlton Gill Hwy
17
196
84
Liberty
Dorchester
Belfast
Sunbury
Seabrook
Riceboro
Julienton
Groundcover Classes
High Reflectance
Juncus roemerianus
Marsh Meadow
Mud
Schoenoplectus americanus and tabernaemontani
Spartina alterniflora (Medium)
Spartina alterniflora (Short)
Spartina alterniflora (Tall)
Submerged
Tree
St Catherine's GCPs
N
0 1.25 2.5 5 7.5 10
Kilometers

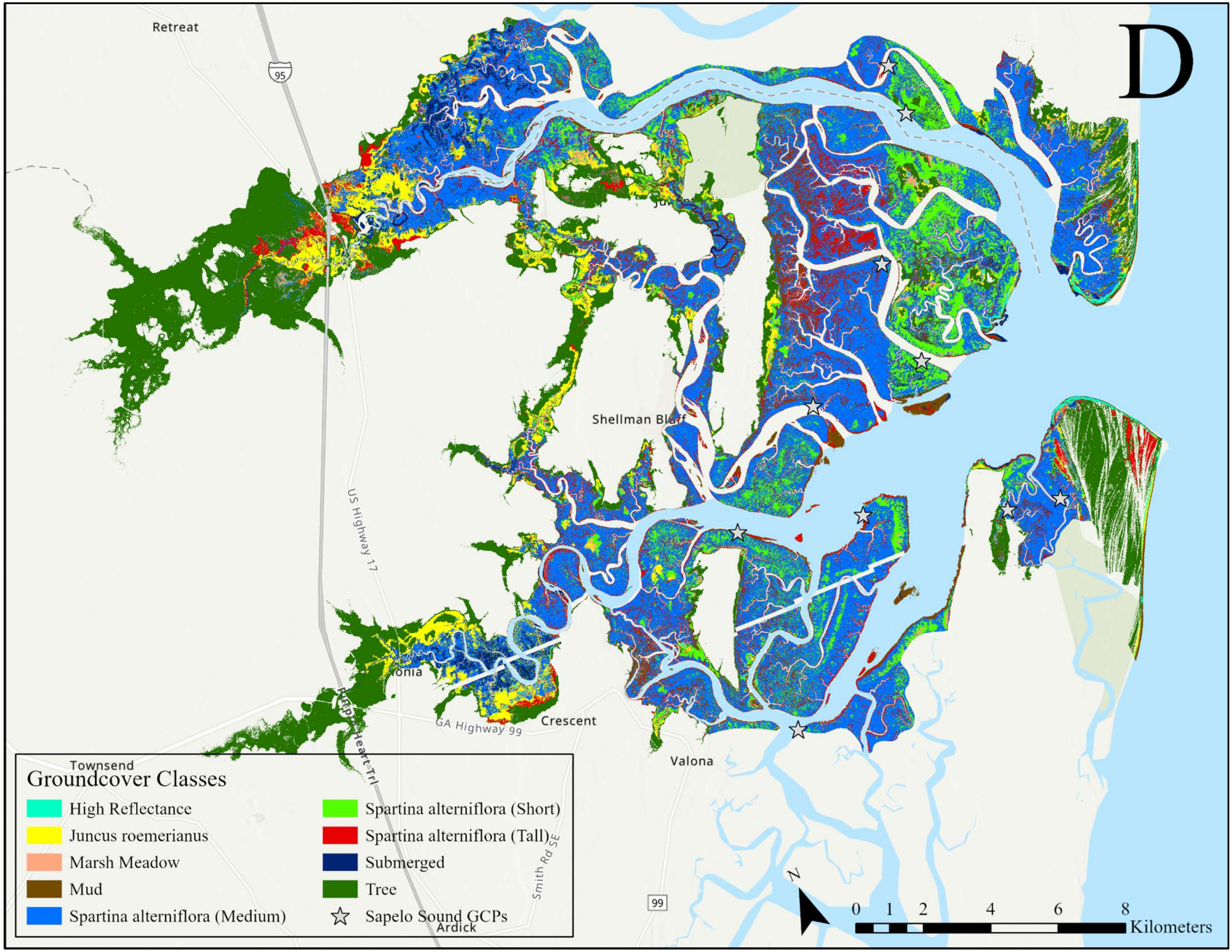
D
Retreat
95
Shellman Bluff
US Highway 17
GA Highway 99
Crescent
Valona
Townsend
Ardick
Smith Rd SE
99
Groundcover Classes
High Reflectance
Juncus roemerianus
Marsh Meadow
Mud
Spartina alterniflora (Medium)
Spartina alterniflora (Short)
Spartina alterniflora (Tall)
Submerged
Tree
Sapelo Sound GCPs
N
0 1 2 4 6 8
Kilometers

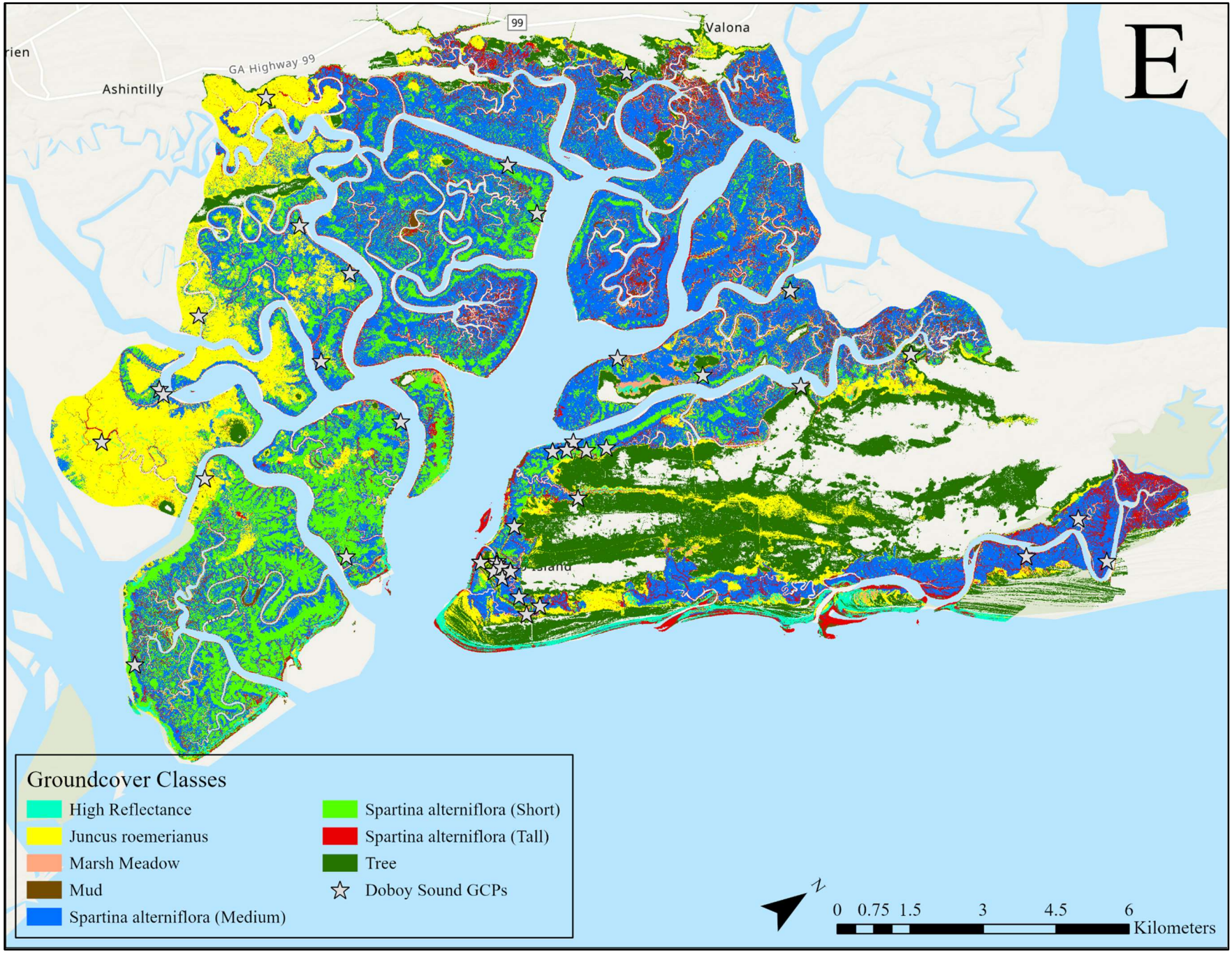
E
99
Valona
GA Highway 99
Ashintilly
Groundcover Classes
High Reflectance
Juncus roemerianus
Marsh Meadow
Mud
Spartina alterniflora (Medium)
Spartina alterniflora (Short)
Spartina alterniflora (Tall)
Tree
Doboy Sound GCPs
N
0 0.75 1.5 3 4.5 6
Kilometers

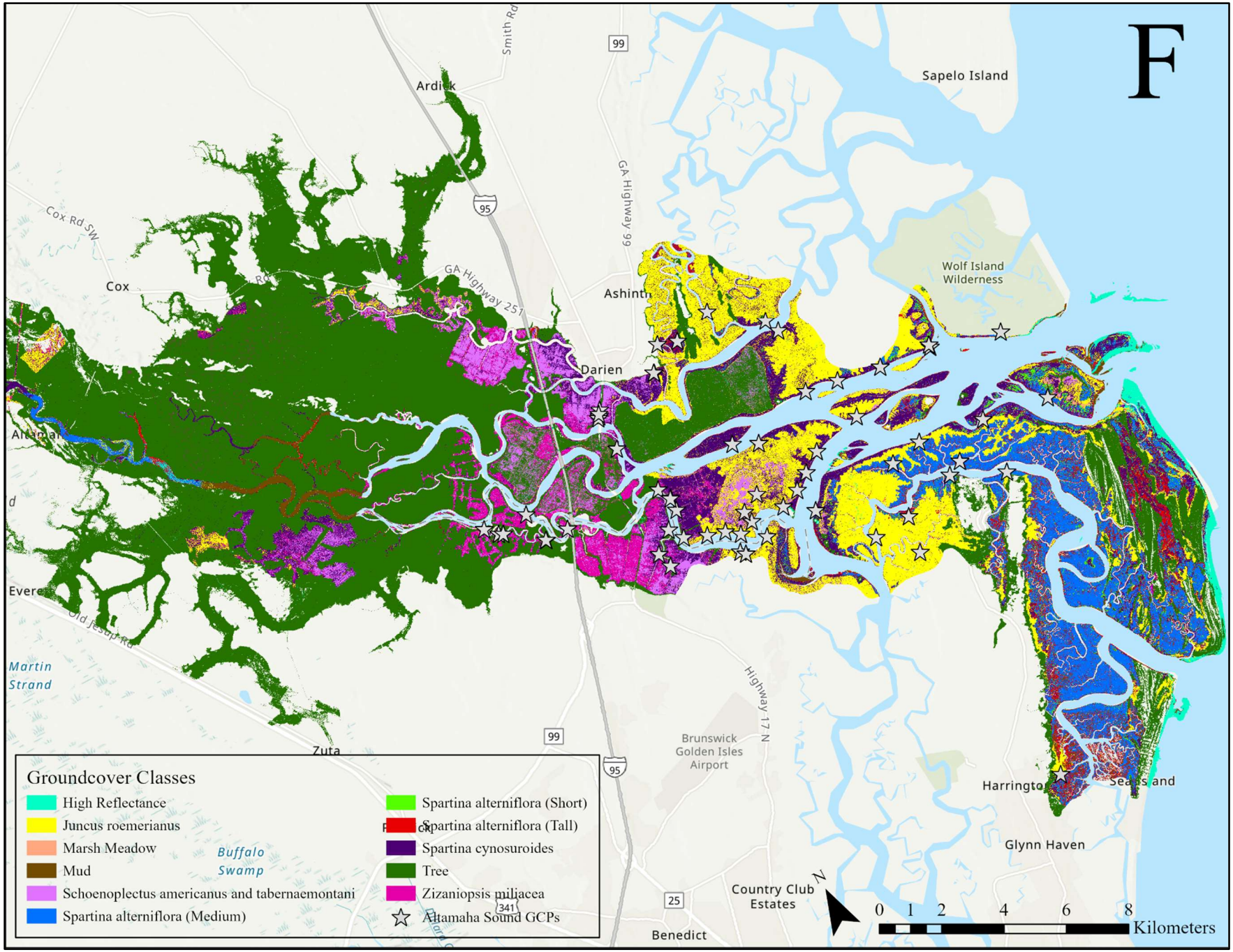
F
Sapelo Island
Wolf Island Wilderness
Darien
Ashinth
Cox
Ardick
Zuta
Martin Strand
Buffalo Swamp
Brunswick Golden Isles Airport
Highway 17 N
Glynn Haven
Country Club Estates
Benedict
Harringto
Sea Is and
Cox Rd SW
Smith Rd
GA Highway 99
GA Highway 251
99
95
25
341
Groundcover Classes
High Reflectance
Juncus roemerianus
Marsh Meadow
Mud
Schoenoplectus americanus and tabernaemontani
Spartina alterniflora (Medium)
Spartina alterniflora (Short)
Spartina alterniflora (Tall)
Spartina cynosuroides
Tree
Zizaniopsis miliacea
Altamaha Sound GCPs
N
0 1 2 4 6 8
Kilometers

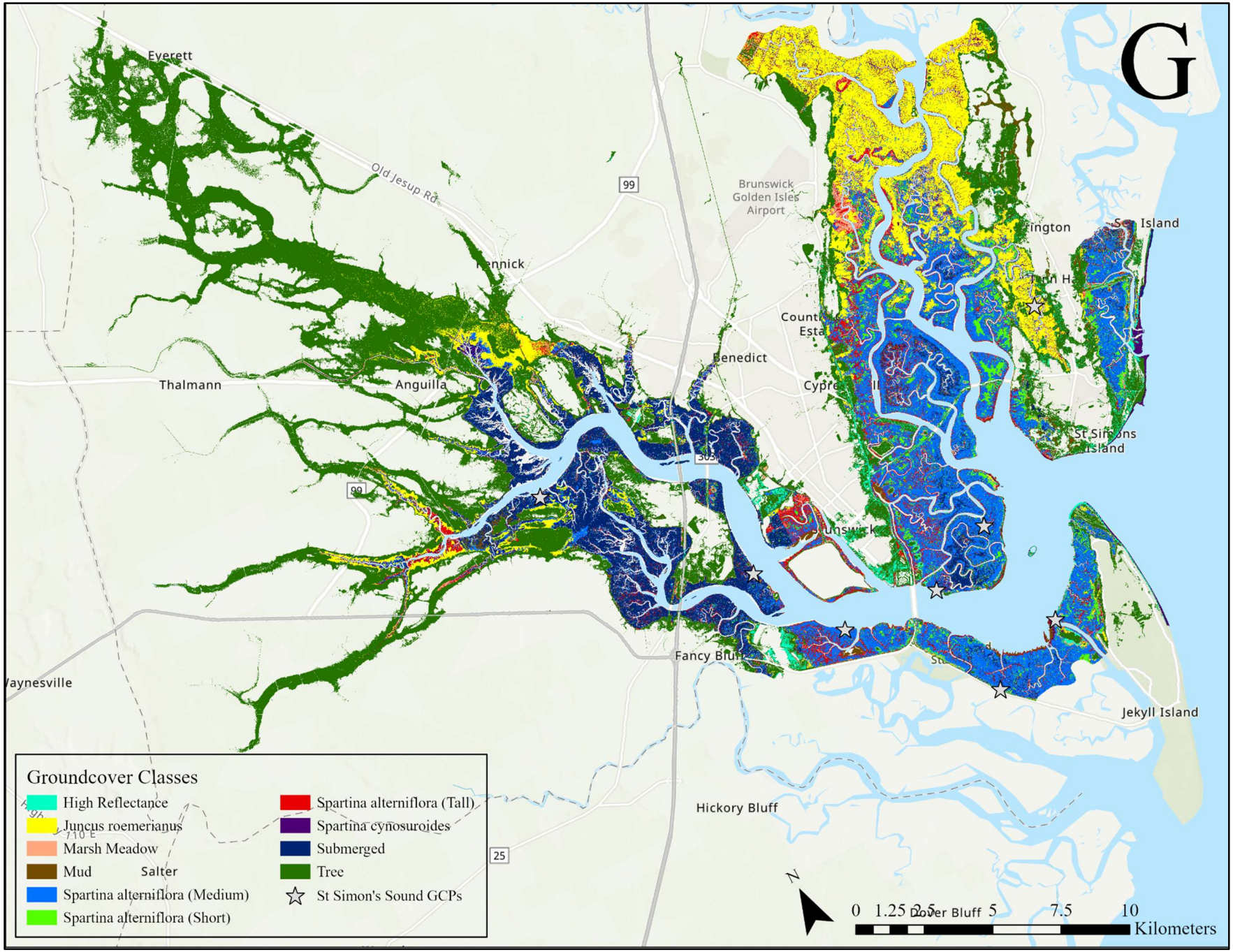
G
Everett
Old Jesup Rd
99
Brunswick
Golden Isles
Airport
Island
Thalmann
Anguilla
Benedict
St Simons
Island
Fancy Bluff
Jekyll Island
Hickory Bluff
Dover Bluff
25
Groundcover Classes
High Reflectance
Juncus roemerianus
Marsh Meadow
Mud
Salter
Spartina alterniflora (Medium)
Spartina alterniflora (Short)
Spartina alterniflora (Tall)
Spartina cynosuroides
Submerged
Tree
St Simon's Sound GCPs
N
0 1.25 2.5 5 7.5 10
Kilometers

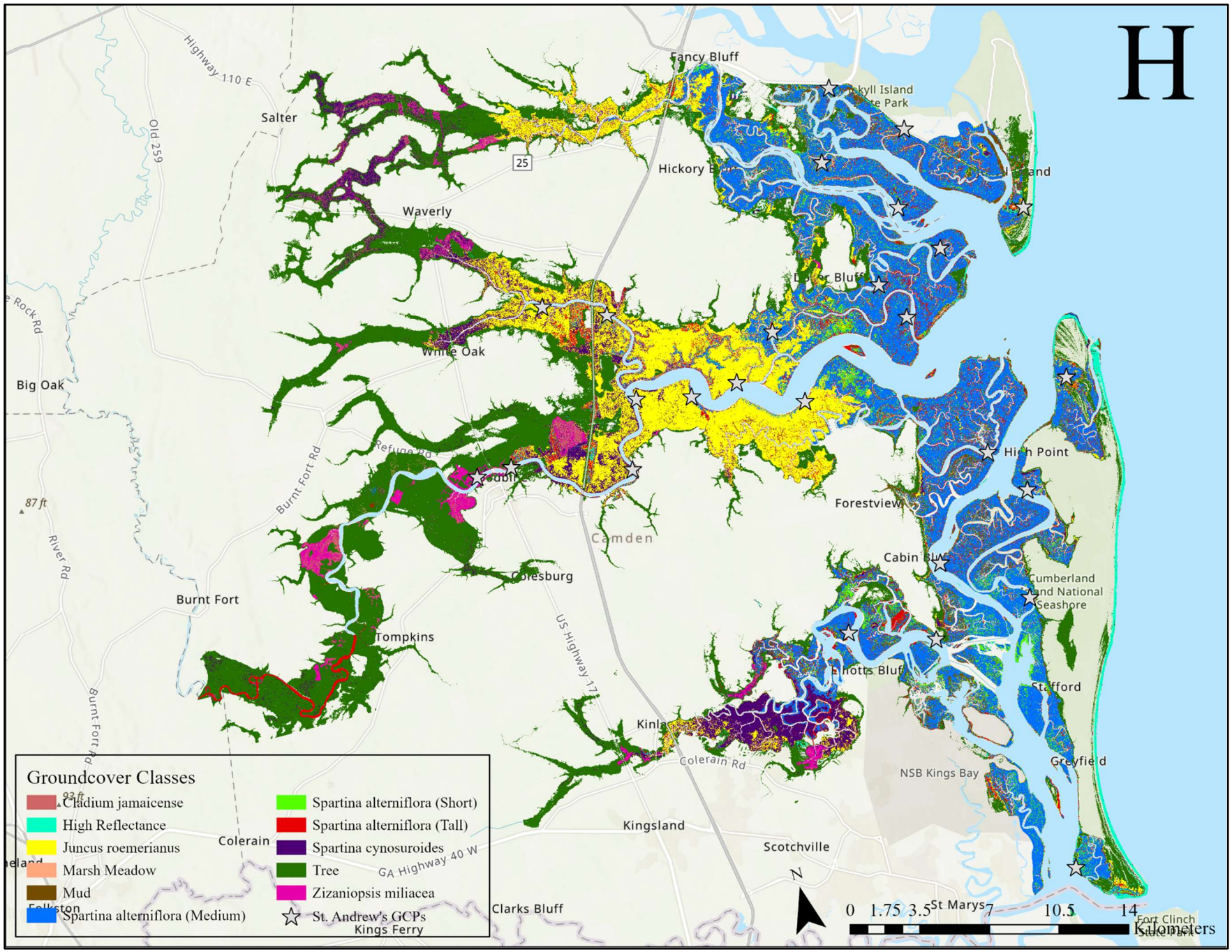
H
Groundcover Classes
Cladium jamaicense
High Reflectance
Juncus roemerianus
Marsh Meadow
Mud
Spartina alterniflora (Medium)
Spartina alterniflora (Short)
Spartina alterniflora (Tall)
Spartina cynosuroides
Tree
Zizaniopsis miliacea
St. Andrew's GCPs
Fancy Bluff
Salter
Waverly
White Oak
Big Oak
Burnt Fort
Tompkins
Colesburg
Camden
Kingsland
Scotchville
Colerain
Clarks Bluff
Kings Ferry
Forestview
High Point
Cabin Bluff
Cumberland Island National Seashore
Greyfield
NSB Kings Bay
St. Marys
Fort Clinch State Park
Highway 110 E
Old 259
Burnt Fort Rd
River Rd
Colerain Rd
US Highway 17
GA Highway 40 W
N
0 1.75 3.5 7 10.5 14
Kilometers

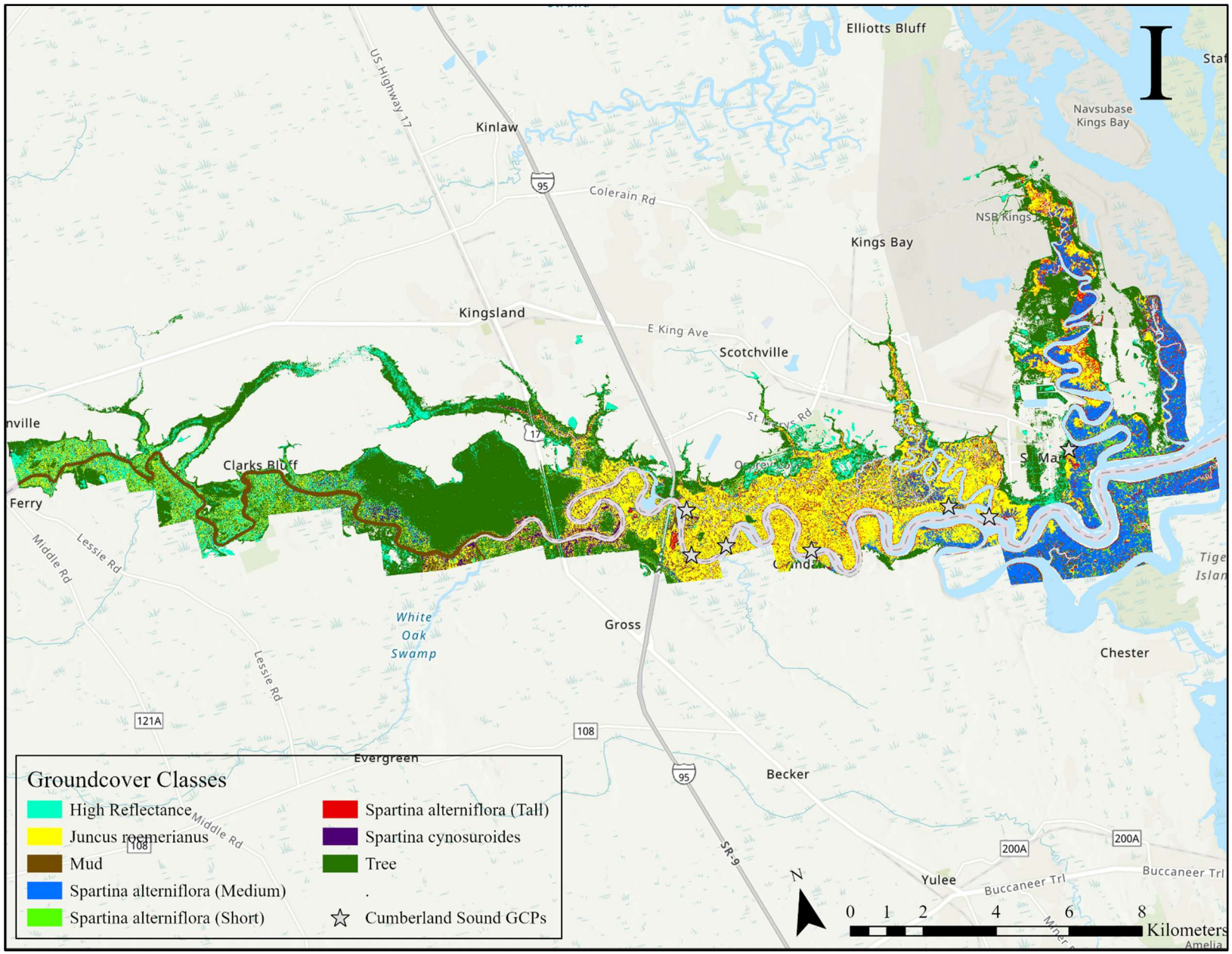
I
Elliotts Bluff
US Highway 17
Kinlaw
95
Colerain Rd
Navsubase Kings Bay
NSB Kings
Kings Bay
Kingsland
E King Ave
Scotchville
Clarks Bluff
Ferry
Middle Rd
Lessie Rd
White Oak Swamp
Gross
Chester
121A
108
Evergreen
Becker
SR-9
200A
Yulee
Buccaneer Trl
Groundcover Classes
High Reflectance
Juncus roemerianus
Mud
Spartina alterniflora (Medium)
Spartina alterniflora (Short)
Spartina alterniflora (Tall)
Spartina cynosuroides
Tree
Cumberland Sound GCPs
N
0 1 2 4 6 8
Kilometers

Table A1. Random Forest classification confusion matrix for the (A) Wassaw Sound, (B) Ossabaw Sound, (C) St. Catherine's Sound, (D) Sapelo Sound, (E) Doboy Sound, (F) Altamaha Sound, (G) St Simon's Sound, (H) St. Andrew's Sound, (I) Cumberland Sound. The rows represent the image data (the classified pixel) while the columns represent the reference data (what the pixel is based on reference data). The shaded cells represent the classification accuracy for each of the classes which is equivalent to the producer's accuracy.

	Ground Reference									A
Classified	High Reflectance	*Juncus roemerianus*	Marsh Meadow	Mud	*Spartina alterniflora* (Medium)	*Spartina alterniflora* (Short)	*Spartina alterniflora* (Tall)	Spartina cynosuroides	Submerged	Tree
High Reflectance	99.14%	0.00%	0.00%	0.00%	0.00%	0.00%	0.00%	0.00%	0.00%	0.00%
Juncus roemerianus	0.41%	91.24%	0.09%	0.00%	0.00%	0.19%	0.43%	7.83%	0.00%	0.00%
Marsh Meadow	0.00%	0.00%	99.64%	0.00%	0.00%	0.19%	0.00%	0.00%	0.00%	0.00%
Mud	0.00%	0.00%	0.00%	100.00%	0.00%	0.00%	0.00%	0.00%	0.00%	0.00%
Spartina alterniflora (Medium)	0.00%	0.18%	0.09%	0.00%	90.86%	0.69%	15.00%	0.40%	0.00%	0.00%
Spartina alterniflora (Short)	0.26%	2.29%	0.18%	0.00%	7.66%	98.94%	6.52%	0.61%	0.00%	0.00%
Spartina alterniflora (Tall)	0.04%	5.56%	0.00%	0.00%	1.48%	0.00%	73.48%	2.56%	0.00%	0.00%
Spartina cynosuroides	0.00%	0.72%	0.00%	0.00%	0.00%	0.00%	4.35%	88.60%	0.28%	0.00%
Submerged	0.00%	0.00%	0.00%	0.00%	0.00%	0.00%	0.00%	0.00%	99.72%	0.00%
Tree	0.15%	0.00%	0.00%	0.00%	0.00%	0.00%	0.22%	0.00%	0.00%	100.00%
Overall Accuracy: 0.950										

Ground Reference

B

Classified	High Reflectance	*Juncus roemerianus*	Marsh Meadow	Mud	*Spartina alterniflora* (Medium)	*Spartina alterniflora* (Short)	*Spartina alterniflora* (Tall)	*Spartina cynosuroides*	Submerged	Tree	*Zizaniopsis miliacea*
High Reflectance	100.00%	0.00%	0.00%	58.46%	0.00%	0.00%	0.48%	0.00%	0.00%	1.21%	0.00%
Juncus roemerianus	0.00%	94.32%	0.00%	0.00%	0.98%	0.03%	6.33%	2.99%	0.00%	0.00%	0.18%
Marsh Meadow	0.00%	0.19%	98.75%	0.00%	1.53%	12.79%	0.85%	0.00%	0.00%	0.00%	0.49%
Mud	0.00%	0.00%	0.00%	41.54%	0.00%	0.00%	0.00%	0.00%	0.00%	0.00%	0.00%
Spartina alterniflora (Medium)	0.00%	0.02%	0.12%	0.00%	83.30%	19.82%	13.83%	4.79%	0.50%	0.00%	0.29%
Spartina alterniflora (Short)	0.00%	0.00%	0.93%	0.00%	5.06%	66.43%	1.17%	3.59%	0.00%	0.00%	1.16%
Spartina alterniflora (Tall)	0.00%	3.45%	0.20%	0.00%	7.96%	0.94%	76.22%	11.98%	0.32%	0.00%	0.29%
Spartina cynosuroides	0.00%	2.02%	0.00%	0.00%	1.02%	0.00%	1.12%	76.05%	0.00%	0.02%	0.82%
Submerged	0.00%	0.00%	0.00%	0.00%	0.16%	0.00%	0.00%	0.00%	99.18%	0.00%	0.00%
Tree	0.00%	0.00%	0.00%	0.00%	0.00%	0.00%	0.00%	0.00%	0.00%	98.78 %	0.00%
Zizaniopsis miliacea	0.00%	0.00%	0.00%	0.00%	0.00%	0.00%	0.00%	0.60%	0.00%	0.00%	96.76%
Overall Accuracy: 0.929											

	Ground Reference									
Classified	High Reflectance	*Juncus roemerianus*	*Marsh Meadow*	Mud	Schoenoplectus americanus and tabernaemontani	Spartina alterniflora (Medium)	Spartina alterniflora (Short)	*Spartina alterniflora (Tall)*	Submerged	Tree
High Reflectance	96.66%	0.00%	51.83%	2.31%	0.00%	0.00%	0.00%	0.10%	0.00%	0.00%
Juncus roemerianus	2.99%	94.40%	21.50%	0.00%	0.77%	0.00%	0.00%	5.65%	0.00%	10.29%
Marsh Meadow	0.31%	0.00%	23.86%	0.00%	0.15%	0.52%	1.98%	0.00%	0.00%	0.00%
Mud	0.00%	0.00%	0.00%	96.92 %	0.00%	0.00%	0.00%	0.00%	0.00%	0.00%
Schoenoplectus americanus and *tabernaemontani*	0.00%	3.11%	0.00%	0.00%	98.31%	0.00%	0.00%	0.00%	0.00%	0.00%
Spartina alterniflora (Medium)	0.04%	0.00%	0.84%	0.00%	0.00%	95.31%	26.12%	0.00%	7.50%	0.00%
Spartina alterniflora (Short)	0.00%	0.00%	0.90%	0.22%	0.00%	0.84%	71.77%	0.05%	0.00%	0.00%
Spartina alterniflora (Tall)	0.00%	0.28%	0.79%	0.55%	0.00%	2.83%	0.12%	94.20%	0.12%	0.00%
Submerged	0.00%	0.00%	0.00%	0.00%	0.00%	0.50%	0.00%	0.00%	92.38%	0.00%
Tree	0.00%	2.21%	0.28%	0.00%	0.77%	0.00%	0.00%	0.00%	0.00%	89.71%
Overall Accuracy: 0.850										

D

	Ground Reference								
Classified	High Reflectance	*Juncus roemerianus*	Marsh Meadow	Mud	Spartina alterniflora (Medium)	Spartina alterniflora (Short)	Spartina alterniflora (Tall)	Submerged	Tree
High Reflectance	96.80%	0.00%	33.47%	5.79%	0.00%	0.08%	0.00%	0.00%	8.99%
Juncus roemerianus	0.00%	97.58%	0.30%	0.00%	0.00%	0.00%	0.00%	0.00%	0.00%
Marsh Meadow	0.00%	2.38%	53.45%	0.00%	0.08%	5.06%	6.90%	0.00%	0.89%
Mud	0.23%	0.00%	0.00%	93.68%	3.23%	0.19%	6.13%	0.00%	0.00%
Spartina alterniflora (Medium)	0.00%	0.02%	0.12%	0.00%	77.70%	7.88%	16.48%	8.41%	0.00%
Spartina alterniflora (Short)	0.00%	0.00%	6.36%	0.00%	10.73%	86.64%	14.56%	0.00%	0.00%
Spartina alterniflora (Tall)	2.52%	0.00%	2.38%	0.00%	8.12%	0.04%	55.56%	0.00%	0.00%
Submerged	0.00%	0.02%	0.00%	0.53%	0.14%	0.11%	0.00%	91.59%	0.00%
Tree	0.46%	0.00%	3.92%	0.00%	0.00%	0.00%	0.38%	0.00%	90.12%
Overall Accuracy: 0.857									

E

	Ground Reference							
Classified	High Reflectance	*Juncus roemerianus*	Marsh Meadow	Mud	*Spartina alterniflora* (Medium)	*Spartina alterniflora* (Short)	*Spartina alterniflora* (Tall)	Tree
High Reflectance	59.32%	0.01%	0.02%	0.00%	0.01%	0.00%	0.37%	0.75%
Juncus roemerianus	1.91%	95.21%	1.06%	0.00%	24.76%	0.28%	0.00%	0.00%
Marsh Meadow	19.07%	0.21%	93.04%	9.35%	11.17%	14.36%	1.22%	0.00%
Mud	0.42%	0.01%	0.00%	41.46%	0.04%	0.02%	6.36%	0.00%
Spartina alterniflora (Medium)	0.85%	3.03%	1.58%	5.28%	54.63%	31.06%	33.41%	0.00%
Spartina alterniflora (Short)	6.99%	0.20%	1.78%	28.86%	6.66%	53.19%	0.00%	0.00%
Spartina alterniflora (Tall)	0.64%	0.10%	1.36%	15.04%	2.72%	1.09%	56.79%	0.00%
Tree	10.81%	1.23%	1.14%	0.00%	0.00%	0.00%	1.84%	99.25%
Overall Accuracy: 0.891								

	Ground Reference										
Classified	High Reflectance	*Juncus roemerianus*	Marsh Meadow	Mud	*Schoenoplectus americanus* and *tabernaemontani*	*Spartina alterniflora* (Medium)	*Spartina alterniflora* (Short)	*Spartina alterniflora* (Tall)	*Spartina cynosuroides*	Tree	*Zizaniopsis miliacea*
High Reflectance	99.93%	2.28%	0.00%	0.00%	0.24%	0.00%	0.00%	0.00%	44.18%	0.57%	1.44%
Juncus roemerianus	0.01%	76.08%	2.59%	0.00%	2.55%	0.00%	0.00%	0.42%	3.42%	0.00%	0.01%
Marsh Meadow	0.00%	0.28%	66.92%	0.00%	2.63%	0.00%	0.00%	0.00%	0.02%	0.15%	0.00%
Mud	0.00%	0.00%	0.00%	97.45 %	0.00%	0.00%	0.00%	0.84%	0.02%	0.00%	0.00%
Schoenoplectus americanus and *tabernaemontani*	0.01%	9.84%	26.83%	0.00%	87.32%	0.00%	0.00%	0.00%	13.07%	0.00%	2.29%
Spartina alterniflora (Medium)	0.00%	0.03%	0.00%	0.00%	0.24%	80.34%	8.64%	2.10%	6.21%	0.00%	0.00%
Spartina alterniflora (Short)	0.00%	0.23%	0.00%	0.00%	0.00%	9.03%	65.45%	0.84%	0.06%	0.00%	0.00%
Spartina alterniflora (Tall)	0.00%	0.10%	0.30%	1.74%	0.08%	8.69%	7.27%	59.03%	0.99%	0.00%	0.00%
Spartina cynosuroides	0.01%	11.03%	3.35%	0.80%	2.32%	1.94%	18.64%	36.76%	31.35%	0.02%	0.75%
Tree	0.02%	0.00%	0.00%	0.00%	0.00%	0.00%	0.00%	0.00%	0.03%	99.25%	0.02%
Zizaniopsis miliacea	0.02%	0.13%	0.00%	0.00%	4.63%	0.00%	0.00%	0.00%	0.66%	0.01%	95.49%
Overall Accuracy: 0.836											

F

	Ground Reference									G
Classified	High Reflectance	*Juncus roemerianus*	Marsh Meadow	Mud	*Spartina alterniflora* (Medium)	*Spartina alterniflora* (Short)	*Spartina alterniflora* (Tall)	*Spartina cynosuroides*	Submerged	Tree
High Reflectance	97.52%	0.00%	3.30%	0.00%	4.57%	3.28%	0.73%	8.14%	0.00 %	0.00%
Juncus roemerianus	0.00%	96.66%	3.07%	0.00%	1.30%	0.00%	0.61%	24.63%	0.00 %	0.13%
Marsh Meadow	0.14%	1.40%	86.32%	0.00%	0.11%	0.00%	0.61%	0.00%	0.00 %	8.73%
Mud	0.55%	0.00%	0.00%	95.25 %	0.13%	0.11%	12.85%	1.04%	6.26 %	0.00%
Spartina alterniflora (Medium)	0.14%	0.21%	2.59%	2.23%	86.60%	49.17%	19.83%	0.63%	0.12 %	0.00%
Spartina alterniflora (Short)	0.00%	0.00%	0.00%	0.00%	6.33%	45.51%	0.24%	0.00%	0.16 %	0.00%
Spartina alterniflora (Tall)	0.83%	0.09%	2.59%	2.23%	0.74%	0.18%	43.08%	4.38%	0.35 %	0.00%
Spartina cynosuroides	0.28%	1.63%	2.12%	0.28%	0.13%	0.00%	22.03%	61.17%	0.04 %	0.00%
Submerged	0.00%	0.00%	0.00%	0.00%	0.09%	1.76%	0.00%	0.00%	93.07 %	0.00%
Tree	0.55%	0.00%	0.00%	0.00%	0.00%	0.00%	0.00%	0.00%	0.00 %	91.14%
Overall Accuracy: 0.8444										

H

	Ground Reference										
Classified	Cladium jamaicense	High Reflectance	*Juncus roemerianus*	Marsh Meadow	Mud	Spartina alterniflora (Medium)	*Spartina alterniflora (Short)*	Spartina alterniflora (Tall)	Spartina cynosuroides	Tree	*Zizaniopsis miliacea*
Cladium jamaicense	73.03%	0.00%	0.00%	0.00%	0.00%	0.00%	0.00%	0.00%	0.00%	0.00%	3.47%
High Reflectance	0.00%	99.40%	0.00%	0.00%	0.00%	0.00%	0.00%	0.00%	1.11%	8.36%	0.00%
Juncus roemerianus	0.00%	0.00%	88.83%	0.00%	0.00%	0.83%	0.00%	5.00%	6.27%	0.18%	0.00%
Marsh Meadow	0.00%	0.00%	4.25%	97.06%	0.00%	0.01%	1.87%	0.49%	1.85%	0.00%	0.00%
Mud	0.00%	0.20%	0.00%	0.00%	64.71 %	0.34%	1.13%	3.41%	0.00%	0.00%	0.00%
Spartina alterniflora (Medium)	0.00%	0.20%	5.64%	0.00%	5.88%	73.05%	33.71%	7.20%	0.00%	0.00%	0.00%
Spartina alterniflora (Short)	0.00%	0.20%	0.04%	0.00%	1.96%	24.88%	62.82%	25.85%	0.00%	5.97%	0.00%
Spartina alterniflora (Tall)	0.00%	0.00%	0.12%	2.94%	23.53 %	0.85%	0.40%	57.20%	0.37%	0.00%	0.00%
Spartina cynosuroides	0.00%	0.00%	0.98%	0.00%	0.00%	0.00%	0.00%	0.00%	90.04%	0.00%	0.00%
Tree	16.10%	0.00%	0.00%	0.00%	0.00%	0.00%	0.00%	0.00%	0.00%	85.49%	79.19%
Zizaniopsis miliacea	10.86%	0.00%	0.13%	0.00%	3.92%	0.04%	0.07%	0.85%	0.37%	0.00%	17.34%
Overall Accuracy: 0.741											

	Ground Reference							
Classified	High Reflectance	*Juncus roemerianus*	Mud	*Spartina alterniflora* (Medium)	*Spartina alterniflora* (Short)	*Spartina alterniflora* (Tall)	*Spartina cynosuroides*	Tree
High Reflectance	99.86%	0.00%	0.00%	0.00%	0.00%	0.00%	0.00%	0.00%
Juncus roemerianus	0.00%	86.52%	0.00%	6.32%	0.00%	0.00%	0.00%	0.00%
Mud	0.00%	0.00%	90.55%	7.17%	34.62%	16.06%	0.63%	0.00%
Spartina alterniflora (Medium)	0.00%	5.61%	3.98%	63.75%	42.31%	0.00%	0.00%	0.00%
Spartina alterniflora (Short)	0.00%	4.59%	5.47%	14.23%	23.08%	0.00%	0.00%	0.00%
Spartina alterniflora (Tall)	0.00%	0.22%	0.00%	8.54%	0.00%	83.94%	0.00%	0.00%
Spartina cynosuroides	0.14%	3.07%	0.00%	0.00%	0.00%	0.00%	99.37%	8.25%
Tree	0.00%	0.00%	0.00%	0.00%	0.00%	0.00%	0.00%	91.75%
Overall Accuracy: 0.861								